Eur. Phys. J. Spec. Top. (2025) 234:8005–8054
https://doi.org/10.1140/epjs/s11734-025-02019-7

THE EUROPEAN PHYSICAL JOURNAL SPECIAL TOPICS

Review

Some topics concerning the standard model, Feynman integrals and renormalization group methods: a review of some recent investigations and results

B. Ananthanarayan[1,a], Sumit Banik[1,2,3,b], Souvik Bera[1,4,c], Abhijit B. Das[1,11,d], Sudeepan Datta[1,e], Samuel Friot[5,6,f], Shayan Ghosh[1,g], M. S. A. Alam Khan[1,7,h], Tanay Pathak[1,8,i], Ratan Sarkar[1,9,j], and Daniel Wyler[10,k]

[1] Centre for High Energy Physics, CV Raman Road, Bangalore, Karnataka 560012, India
[2] Physik-Institut, Universität Zürich, Winterthurerstrasse 190, Zürich 8057, Switzerland
[3] Laboratory for Particle Physics, PSI Center for Neutron and Muon Sciences, Forschungsstrasse 111, Villigen 5232, Switzerland
[4] Asia Pacific Center for Theoretical Physics, Pohang, Gyeongsangbuk-do 37673, Korea
[5] Université Paris-Saclay, CNRS/IN2P3, IJCLab, Orsay 91405, France
[6] Univ Lyon Univ Claude Bernard Lyon 1, CNRS/IN2P3, IP2I Lyon, Villeurbanne 69622, France
[7] Department of Physics, Indian Institute of Technology Gandhinagar, Palaj, Gandhinagar, Gujarat 382355, India
[8] Department of Physics, Kyoto University, Kitashirakawa Oiwakecho, Sakyo-ku, Kyoto 606-8502, Japan
[9] The Institute of Mathematical Sciences, A CI of Homi Bhabha National Institute, Taramani, Chennai, Tamil Nadu 600113, India
[10] Physik-Institut, Universität Zürich, Winterthurerstrasse, 190, Zürich 8057, Switzerland
[11] DENSO, Global R&D Tokyo, Ota City, Hanedakuko 144-0041, Japan

Received 28 May 2025 / Accepted 10 October 2025 / Published online 10 November 2025

Abstract In this review, we present a comprehensive overview of some of our work carried out in numerous collaborations on important topics in the context of higher-order calculations in perturbative quantum field theories. The approach of this review is one where analytical methods are given prominence. Thus, we primarily concern ourselves with the study of multi-loop scalar Feynman integrals appearing in simplified and idealized models on the one hand, and on the other, to methods for obtaining analytic results for such integrals that are amenable to an implementation on *Mathematica* as the computer algebra software of choice. After a preliminary discussion of some of the commonly used parametric representations for Feynman integrals, we review (a) the construction of an algorithm and an automated program to find the 'regions' of Feynman integrals using Landau equations and power geometry, (b) the analysis of a non-trivial two-loop non-planar Feynman integral using Hopf algebras, (c) some basic aspects of multi-variable hypergeometric functions, namely, their regions of convergence and analytic continuations, (d) the interplay between the theory of multi-variable hypergeometric functions and Feynman integrals, including an algorithmic method for finding series representations for multi-fold Mellin-Barnes representations of Feynman integrals, the interpretation of Feynman integrals as GKZ hypergeometric functions and an automated program that uses this idea for obtaining series solutions, the ϵ-expansion for multi-variable hypergeometric functions arising from dimensionally regularized Feynman integrals, algebraic relations for products of propagators, and (e) the summation of large logarithms for renormalizable as well as non-renormalizable quantum field theories.

[a] e-mail: anant@iisc.ac.in
[b] e-mail: sumit.banik@psi.ch
[c] e-mail: souvik.bera@apctp.org
[d] e-mail: abhijit@alum.iisc.ac.in
[e] e-mail: sudeepand@iisc.ac.in
[f] e-mail: samuel.friot@ijclab.in2p3.fr
[g] e-mail: shayanghosh@alum.iisc.ac.in
[h] e-mail: alam.khan1909@gmail.com
[i] e-mail: pathak.tanay.4s@kyoto-u.ac.jp
[j] e-mail: ratansarkar@imsc.res.in
[k] e-mail: wyler@physik.uzh.ch (corresponding author)

1 Introduction

The Standard Model of the electroweak and strong interactions is a relativistic quantum field theory based on the gauge group $SU(3)_C \times SU(2)_L \times U(1)_Y$. It has so far demonstrated a high degree of success in being able to explain and predict a wide variety of experimental observations related to matter at its lowest accessible length scales, despite the presence of many other observations that cannot be satisfactorily explained by it. At sufficiently high energy (or, low distance) scales, the coupling parameters in the Lagrangian densities governing these interactions are small enough to admit an expansion of the scattering S-matrix elements. The contribution to each order in this expansion can be pictorially understood in terms of the so-called Feynman diagrams, the number of which has a factorial growth with the rise in the order of the expansion. For a specific physical process involving elementary particles of the Standard Model, the number of external states participating in the said process is fixed, therefore, going to higher orders in the expansion necessarily involves dealing with Feynman diagrams with a higher number of loops.

In particle physics experiments, most elementary particle processes at the leading order (LO) in perturbation theory are described by tree Feynman diagrams. Such diagrams correspond to rational functions of the kinematic invariants, and thus have a relatively simple pole structure. At higher orders in perturbation, diagrams with loops appear, which correspond to integrals of rational functions, thus possessing a more complicated analytic structure, such as the presence of logarithmic branch cuts. The precise analytic behavior of multi-loop Feynman integrals depends on the number of scales involved, arising from off-shell external states and/or massive particles circulating in the loops, and is a significantly challenging problem to settle in all generality. Precision studies that go beyond the LO have to deal with such integrals. The procedure for evaluating one-loop integrals appearing at the next-to-leading-order (NLO) in perturbation theory is relatively straightforward, owing much of its success to the development of powerful unitarity-based methods and recursion relations, which bypass much of the complexity and ambiguity inherent in the diagrammatic approach. However, for diagrams appearing at the next-to-next-to-leading-order (NNLO) in perturbation and beyond, unitarity-based methods, while successful for very specific studies, are yet to observe a level of adoption that is commonplace in the one-loop case. As a result, fully analytic results for such integrals are often obtained using the traditional diagrammatic approach, which plays a critical role and is often the key bottleneck in pushing the frontier for precision in theoretical particle physics calculations that may complement the experimental advances in the precision frontier. For obtaining renormalized results, such calculations are often performed in the well-known dimensional regularization scheme, wherein the space-time dimension is analytically continued from D_0 to $\mathrm{D} = \mathrm{D}_0 - 2\epsilon$, where D_0 is the original space-time dimension, and ϵ is a small number called the 'dimensional regularization parameter'. For our purposes, it is enough to consider $\mathrm{D}_0 = 4$, even though it is quite usual to consider dimension shifts for Feynman integrals such as computing integrals in dimension $\mathrm{D}_0 = 2$.

At lower energies, the relevant degrees of freedom of the strong interactions are the mesons and baryons. They find their use in various effective field theories such as the Chiral Perturbation Theory (ChPT) and variants thereof. Feynman diagrammatic calculations can be performed in such theories, although the expansion is no longer performed in terms of the coupling parameters, but rather, in terms of the momenta instead, precisely owing to the sufficiently low values of the latter. A recent review on ChPT can be found in [1].

By a sequence of intelligently designed calculation-organizing principles and automated programs, the procedure of computing the set of Feynman integrals contributing to a given physics process at some given order in perturbation results in the emergence of the so-called 'master integrals', which are a much smaller set than the initial set of integrals. There has been significant progress in the development of novel algorithms and automated computational tools to get to the step of master integrals starting from the initial set, references for which can be found in the reviews [2–4]. The master integrals are scalar Feynman integrals, meaning they are devoid of any Lorentz and spinor indices in the numerator. Such integrals admit various parametric representations, some of which quite readily provide a connection of the integrals to hypergeometric functions in one or more variables. For simple enough cases, the integrals could be relatively straightforwardly written in a closed form in terms of well-known hypergeometric functions, such as the single-variable Gauss ${}_2F_1$ and the generalized ${}_pF_q$ functions. For relatively more complicated cases, it might be possible to obtain closed-forms in terms of hypergeometric functions of two or more variables, some of which have been discussed at length later in this review. For yet more complicated cases, it is not easy to obtain closed-form representations in terms of known hypergeometric functions. Instead, one obtains generic series solutions converging in different domains of convergence. For perturbative studies, it is standard practice to also write the result so obtained (closed-form or series) as a Laurent expansion in the parameter ϵ.

Our work in the frontier of analytic evaluation of multi-loop Feynman integrals started with the consideration of two-loop diagrams arising in the context of ChPT, and our advocacy of the 'Mellin-Barnes' (MB) method in this context. It helped us find a representation for some of the quantities relevant to calculations in ChPT as a series expansion in ratios of physical quantities and make contact with lattice computations. Such a series expansion is also closely related to an approach known as the 'Method of Regions' (MoR), which was also applied in ChPT.

An alternative approach for the isolation of regions was introduced by us, leading to an algorithm that was named ASPIRE, and a *Mathematica*-based program was developed, tested, and validated against several known examples in the existing literature. An extension of the approach which required the essential use of Newton polytopes was found as an expression of unitarity and the top and bottom facets. Unitarity revealed cut structures were studied by us in the example of a non-planar diagram at two loops and established the existence of an alphabet and a co-action using a Hopf-algebra based method. This work was an extension of earlier works on cut Feynman diagrams primarily for planar examples of Feynman diagrams which can be represented using a special class of transcendental functions called the Multiple polylogarithms (MPLs).

These studies naturally led to the exploration of the properties of hypergeometric functions. As mentioned earlier, the simplest of the hypergeometric functions are those in one variable, such as the Gauss hypergeometric function and its higher-order generalizations. For the two variable case, there are 14 distinct complete hypergeometric functions of order 2, which are called Appell and Horn's functions. Investigating the analytic continuations of these hypergeometric functions is essential for deriving expressions applicable beyond their defining domain of convergence, thereby enabling the determination of numerical values. A systematic analysis of the analytic continuations was carried out by Olsson for the two-variable Appell F_1 function by using the transformation theory of one variable, the Gauss hypergeometric ${}_2F_1$ function. This approach is hereafter referred to as the method of Olsson. Using this method, we found a detailed list of analytic continuations of the Appell F_2 function. Subsequently, these analytic continuations were used in the package `AppellF2.wl` for the purpose of numerical evaluation. The method of Olsson for finding analytic continuations of multi-variable hypergeometric series is also automated in the form of a *Mathematica* [5] package called `Olsson.wl`. A companion package called `ROC2.wl` was also introduced along with it, which allows for the automatic evaluation of regions of convergence for two-variable hypergeometric series, which is an important step in the process of analytic continuation. These packages have been instrumental in deriving the analytic continuations of various other two- and three-variable hypergeometric series such as the Appell F_1, Appell F_3, Horn H_1 and Horn H_5 and the Lauricella F_D and Lauricella-Saran F_S series in three variables. Along with the computation of analytic continuations, automated packages were also developed for the numerical evaluation of these functions.

The MB approach mentioned earlier was further pursued, and efforts to obtain a general series solution to multi-fold MB integrals in the case of Yangian systems and conformal Feynman integrals led to the development of yet another automated program in the form of a *Mathematica* package called `MBConicHulls.wl`. In association to this, studies of the 'Method of Brackets' (MoB) and its applicability to Feynman integral evaluation were also undertaken, with a first evaluation of several quartic and quadratic integrals using MoB. The interconnections of the MB and MoB techniques were further explored, using which, Ising integrals and other related integrals were tackled, and further advancements towards the improvement of these methods were suggested. Around the time of these studies, the idea of interpreting generalized Feynman integrals as solutions to GKZ partial-differential-equation systems gathered momentum amongst physicists. The solutions admitted by these PDE systems can be conveniently and algorithmically expressed in terms of series expressions, and a *Mathematica* package `FeynGKZ` was developed to obtain such solutions for Feynman integrals. A brief summary of the most basic workflow using `FeynGKZ` is discussed in this article. Furthermore, when Feynman integrals are expressed in closed form as known hypergeometric functions, the parameter ϵ appears in the parameters of the latter. To obtain the Laurent expansion of these Feynman integrals, it is essential to expand the multi-variable hypergeometric functions with respect to their parameters. We have developed an algorithm for this expansion, which has been implemented in the *Mathematica* based package `MultiHypExp.wl`. This article briefly discusses the algorithm and its application through examples.

We also discuss some specific examples of these investigations. In one of these, the effectiveness of the MB approach is demonstrated by using it to solve the non-trivial double-box and hexagon conformal Feynman integrals. In another, we demonstrate a use of the `MultiHypExp` package for obtaining ϵ-expansions of hypergeometric functions encountered upon trying to analytically evaluate some boundary Feynman integrals originating in the context of three-loop QCD corrections to heavy-to-light form factors. The final example involves a brief discussion of the sunset Feynman integral in ChPT and specific QED corrections to the charged lepton $(g-2)_l$.

It may be worth noting that results at higher perturbative orders usually suffer from the presence of large logarithms. Thus, to ensure better convergence behavior of the perturbation expansion to all orders, the results obtained at higher orders should be suitably optimized to control the large logarithms or to reduce the dependence of the extra renormalization scale introduced in the regularization procedure. These issues are dealt with using renormalization group techniques and are discussed in the latter part of this review. These techniques are discussed for the summation of large leading-logarithms first for the case of massless models, and then subsequently also for QCD. In the case of QCD, we also provide a brief discussion of the RG improvement of the perturbation series, as well as its use in the determination of the Standard Model parameters using QCD sum rules.

The organization of this article is as follows: in Sect. 2, we discuss the various parameterizations of scalar Feynman integrals. To evaluate the Feynman integrals to higher orders, we first discuss the MoR in Sect. 3, following which the method of Hopf algebras is discussed in Sect. 4. Sections 5 and 6 explore the properties of some special hypergeometric functions, their numerical evaluation, and the associated automated programs. In

Sect. 7, we discuss some examples of the evaluation of Feynman diagrams using some of our recently-developed automated programs, as well as new analytical results for some three-loop contributions to the charged-lepton $(g-2)_l$ using the MB method. Next, we discuss the issue of large logarithms in simple massless models as well as their all-order summation in Sect. 8. Subsequently, in Sect. 9, we discuss the application of the RG-summation of large logarithms in QCD and electroweak theory, as well as phenomenological application in the determination of some Standard Model parameters using QCD sum rules. In Sect. 10, we summarize the results of our studies and provide possible future directions for further investigation.

2 Parametric representations for Feynman integrals

In this section, we give a brief introduction to three popular parametric representations of Feynman integrals. Here, we consider the parametric representation of a general scalar L-loop Feynman integral with m propagators, E external momenta (p_1, p_2, ..., p_E), and L internal momenta (l_1, l_2, ..., l_L). Thus, its momentum representation in dimensional regularization is,

$$I(n_1,\, n_2,\, ..,\, n_m) = \int \prod_{i=1}^{L} \frac{d^{\mathrm{D}} l_i}{\left(i\pi^{\frac{\mathrm{D}}{2}}\right)^{L}} \prod_{\alpha=1}^{m} {D_\alpha}^{-n_\alpha}, \tag{1}$$

where $D_\alpha = A_\alpha^{ij} l_i.l_j + 2B_\alpha^{ik} l_i.p_k + C_\alpha$ are the propagator factors. A and B are $L\times L$ and $L\times E$ matrices respectively, and C_α are constants.

2.1 Feynman parameters

This is one of the most popular representations is based on the identity:

$$\begin{aligned}\frac{1}{A_1^{\alpha_1}\cdots A_n^{\alpha_n}} = \frac{\Gamma(\alpha_1+\cdots+\alpha_n)}{\Gamma(\alpha_1)\cdots\Gamma(\alpha_n)} \int_0^1 du_1 \cdots \\ \times \int_0^1 du_n \frac{\delta(1-\sum_{k=1}^{n} u_k) u_1^{\alpha_1-1}\cdots u_n^{\alpha_n-1}}{\left(\sum_{k=1}^{n} u_k A_k\right)^{\sum_{k=1}^{n}\alpha_k}},\end{aligned} \tag{2}$$

where $\mathrm{Re}(\alpha_j) > 0$ for all $1 \le j \le n$. In the case of Feynman integrals, we use Eq. (2) to combine all the propagators into a single factor in the denominator by introducing Feynman parameters x_α for each propagator, as follows

$$\prod_{\alpha=1}^{m} {D_\alpha}^{-n_\alpha} = \frac{\Gamma(\sum_{\alpha=1}^{m} n_\alpha)}{\prod_\alpha \Gamma(n_\alpha)} \prod_{\alpha=1}^{m} \int_0^1 \mathrm{d}x_\alpha (x_\alpha)^{n_\alpha-1} \frac{\delta(1-\sum_{\alpha=1}^{m} x_\alpha)}{(x_\alpha D_\alpha)^{\sum_\alpha n_\alpha}}. \tag{3}$$

Substituting this expression into the momentum representation Eq. (1) and performing the internal loop integration leads to the following expression,

$$\begin{aligned} I(n_1,\, n_2,\, ..,\, n_m) = \frac{\Gamma(\frac{L\,\mathrm{D}}{2} - \sum_\alpha n_\alpha)}{\prod_\alpha \Gamma(n_\alpha)} \int_0^1 \prod_{\alpha=1}^{m} \mathrm{d}x_\alpha {x_\alpha}^{n_\alpha-1} \\ \times \delta(1-\sum_{\alpha=1}^{m} x_\alpha) \frac{(\mathcal{F})^{\frac{L\,\mathrm{D}}{2}-\sum_\alpha n_\alpha}}{(\mathcal{U})^{\frac{(L+1)\,\mathrm{D}}{2}-\sum_\alpha n_\alpha}}, \end{aligned} \tag{4}$$

which is called the Feynman parametric representation. In the above expression, $\mathcal{U}$ and $\mathcal{F}$ are homogeneous polynomials in Feynman parameters x_α of degree L and $L+1$ respectively. They are commonly called the first and second Symanzik polynomials, and expressed as,

$$\mathcal{U} = \det(A)\,, \tag{5}$$

$$\mathcal{F} = \det(AC) - (A^{\mathrm{adj}})^{ij} B^i B^j\,, \tag{6}$$

with $A = \sum_\alpha x_\alpha A^{ij}_\alpha$, $B^i = \sum_\alpha x_\alpha B^{ij}_\alpha p_j$, $C = \sum_\alpha x_\alpha C_\alpha$ and $A^{\rm adj} = \frac{\det(A)}{A^{-1}}$. Alternatively, they can be computed graphically as discussed in Ref. [6] and implemented in the *Mathematica* package `UF.m` by A. Smirnov.

2.2 Schwinger representation

This parametrization is based on the Schwinger trick

$$\frac{1}{t^n} = \int_0^\infty \frac{{\rm d}x\, x^{n-1}}{\Gamma(n)} e^{-xt}\,, \tag{7}$$

which can be applied individually to each propagator factor in the denominator of Eq. (1) and yields the following expression,

$$I(n_1,\, n_2,\, ..,\, n_m) = \int \prod_{i=1}^{L} \frac{d^{\rm D} l_i}{\left(i\pi^{\frac{\rm D}{2}}\right)^L} \prod_{\alpha=1}^{m} \frac{1}{\Gamma(n_\alpha)} \int_0^\infty {\rm d}x_\alpha\, x_\alpha^{n_\alpha - 1}\, e^{-x_\alpha D_\alpha}\,, \tag{8}$$

where x_α are called alpha parameters that are introduced for each propagator.

The integration over loop momenta is now a Gaussian integral, which can be integrated easily by completing the squares. The final expression after integrating out the loop-momenta is

$$I(n_1,\, n_2,\, ..,\, n_m) = \prod_{\alpha=0}^{m} \frac{1}{\Gamma(n_\alpha)} \int_0^\infty {\rm d}x_\alpha\, x_\alpha^{n_\alpha - 1}\, \mathcal{U}^{-\frac{\rm D}{2}}\, e^{-\frac{\mathcal{F}}{\mathcal{U}}}\,, \tag{9}$$

which is called the Schwinger parametric representation. Polynomials $\mathcal{U}$ and $\mathcal{F}$ in the above expression are the same as those in Eq. (4).

2.3 MB representation

The MB integrals are a particular type of contour integrals where the integrand, in its most general form, is made of a ratio of products of Euler-Gamma functions multiplied by parameters (dimensionless scales) raised to the power of the integration variables. The general form of an N-fold MB representation is

$$I(x_1,\, x_2,\, \cdots,\, x_N) = \int_{-i\infty}^{+i\infty} \frac{dz_1}{2\pi i} \cdots \int_{-i\infty}^{+i\infty} \frac{dz_N}{2\pi i}\, \frac{\prod_{i=1}^{k} \Gamma^{a_i}(\mathbf{e}_i \cdot \mathbf{z} + g_i)}{\prod_{j=1}^{l} \Gamma^{b_j}(\mathbf{f}_j \cdot \mathbf{z} + h_j)} x_1^{z_1} \cdots x_N^{z_N}\,, \tag{10}$$

where a_i, b_j, k, l and N are positive integers, $\mathbf{z} = (z_1,\, ...,\, z_N)$, and $\mathbf{e}_i$ and $\mathbf{f}_j$ are N-dimensional vectors. In the context of Feynman integrals, $x_1,\, \cdots x_N$ are dimensionless scales. The contours of the integration are such that they do not split the poles of each numerator Gamma function into different subsets.

The MB representation of a scalar Feynman integral can be derived either from the momentum representation by repeated application of the following identity

$$\frac{1}{(A+B)^\nu} = \frac{1}{\Gamma(\nu)} \int_{-i\infty}^{+i\infty} \frac{{\rm d}z}{2\pi i} \Gamma(-z)\Gamma(\nu+z) \frac{A^z}{B^{z+\nu}}\,, \tag{11}$$

to convert massive propagators into massless ones and, subsequently, compute the simpler massless integrals to get the final MB representation. Alternatively, the MB representation can be derived by first applying the following identities

1). Cahen-Mellin formula:

$$e^{-x} = \int_{c-i\infty}^{c+i\infty} \frac{{\rm d}z}{2\pi i}\, x^z \Gamma(-z)\,. \tag{12}$$

2). Multinomial Expansion:

$$(x_1+\cdots+x_n)^{\alpha}=\frac{1}{\Gamma(-\alpha)}\int\limits_{c_1-i\infty}^{c_1+i\infty}\frac{\mathrm{d}z_1}{2\pi i}\cdots\int\limits_{c_{n-1}-i\infty}^{c_{n-1}+i\infty}\frac{\mathrm{d}z_{n-1}}{2\pi i}\,(x_1)^{z_1}\cdots(x_{n-1})^{z_{n-1}}$$
$$\times\,(x_n)^{\alpha-z_1-\cdots-z_{n-1}}\Gamma(-z_1)\cdots\Gamma(-z_{n-1})\Gamma(-\alpha+z_1+\cdots+z_{n-1})\,, \tag{13}$$

on any of the three parametric representations discussed above, and then use the Inverse Mellin Transform, which says if

$$f(x)=\int\limits_{c-i\infty}^{c+i\infty}\frac{\mathrm{d}z}{2\pi i}\,x^{z}F(z)\,, \tag{14}$$

then,

$$\int\limits_{0}^{\infty}\mathrm{d}x\;x^{\alpha-1}f(x)=F(-\alpha)\,, \tag{15}$$

to yield the final MB representation.

The MB representation is a valuable tool in mathematical physics and helps us to study and evaluate Feynman integrals and various other kinds of definite integrals as well. For example, one can perform numerical integration [7–9], resolve epsilon singularity [10, 11], derive analytic series solutions in terms of hypergeometric functions [12, 13], derive differential equations [14, 15], count the number of master integrals (in some cases) [16], evaluate various kinds of improper integrals [17] etc. Another motivation to study MB integrals is that they are a valuable tool in the theory of hypergeometric functions. In particular, many multivariable hypergeometric functions have an MB representation which can help to derive analytic continuations of multivariable hypergeometric series.

3 Method of regions

The description of high-energy scattering amplitudes consists of physics coming from various scales. It is important to decouple the physics of different scales for the precise prediction of physical observables. Evaluation of amplitudes becomes non-trivial when one considers higher-order corrections for observables for specific processes, due to the presence of increased loops and scales in the Feynman diagrams. It is useful to consider systematic approximations to simplify calculations. The MoR [18–22] is one of the approaches that gives an asymptotic expansion of a given Feynman integral in a given limit. For more recent developments, see Refs. [23–30]. One can also study their analytic structure at the integrand level using homological methods [31, 32].

The steps one has to follow within MoR:

1). Identify the scales (masses and momenta) to set up a hierarchy and construct a small expansion parameter using the hierarchy.
2). Divide the loop momentum space into regions based on scale prescriptions.
3). In each of the regions, the integrand of the original integral is Taylor expanded.
4). After the expansion, integrate the expanded terms over the whole loop momentum space.
5). Within dimensional regularization, the scaleless contributions vanish.
6). Sum of contributions from each region gives the asymptotic expansion of the original integral in the limit considered.

In the geometric construction of the MoR, one deals with the parametric representation of a given Feynman integral expressed in terms of the Symanzik polynomials $\mathcal{U}$ and $\mathcal{F}$ (see Refs. [33, 34] for details about $\mathcal{U}$, $\mathcal{F}$). The polynomial $\mathcal{F}$ encodes all the kinematic information of multi-loop Feynman integrals. The neighborhoods of the Landau singularities of these integrals give the set of different regions which can be seen as the manifested scaling behavior of the parametric variables, when treated geometrically.

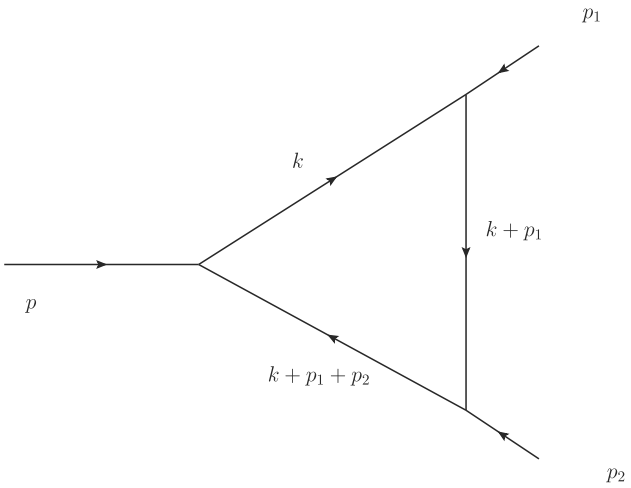

Fig. 1 One-loop Sudakov form factor

Isolation of regions in parametric space had been pioneered by Pak and Smirnov and implemented in the publicly available *Mathematica* package ASY [35]. Later on, the algorithm had been improved with the inclusion of certain linear transformations in the α-parameters to detect missing regions like potential and Glauber in ASY2 [36].

An alternative algorithm ASPIRE based on Landau singularities and Power Geometry [37] had been constructed in Ref. [38]. Within ASPIRE, one first constructs $\mathcal{G} = \mathcal{U} + \mathcal{F}$ and finds the Gröbner basis of set of equations $\{\mathcal{F}, \frac{\partial \mathcal{F}}{\partial \alpha_i}\}$, where $i = 1, \cdots, n$ denote the number of internal lines. If the Gröbner basis elements contain terms like $(\alpha_i - \alpha_j)$, one makes linear transformations of the types $\{\alpha_i \to \alpha_i + a\alpha_j, \alpha_j \to a\alpha_j\}$ or $\{\alpha_i \to a\alpha_i, \alpha_j \to a\alpha_i + \alpha_j\}$ (with $a \in \mathbb{R}$ and the delta function constraint in Feynman parameter space $\sum_{i=1}^{n} \alpha_i = 1$) to map those singular surfaces to the co-ordinate space $\alpha_i = 0$ or $\alpha_j = 0$. Those linear transformations are then applied to $\mathcal{G}$ to obtain a set of polynomials $G = \{\mathcal{G}, \mathcal{G}_1, \mathcal{G}_2, \cdots\}$. Corresponding to each monomial term of each of these polynomials, the vector exponents are extracted as the power of the variables in the coordinates $\{\lambda, \alpha_1, \cdots, \alpha_n\}$, λ being the expansion parameter. The set of vector exponents of monomial terms of a polynomial is called the support $\mathcal{S}$ of the polynomial. Thus for G, the supports are $S = \{\mathcal{S}, \mathcal{S}_1, \mathcal{S}_2, \cdots\}$. Convex hull of these supports S gives the Newton polytope $N = \{\mathcal{N}, \mathcal{N}_1, \mathcal{N}_2, \cdots\}$. For each of N, one finds a normal vector for each of the facets with the condition that the component of the normal vector corresponding to the coordinate-λ in $\{\lambda, \alpha_1, \cdots, \alpha_n\}$ has to be non-zero. Set of unique normal vectors $\{v_1, v_2, \cdots, v_n\}$ provides the scaling of each of $\{\alpha_1, \cdots, \alpha_n\}$ meaning that $\{\alpha_1 \sim \lambda^{v_1}\alpha_1, \alpha_2 \sim \lambda^{v_2}\alpha_2, \cdots, \alpha_n \sim \lambda^{v_n}\alpha_n\}$ and thus represents the set of regions $R = \{R_1, R_2, \cdots, R_m\}$ with $m \in \mathbb{N}$.

To demonstrate the MoR, we consider a one-loop three-point integral, depicted in Fig. 1, in $\mathrm{D} = 4 - 2\epsilon$ as an example. The Feynman integral for this diagram is given by

$$I(p_1^2, p_2^2; \epsilon) = \int \frac{d^{\mathrm{D}}k}{i\pi^{\frac{\mathrm{D}}{2}}} \frac{1}{k^2(k+p_1)^2(k+p_1+p_2)^2}, \tag{16}$$

where k is the internal loop-momentum and the external momenta are $\{p, p_1, p_2\}$ with $p = p_1 + p_2$. We construct the expansion parameter ($\lambda \sim \frac{p_1^2}{p^2} \sim \frac{p_2^2}{p^2}$) based on the following limit,

$$p_1^2 \sim p_2^2 << p^2,$$

and, using ASPIRE, we obtain four regions

$$\{0, 0, 0\}, \{0, -1, -1\}, \{-1, -1, 0\}, \{-1, -2, -1\}.$$

Evaluation of these regions in the Schwinger parametric space involves the following template integrals [39]

$$I_{R_i} = \int_0^\infty \prod_{j=1}^{n} \frac{d\alpha_j \alpha_j^{\lambda_j}}{\Gamma(1+\lambda_j)} \mathcal{U}_{R_i}^{-\mathrm{D}/2} e^{-\frac{\mathcal{F}_{R_i}}{\mathcal{U}_{R_i}}}, \tag{17}$$

where $\mathcal{U}_{R_i}$ and $\mathcal{F}_{R_i}$ are the first and second Symanzik polynomials for the region R_i and λ_j are the analytic regulators required to be considered when contributions of some of the regions are not well defined in $\mathrm{D} = 4 - 2\epsilon$ dimension [40].

Let us evaluate the integral for the hard region $\{0, 0, 0\}$. The Symanzik polynomials for the integral in Eq. (16) are

$$\begin{aligned}\mathcal{U} &= \alpha_1 + \alpha_2 + \alpha_3\,,\\ \mathcal{F} &= -p_1^2\alpha_1\alpha_2 - p_2^2\alpha_2\alpha_3 - p^2\alpha_1\alpha_3\,.\end{aligned}$$

We take $-p^2 = P^2$, $-p_1^2 = P_1^2$, $-p_2^2 = P_2^2$ and consider the kinematic region $P^2 > 0$, $P_1^2 > 0$, $P_2^2 > 0$ to make the second Symanzik polynomial $\mathcal{F}$ positive definite. For the hard region, we have the following scaling behavior

$$p^2 \sim \lambda^0 p^2,\ p_1^2 \sim \lambda^1 p_1^2,\ p_2^2 \sim \lambda^1 p_2^2,\ \alpha_1 \sim \lambda^0\alpha_1,\ \alpha_2 \sim \lambda^0\alpha_2,\ \alpha_3 \sim \lambda^0\alpha_3\,.$$

Using these scaling behaviors for hard region, we have

$$\begin{aligned}\mathcal{U}_{hard} &= \alpha_1 + \alpha_2 + \alpha_3\\ \mathcal{F}_{hard} &= -p^2\alpha_1\alpha_3\,.\end{aligned}$$

The leading order contribution for the hard region with $-p^2 = P^2$ is

$$\begin{aligned}I_{hard} &= \int_0^\infty \prod_{j=1}^{3} \frac{d\alpha_j \alpha_j^{\lambda_j}}{\Gamma(1+\lambda_j)} (\alpha_1+\alpha_2+\alpha_3)^{-\mathrm{D}/2} e^{-\frac{P^2\alpha_1\alpha_3}{\alpha_1+\alpha_2+\alpha_3}}\\ &= \frac{\Gamma(-\mathrm{D}/2+3+\lambda_1+\lambda_2+\lambda_3)\Gamma(\mathrm{D}/2-2-\lambda_1-\lambda_3)\Gamma(\mathrm{D}/2-2-\lambda_1-\lambda_2)}{\Gamma(1+\lambda_1)\Gamma(1+\lambda_3)\Gamma(-3+\mathrm{D}-\lambda_1-\lambda_2-\lambda_3)}\\ &\quad\times (P^2)^{\mathrm{D}/2-3-\lambda_1-\lambda_2-\lambda_3}\,.\end{aligned} \tag{18}$$

We now take the limit $\lambda_i \to 0$ for $i = 1, 2, 3$ and the Taylor expansion around $\epsilon = 0$, considering the prefactor $e^{\epsilon\gamma_E}(\mu^2)^\epsilon$ of the integral, gives

$$I_{hard} = \frac{1}{P^2\epsilon^2} + \frac{1}{P^2\epsilon}\log\left(\frac{\mu^2}{P^2}\right) + \mathcal{O}(\epsilon^0)\,, \tag{19}$$

where μ^2 is a scale introduced to make the coupling constant of the considered theory dimensionless. The region $\{-1, -1, 0\}$ is collinear to momentum p_1 and the integral for p_1-collinear region is

$$I_{p_1-collinear} = \int_0^\infty \prod_{j=1}^{3} \frac{d\alpha_j \alpha_j^{\lambda_j}}{\Gamma(1+\lambda_j)} (\alpha_1+\alpha_2)^{-\mathrm{D}/2} e^{-\frac{P_1^2\alpha_1\alpha_2+P^2\alpha_1\alpha_3}{\alpha_1+\alpha_2}}\,. \tag{20}$$

Solving this integral and taking the limits $\lambda_i \to 0$ and then expanding around $\epsilon = 0$, we get

$$I_{p_1-collinear} = -\frac{1}{P^2\epsilon^2} - \frac{1}{P^2\epsilon}\log\left(\frac{\mu^2}{P_1^2}\right) + \mathcal{O}(\epsilon^0)\,. \tag{21}$$

The contributions from p_2-collinear region $\{0, -1, -1\}$ and soft region $\{-1, -2, -1\}$ are

$$I_{p_2-collinear} = -\frac{1}{P^2\epsilon^2} - \frac{1}{P^2\epsilon}\log\left(\frac{\mu^2}{P_2^2}\right) + \mathcal{O}(\epsilon^0)\,, \tag{22}$$

$$I_{soft} = \frac{1}{P^2\epsilon^2} + \frac{1}{P^2\epsilon}\log\left(\frac{\mu^2 P^2}{P_1^2 P_2^2}\right) + \mathcal{O}(\epsilon^0)\,. \tag{23}$$

After summing over the regions, we reproduce the correct expression for the integral in Eq. (16). Interested readers can find other examples solved with the ASPIRE algorithm in the ancillary files provided with Refs. [38, 41].

4 Cuts of Feynman integrals and Hopf algebras

A large class of Feynman integrals can be expressed in terms of transcendental functions called the MPLs, which are defined in terms of a certain kind of iterated integrals, and include the classical polylogarithms as a special case. The MPLs form a Hopf algebra (see Refs. [42, 43] for further details), which involves a co-product denoted as Δ. The discontinuity across some channel of a given Feynman integral is related to the coproduct. The product of the function, in turn, is related to the symbol alphabet of the Feynman integral, which encodes the analytic structure of the function. Thus, an analytic evaluation of the discontinuity can lead us to determine an ansatz for the original Feynman integral in terms of the MPLs.

The method of using Hopf algebra to evaluate Feynman integrals analytically developed in Ref. [42] was applied for the first time to the two-loop non-planar on-shell diagram with massless propagators and three external mass scales [43]. We now provide a summary of this work. We show that the existence of the method of cut Feynman diagrams comprising the co-product, the first entry condition, and the integrability condition which was found to hold for the planar case, also holds for the non-planar case. Furthermore, the non-planar symbol alphabet is found to be the same as that for the planar case. This is one of the main results of the work, and has been obtained by a systematic analysis of the relevant cuts, using the symbolic manipulation *Mathematica* codes `HypExp` and `PolyLogTools`. The obtained result for the symbol is cross-checked by an analysis of the known two-loop original Feynman integral result. In addition, we reconstruct the full analytic result from the symbol. This is another important result in this work.

Consider the two-loop non-planar diagram in Fig. 2 that can be evaluated using direct integration, and the result is given by [44]:

$$C(p_1^2, p_2^2, p_3^3) = \left(\frac{i\,\pi}{\lambda p_3^2}\right)^2 \left[2(\mathrm{Li}_2(-\rho x) - \mathrm{Li}_2(-\rho y)) + \log(\rho x)\log(\rho y) + \frac{\pi^2}{3} + \log\left(\frac{y}{x}\right)\log\left(\frac{1+\rho y}{1+\rho x}\right)\right]^2, \tag{24}$$

where,

$$\lambda = \sqrt{(1-x-y)^2 - 4xy}, \quad \rho(x, y) = \frac{2}{1-x-y+\lambda}, \quad x = \frac{p_1^2}{p_3^2}, \quad y = \frac{p_2^2}{p_3^2}. \tag{25}$$

We will try to evaluate it using the method of cut diagrams. We first evaluate the first cut and second cut that are obtained by cutting two and three propagators (see Fig. 2), respectively. In the next step, the full function is obtained from the reconstruction of the symbol. We briefly discuss the results obtained in the next three subsections.

4.1 The first cut

The Feynman integral for the first cut is given by

$$\mathrm{Cut}\left[(l-p_2)^2, l^2\right] = -(2\pi)^2\, e^{2\gamma_E \epsilon} \int \frac{d^{\mathrm{D}}l}{i\pi^{\frac{\mathrm{D}}{2}}} \frac{d^{\mathrm{D}}k}{i\pi^{\frac{\mathrm{D}}{2}}} \frac{\delta^+(l^2)\,\delta^+\left((l-p_2)^2\right)}{(k+l-p_1)^2(k+l-p_2)^2(k-p_1)^2(k)^2}. \tag{26}$$

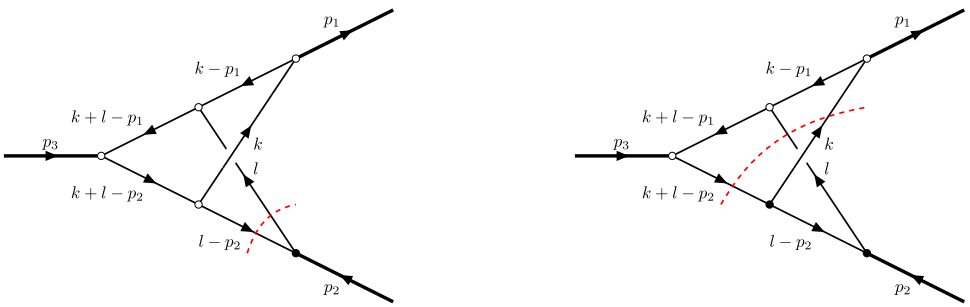

(a) Cut $\left[(l-p_2)^2, l^2\right]$ (b) Cut $\left[(k+l-p_2)^2, l^2, k^2\right]$

Fig. 2 Two-loop non-planar Feynman diagram and associated cut diagrams, all shown at uniform scale

We have carried out the integrations term by term using the *Mathematica* packages `HypExp` and `PolyLogTools`. The results are as follows:

$$\text{Cut}\left[(l-p_2)^2,\, l^2\right] = (-1)^{\epsilon}\frac{4\pi c_\Gamma e^{\gamma_E \epsilon}}{\Gamma(1-\epsilon)}\frac{(z\bar{z})^{-\epsilon}}{(z-\bar{z})^2}(p_1^2)^{-2-2\epsilon}\sum_{k=-1}^{\infty}\epsilon^k[f^{(k)}(z,\,\bar{z})]\,, \tag{27}$$

where,

$$u_i = \frac{p_i^2}{p_1^2}\,, \qquad z = \frac{1}{2}(1+u_2-u_3+\sqrt{\lambda})\,, \qquad \bar{z} = \frac{1}{2}(1+u_2-u_3-\sqrt{\lambda})\,, \tag{28}$$

and

$$f^{(-1)}(z,\,\bar{z}) = G\Big(1,\,\frac{\bar{z}-1}{\bar{z}-z},\,1\Big) + G\Big(1,\,\frac{z-1}{z-\bar{z}},\,1\Big) - G\Big(0,\,\frac{z-1}{z-\bar{z}},\,1\Big) - G\Big(0,\,\frac{\bar{z}-1}{\bar{z}-z},\,1\Big)\,. \tag{29}$$

The expression obtained for $f^{(0)}(z,\,\bar{z})$ is completely in terms of MPLs which is rather long and the interested reader can find it in Ref. [43].

4.2 The second cut

The Feynman Integral for the second cut is given by

$$\text{Cut}\left[(k+l-p_2)^2,\, l^2,\, k^2\right] = -(2\pi)^3\, e^{2\gamma_E\epsilon}\int\frac{d^{\mathrm{D}}l}{i\pi^{\frac{\mathrm{D}}{2}}}\frac{d^{\mathrm{D}}k}{i\pi^{\frac{\mathrm{D}}{2}}}\frac{\delta^+(l^2)\,\delta^+\big((k+l-p_2)^2\big)\,\delta^+\big(k^2\big)}{(k+l-p_1)^2(k-p_1)^2(l-p_2)^2}\,, \tag{30}$$

where the above integration can be done using `PolyLogTools` which results in

$$\text{Cut}\left[(k+l-p_2)^2,\, l^2,\, k^2\right] = \frac{4\pi c_\Gamma e^{\gamma_E \epsilon}}{\Gamma(1-\epsilon)}\frac{(z\bar{z})^{-\epsilon}}{(z-\bar{z})^2}(p_1^2)^{-2-2\epsilon}\sum_{k=-1}^{\infty}\epsilon^k[g^{(k)}(z,\,\bar{z})]\,, \tag{31}$$

with

$$g^{(-1)}(z,\,\bar{z}) = G\left(0,\,\frac{z-1}{z-\bar{z}},\,1\right) + G\left(0,\,\frac{\bar{z}-1}{\bar{z}-z},\,1\right) - G\left(1,\,\frac{z-1}{z-\bar{z}},\,1\right) - G\left(1,\,\frac{\bar{z}-1}{\bar{z}-z},\,1\right), \tag{32}$$

and

$$g^{(0)}(z,\,\bar{z}) = g_M^{(0)}(z,\,\bar{z}) + g_{\epsilon^1}^{(0)}(z,\,\bar{z}) + g_{\epsilon^{-1}}^{(0)}(z,\,\bar{z}) + g_P^{(0)}(z,\,\bar{z})\,. \tag{33}$$

We find that the divergences present in Eq. (29) and Eq. (29) cancel in the sum:

$$f^{(-1)}(z,\,\bar{z}) + g^{(-1)}(z,\,\bar{z}) = 0\,. \tag{34}$$

4.3 Reconstruction of the symbol and the full function

After employing similar methods as in the planar diagram for the symbol of the non-planar diagram, we get the symbol. Using this, the full function can be constructed, which in terms of the ordinary logarithms, is given by

$$\left[-2\text{Li}_2(\bar{z}) - \log^2(-\bar{z}) - \log(-z)\log(-\bar{z}) + \log(z\bar{z})\Big(\log\Big(-\frac{1-z}{1-\bar{z}}\Big) + \log(\bar{z})\Big) + 2\text{Li}_2(z)\right]^2, \tag{35}$$

which matches with Eq. (24) and the result in literature [44].

5 Theory of multi-variable hypergeometric functions

In this section, we give a brief review of the general hypergeometric function theory. We will mention some two and three-variable hypergeometric series along with an outline of various methods that are used to find their analytic continuation and their efficient numerical implementation. Horn's theorem, which is the main ingredient in finding the region of convergence of these multi-variable hypergeometric series is also discussed. These methods are applicable to series with more than two variables as well. However, for ease, the discussion below is focused on the two-variable hypergeometric series. We start by giving a general definition of two-variable hypergeometric functions. Assume the following double power series

$$F(x,\, y) = \sum_{m,\, n=0}^{\infty} C(m,\, n) x^m y^n \,, \tag{36}$$

We define two ratios

$$\begin{aligned} f(m,\, n) &= \frac{C(m+1,\, n)}{C(m,\, n)} \,, \\ g(m,\, n) &= \frac{C(m,\, n+1)}{C(m,\, n)} \,, \end{aligned} \tag{37}$$

and $F(x)$ is called a hypergeometric series, if $f(n,\, m)$ and $g(n,\, m)$ are rational functions of m and n. We can write

$$\begin{aligned} f(m,\, n) &= \frac{F(m,\, n)}{F'(m,\, n)} \,, \\ g(m,\, n) &= \frac{G(m,\, n)}{G'(m,\, n)} \,, \end{aligned} \tag{38}$$

where F, F', G and G' are polynomials in m and n. The largest degree among all these polynomials is called the order of the hypergeometric function. As a simple example of ${}_2F_1(x)$, the well-known Gauss hypergeometric function has an order of 2. Its higher-order generalization such as the ${}_pF_{p-1}(x)$ has order p. Further generalizations of Gauss hypergeometric, in 2-variables, we can define 14 distinct and complete hypergeometric series of order 2 [45, 46]. These include the four Appell functions F_1, F_2, F_3, F_4 and 10 Horn functions G_1, G_2, G_3, H_1, $\cdots$, H_7. The most important aspects of these hypergeometric functions essential to Feynman integrals involve the study of their analytic continuation, efficient numerical implementation, and finding the region of convergence of the analytic continuation involved. We will study more about the technical details in the upcoming subsections with their application to some of the series of Horn's list along with some 3-variable generalizations.

5.1 Appell functions

The Appell functions are defined as follows

$$F_1(a,\, b_1,\, b_2;\, c|x,\, y) = \sum_{m,\, n=0}^{\infty} \frac{(a)_{m+n} (b_1)_m (b_2)_n}{(c)_{m+n}} \frac{x^m}{m!} \frac{y^n}{n!}, \quad |x|< 1 \wedge |y|< 1 \,, \tag{39}$$

$$F_2(a,\, b_1,\, b_2;\, c_1,\, c_2|x,\, y) = \sum_{m,\, n=0}^{\infty} \frac{(a)_{m+n} (b_1)_m (b_2)_n}{(c_1)_m (c_2)_n} \frac{x^m}{m!} \frac{y^n}{n!}, \quad |x|+|y|< 1 \,, \tag{40}$$

$$F_3(a_1,\, a_2,\, b_1,\, b_2;\, c|x,\, y) = \sum_{m,\, n=0}^{\infty} \frac{(a_1)_m (a_2)_n (b_1)_m (b_2)_n}{(c)_{m+n}} \frac{x^m}{m!} \frac{y^n}{n!}, \quad |x|< 1 \wedge |y|< 1 \,, \tag{41}$$

$$F_4(a,\, b;\, c_1,\, c_2|x,\, y) = \sum_{m,\, n=0}^{\infty} \frac{(a)_{m+n} (b)_{m+n}}{(c_1)_m (c_2)_n} \frac{x^m}{m!} \frac{y^n}{n!}, \quad \sqrt{|x|} + \sqrt{|y|} < 1 \,, \tag{42}$$

where $(a)_m = \frac{\Gamma(a+m)}{\Gamma(a)}$ is the Pochhammer symbol. All the above series are reduced, when one of its arguments is zero, to the celebrated Gauss ${}_2F_1$ hypergeometric series. The defining domains of convergence of the series are

shown as well. To find the value of the function beyond the defining domain of convergence, it is necessary to find an analytic continuation.

We shall briefly describe the method of Olsson [47] to find analytic continuation below. The method is based on the fact that it is possible to derive the transformation properties of a multivariable hypergeometric series using the transformation theory of the hypergeometric function with a lesser number of variables. For instance, in the case of F_2, it suffices to know the transformation properties of one variable hypergeometric functions ${}_pF_{p-1}$. Some of these properties for some frequently used functions are listed below.

1). Pfaff-Euler transformation: These are the three transformations of the hypergeometric ${}_2F_1$ function, which are as follows

$$\begin{aligned} {}_2F_1(a,\, b,\, c; z) &= (1-z)^{-a} \quad {}_2F_1\left(a,\, c-b,\, c,\, \frac{z}{z-1}\right) \\ &= (1-z)^{-b} \quad {}_2F_1\left(c-a,\, b,\, c,\, \frac{z}{z-1}\right) \\ &= (1-z)^{c-a-b} \quad {}_2F_1(c-a,\, c-b,\, c,\, z)\,, \end{aligned} \tag{43}$$

These can be easily derived using proper Euler-type transformation in the integral representation of the hypergeometric ${}_2F_1$ function.

2). Another important transformation is the analytic continuation of ${}_2F_1(z)$ around $z = 1$ which is as follows

$$\begin{aligned} {}_2F_1(a,\, b,\, c; z) = {} & \frac{\Gamma(c)\Gamma(a+b-c)}{\Gamma(a)\Gamma(b)}(1-z)_2^{c-a-b}F_1(c-a,\, c-b,\, c-a-b+1; 1-z) \\ & + \frac{\Gamma(c)\Gamma(c-a-b)}{\Gamma(c-a)\Gamma(c-b)}\, {}_2F_1(a,\, b,\, a+b-c+1; 1-z)\,. \end{aligned} \tag{44}$$

3). The analytic continuation of ${}_2F_1$ around $z = \infty$ is given by

$$\begin{aligned} {}_2F_1(a,\, b,\, c; z) = {} & \frac{\Gamma(c)\Gamma(b-a)}{\Gamma(b)\Gamma(c-a)}(-z)^{-a}\, {}_2F_1\left(a,\, a-c+1,\, a-b+1; \frac{1}{z}\right) \\ & + \frac{\Gamma(c)\Gamma(a-b)}{\Gamma(a)\Gamma(c-b)}(-z)^{-b}\, {}_2F_1\left(b,\, b-c+1,\, b-a+1; \frac{1}{z}\right). \end{aligned} \tag{45}$$

4). The last set of transformations important for us is the analytic continuation of the hypergeometric function ${}_pF_{p-1}(z)$ around $z = \infty$, which we do not present here.

5.2 Lauricella functions

The three-variable generalizations of the Appell functions are the Lauricella function $F_A^{(3)}$, $F_B^{(3)}$, $F_C^{(3)}$ and $F_D^{(3)}$ [45]. Another three-variable hypergeometric series of interest in Feynman integral evaluation that appears as a solution to scalar one-loop integral is the Lauricella-Saran $F_S^{(3)}$ function, which has the following series representation

$$F_S^{(3)} \equiv F_S^{(3)}(a_1,\, a_2,\, b_1,\, b_2,\, b_3; c|x,\, y,\, z) = \sum_{m,\, n,\, p=0}^{\infty} \frac{(a_1)_m (a_2)_{n+p} (b_1)_m (b_2)_n (b_3)_p}{(c)_{m+n+p}} \frac{x^m y^n z^p}{m!\, n!\, p!}\,. \tag{46}$$

In the following subsection, we demonstrate the method of Olsson to find analytic continuation with the example of the triple variable Lauricella $F_S^{(3)}$.

5.3 Analytic continuation using the method of Olsson

Appell and Kampé de Feŕiet [48] have pointed out that analytic continuations of a multivariable hypergeometric function can be derived by leveraging the known analytic continuations of the hypergeometric functions with variables lower in number than that of the former function. In Ref. [47], Olsson obtained the analytic continuations of the double variable Appell F_1 function [49] employing the linear transformation formulae of the Gauss ${}_2F_1$ function. The same technique has been used to find the analytic continuations of the Appell F_2 recently, which

are the backbone of the numerical package `AppellF2.wl` [50]. Furthermore, it has been used to find the analytic continuations of other multivariable hypergeometric functions of interest to Feynman integral calculation, including two-variable Appell F_1, Appell F_3, and 3-variable Lauricella F_D and Lauricella-Saran F_s. The analytical results of the analytic continuations of these function as well as their numerical implementation is now available with open access on GitHub.[1] The analytic continuations of Horn H_1 and H_5 are the two remaining two-variable hypergeometric functions of special mathematical interest, as these cannot be written as a transformation of Appell F_2. Their analytic continuation is also found using the method of Olsson, and the numerical implementation is available on GitHub.[2] Appell F_4 has already been considered in detail in Ref. [51]. This powerful technique to find the analytic continuations of multivariable hypergeometric functions is automated in the *Mathematica* based package `Olsson.wl` [52], which eases the calculations significantly. Other methods to find the analytic continuation have also been explored recently in Ref. [53]. Preliminary tests suggest that the result obtained using methods and packages in [53] matches with various packages mentioned previously.

We illustrate the method in this section by finding the analytic continuations of the Lauricella-Saran function around $(0, \infty, \infty)$ and (∞, ∞, ∞) using the method of Olsson.

One can immediately observe the following symmetry of the F_S

$$F_S^{(3)}(a_1, a_2, b_1, b_2, b_3; c|x, y, z) = F_S^{(3)}(a_1, a_2, b_1, b_3, b_2; c|x, z, y)\,. \tag{47}$$

We observe that summing over one of the summation indices, one can write the summand in terms of the double variable Appell F_1 or F_3 function

$$\begin{aligned} F_S^{(3)}(a_1, a_2, b_1, b_2, b_3; c|x, y, z) &= \sum_{m=0}^{\infty} \frac{(a_1)_m (b_1)_m}{(c)_m} \frac{x^m}{m!} F_1(a_2; b_2, b_3; c+m|y, z) \\ &= \sum_{n=0}^{\infty} \frac{(a_2)_n (b_2)_n}{(c)_n} \frac{y^n}{n!} F_3(a_1, b_3, b_1, a_2+n; c+n|x, z) \\ &= \sum_{p=0}^{\infty} \frac{(a_2)_p (b_3)_p}{(c)_p} \frac{z^p}{p!} F_3(a_1, b_2, b_1, a_2+p; c+p|x, y)\,. \end{aligned} \tag{48}$$

Thus, a good use of the analytic continuations of the Appell functions can be made to find the analytic continuations of $F_S^{(3)}$. We briefly outline the method and use it to find the analytic continuation of the Lauricella-Saran function around $(0, \infty, \infty)$ [54]. We use the analytic continuation of the Appell F_1 around (∞, ∞) from Ref. [47] (precisely Eq. (22) of the Ref. [47]), which is shown below.

$$\begin{aligned} F_1(a, b_1, b_2; c|x, y) &= (-x)^{-b_1} (-y)^{b_1-a} \frac{\Gamma(c)\Gamma(a-b_1)\Gamma(-a+b_1+b_2)}{\Gamma(a)\Gamma(b_2)\Gamma(c-a)} \\ &\quad \times G_2\left(b_1, a-c+1, a-b_1, -a+b_1+b_2 \middle| -\frac{y}{x}, -\frac{1}{y}\right) \\ &\quad + (-x)^{-a} \frac{\Gamma(c)\Gamma(b_1-a)}{\Gamma(b_1)\Gamma(c-a)} F_1\left(a, a-c+1, b_2; a-b_1+1 \middle| \frac{1}{x}, \frac{y}{x}\right) \\ &\quad + (-x)^{-b_1} (-y)^{-b_2} \frac{\Gamma(c)\Gamma(a-b_1-b_2)}{\Gamma(a)\Gamma(c-b_1-b_2)} \\ &\quad \times F_1\left(b_1+b_2-c+1, b_1, b_2; -a+b_1+b_2+1 \middle| \frac{1}{x}, \frac{1}{y}\right), \end{aligned} \tag{49}$$

where G_2 is the one of Horn's functions defined as

$$G_2(a, a', b, b'|x, y) = \sum_{m,\, n=0}^{\infty} (a)_m (a')_n (b)_{n-m} (b')_{m-n} \frac{x^m}{m!} \frac{y^n}{n!}\,, \quad \frac{1}{|x|} < 1 \wedge \frac{1}{|y|} < 1 \wedge \left|\frac{y}{x}\right| < 1\,.$$

[1] https://github.com/souvik5151/Appell_Lauricella_Saran_functions.
[2] https://github.com/souvik5151/Horn_H1_H5.git.

Inserting the above expression in Eq. (48) and simplifying the Gamma functions and Pochhammer symbols, we obtain the analytic continuation of $F_S^{(3)}$ around $(0,\infty,\infty)$ as

$$\begin{aligned}
F_S^{(3)} &= (-y)^{-a_2}\frac{\Gamma(c)\Gamma(b_2-a_2)}{\Gamma(b_2)\Gamma(c-a_2)}\times\sum_{m,n,p=0}^{\infty}\frac{(a_1)_m(b_1)_m(b_3)_p(a_2)_{n+p}(-c+a_2+1)_{n-m}}{(a_2-b_2+1)_{n+p}}\frac{(-x)^m y^{-n-p}z^p}{m!\,n!\,p!}\\
&\quad (-y)^{-b_2}(-z)^{b_2-a_2}\frac{\Gamma(c)\Gamma(a_2-b_2)\Gamma(-a_2+b_2+b_3)}{\Gamma(a_2)\Gamma(b_3)\Gamma(c-a_2)}\\
&\quad\times\sum_{m,n,p=0}^{\infty}\frac{(a_1)_m(b_1)_m(b_2)_n(a_2-b_2)_{p-n}(-c+a_2+1)_{p-m}}{(a_2-b_2-b_3+1)_{p-n}}\frac{(-x)^m y^{-n}z^{n-p}}{m!\,n!\,p!}\\
&\quad +(-y)^{-b_2}(-z)^{-b_3}\frac{\Gamma(c)\Gamma(a_2-b_2-b_3)}{\Gamma(a_2)\Gamma(c-b_2-b_3)}\\
&\quad\times\sum_{m,n,p=0}^{\infty}\frac{(a_1)_m(b_1)_m(b_2)_n(b_3)_p(-c+b_2+b_3+1)_{-m+n+p}}{(-a_2+b_2+b_3+1)_{n+p}}\frac{(-x)^m y^{-n}z^{-p}}{m!\,n!\,p!}\,,
\end{aligned}\tag{50}$$

which can be written in terms of other triple variable hypergeometric functions as

$$\begin{aligned}
F_S^{(3)} &= (-y)^{-a_2}\frac{\Gamma(c)\Gamma(b_2-a_2)}{\Gamma(b_2)\Gamma(c-a_2)}\times F_{5c}\left(a_2,\,b_3,\,a_1,\,b_1,\,1+a_2-c;1+a_2-b_2\middle|\frac{z}{y},\,\frac{1}{y},\,-x\right)\\
&\quad +(-y)^{-b_2}(-z)^{b_2-a_2}\frac{\Gamma(c)\Gamma(a_2-b_2)\Gamma(-a_2+b_2+b_3)}{\Gamma(a_2)\Gamma(b_3)\Gamma(c-a_2)}\\
&\quad\times F_{1e}\left(b_2,\,a_1,\,b_1,\,b_2+b_3-a_2,\,1+a_2-c,\,a_2-b_2\middle|-\frac{z}{y},\,-\frac{1}{z},\,-x\right)\\
&\quad +(-y)^{-b_2}(-z)^{-b_3}\frac{\Gamma(c)\Gamma(a_2-b_2-b_3)}{\Gamma(a_2)\Gamma(c-b_2-b_3)}\\
&\quad\times F_{5b}\left(b_3,\,b_2,\,b_1,\,a_1,\,1+b_2+b_3-c;1-a_2+b_2+b_3\middle|\frac{1}{z},\,\frac{1}{y},\,-x\right).
\end{aligned}$$

The domain of convergence can be found using Horn's theorem, which has already been discussed in Sect. 5.4, and the above analytic continuation is valid in:

$$|x|<1\wedge\frac{1}{|y|}+1<\frac{1}{|x|}\wedge\frac{1}{|y|}<1\wedge\frac{1}{|z|}+1<\frac{1}{|x|}\wedge\frac{1}{|z|}<1\wedge\left|\frac{z}{y}\right|<1\,.$$

One can immediately find another analytic continuation of the $F_S^{(3)}$ around $(0,\infty,\infty)$ using the symmetry relation (i.e., Eq. (47)), which we do not present here explicitly.

Next, we find the analytic continuation around (∞,∞,∞) by taking each of the three series of Eq. (50), summing over the index m and using the analytic continuation of ${}_2F_1(x)$ around $x=\infty$ (i.e., Eq. (45)). Let us denote the first series of Eq. (50) as S_1

$$\begin{aligned}
S_1 &= \sum_{m,n,p=0}^{\infty}\frac{(a_1)_m(b_1)_m(b_3)_p(a_2)_{n+p}(-c+a_2+1)_{n-m}}{(a_2-b_2+1)_{n+p}}\frac{(-x)^m y^{-n-p}z^p}{m!\,n!\,p!}\\
&= \sum_{n,p=0}^{\infty}\frac{(b_3)_p(-c+a_2+1)_n(a_2)_{n+p}}{(a_2-b_2+1)_{n+p}}\frac{y^{-n-p}z^p}{n!\,p!}\,{}_2F_1(a_1,\,b_1;c-n-a_2|x)\,.
\end{aligned}\tag{51}$$

In the second equality, the summation over the index m is explicitly taken. As a result, the Gauss ${}_2F_1$ appears in the summand. Now, we use Eq. (45) to find the analytic continuation of the series S_1 which we denote here as S_1' and it has following form

$$S_1' = (-x)^{-a_1}\frac{\Gamma(b_1-a_1)\Gamma(c-a_2)}{\Gamma(b_1)\Gamma(c-a_1-a_2)}\times\sum_{m,n,p=0}^{\infty}\frac{(a_1)_m(b_3)_p(a_2)_{n+p}(-c+a_1+a_2+1)_{m+n}}{(a_1-b_1+1)_m(a_2-b_2+1)_{n+p}}\frac{x^{-m}y^{-n-p}z^p}{m!\,n!\,p!}$$

$$
\begin{aligned}
&+(-x)^{-b_1}\frac{\Gamma(a_1-b_1)\Gamma(c-a_2)}{\Gamma(a_1)\Gamma(c-a_2-b_1)}\times\sum_{m,\,n,\,p=0}^{\infty}\frac{(b_1)_m(b_3)_p(a_2)_{n+p}(-c+a_2+b_1+1)_{m+n}}{(-a_1+b_1+1)_m(a_2-b_2+1)_{n+p}}\frac{x^{-m}y^{-n-p}z^p}{m!\,n!\,p!}\\
&=(-x)^{-a_1}\frac{\Gamma(b_1-a_1)\Gamma(c-a_2)}{\Gamma(b_1)\Gamma(c-a_1-a_2)}\times F_M\left(a_2,\,1+a_1+a_2-c,\,b_3,\,a_1;1+a_2-b_2,\,1+a_1-b_1\middle|\frac{z}{y},\,\frac{1}{y},\,\frac{1}{x}\right)\\
&\quad+(-x)^{-b_1}\frac{\Gamma(a_1-b_1)\Gamma(c-a_2)}{\Gamma(a_1)\Gamma(c-a_2-b_1)}\times F_M\left(a_2,\,1+b_1+a_2-c,\,b_3,\,b_1;1+a_2-b_2,\,1+b_1-a_1\middle|\frac{z}{y},\,\frac{1}{y},\,\frac{1}{x}\right). \qquad (52)
\end{aligned}
$$

Similarly, taking the second series of Eq. (50), denoted here as S_2, and proceeding as before gives us

$$
\begin{aligned}
S_2&=\sum_{m,\,n,\,p=0}^{\infty}\frac{(a_1)_m(b_1)_m(b_2)_n(a_2-b_2)_{p-n}(-c+a_2+1)_{p-m}}{(a_2-b_2-b_3+1)_{p-n}}\frac{(-x)^m y^{-n}z^{n-p}}{m!\,n!\,p!}\\
&=\sum_{n,\,p=0}^{\infty}\frac{(b_2)_n(-c+a_2+1)_p(a_2-b_2)_{p-n}}{(a_2-b_2-b_3+1)_{p-n}}\frac{y^{-n}z^{n-p}}{n!\,p!}\,{}_2F_1(a_1,\,b_1;c-p-a_2|x)\,. \qquad (53)
\end{aligned}
$$

Again, using the analytic continuation of ${}_2F_1(\ldots;x)$ around $x=\infty$, we obtain the analytic continuation of S_2 as

$$
\begin{aligned}
S_2'&=(-x)^{-a_1}\frac{\Gamma(b_1-a_1)\Gamma(c-a_2)}{\Gamma(b_1)\Gamma(c-a_1-a_2)}\times\sum_{m,\,n,\,p=0}^{\infty}\frac{(a_1)_m(b_2)_n(a_2-b_2)_{p-n}(-c+a_1+a_2+1)_{m+p}}{(a_1-b_1+1)_m(a_2-b_2-b_3+1)_{p-n}}\frac{x^{-m}y^{-n}z^{n-p}}{m!\,n!\,p!}\\
&\quad+(-x)^{-b_1}\frac{\Gamma(a_1-b_1)\Gamma(c-a_2)}{\Gamma(a_1)\Gamma(c-a_2-b_1)}\sum_{m,\,n,\,p=0}^{\infty}\frac{(b_1)_m(b_2)_n(a_2-b_2)_{p-n}(-c+a_2+b_1+1)_{m+p}}{(-a_1+b_1+1)_m(a_2-b_2-b_3+1)_{p-n}}\frac{x^{-m}y^{-n}z^{n-p}}{m!\,n!\,p!}\\
&=(-x)^{-a_1}\frac{\Gamma(b_1-a_1)\Gamma(c-a_2)}{\Gamma(b_1)\Gamma(c-a_1-a_2)}\times F_{4h}\left(1+a_1+a_2-c,\,a_1,\,b_2,\,a_2-b_2,\,-a_2+b_2+b_3;1+a_1-b_1\middle|-\frac{1}{z},\,\frac{1}{x},\,-\frac{z}{y}\right)\\
&\quad+(-x)^{-b_1}\frac{\Gamma(a_1-b_1)\Gamma(c-a_2)}{\Gamma(a_1)\Gamma(c-a_2-b_1)}\times F_{4h}\left(1+b_1+a_2-c,\,b_1,\,b_2,\,a_2-b_2,\,-a_2+b_2+b_3;1+b_1-a_1\middle|-\frac{1}{z},\,\frac{1}{x},\,-\frac{z}{y}\right).
\end{aligned} \qquad (54)
$$

Finally, we consider the third series, denoted here as S_3, and it has the following form

$$
\begin{aligned}
S_3&=\sum_{m,\,n,\,p=0}^{\infty}\frac{(a_1)_m(b_1)_m(b_2)_n(b_3)_p(-c+b_2+b_3+1)_{-m+n+p}}{(-a_2+b_2+b_3+1)_{n+p}}\frac{(-x)^m y^{-n}z^{-p}}{m!\,n!\,p!}\\
&=\sum_{n,\,p=0}^{\infty}\frac{(b_2)_n(b_3)_p(-c+b_2+b_3+1)_{n+p}}{(-a_2+b_2+b_3+1)_{n+p}}\frac{y^{-n}z^{-p}}{n!\,p!}{}_2F_1(a_1,\,b_1;c-n-p-b_2-b_3|x)\,. \qquad (55)
\end{aligned}
$$

Using the analytic continuation of ${}_2F_1(\ldots;x)$ around $x=\infty$, we find the analytic continuation of S_3 (denoted as S_3')

$$
\begin{aligned}
S_3'&=(-x)^{-a_1}\frac{\Gamma(b_1-a_1)\Gamma(c-b_2-b_3)}{\Gamma(b_1)\Gamma(c-a_1-b_2-b_3)}\\
&\qquad\times\sum_{m,\,n,\,p=0}^{\infty}\frac{(a_1)_m(b_2)_n(b_3)_p(-c+a_1+b_2+b_3+1)_{m+n+p}}{(a_1-b_1+1)_m(-a_2+b_2+b_3+1)_{n+p}}\frac{x^{-m}y^{-n}z^{-p}}{m!\,n!\,p!}\\
&\qquad+(-x)^{-b_1}\frac{\Gamma(a_1-b_1)\Gamma(c-b_2-b_3)}{\Gamma(a_1)\Gamma(c-b_1-b_2-b_3)}\\
&\qquad\times\sum_{m,\,n,\,p=0}^{\infty}\frac{(b_1)_m(b_2)_n(b_3)_p(-c+b_1+b_2+b_3+1)_{m+n+p}}{(-a_1+b_1+1)_m(-a_2+b_2+b_3+1)_{n+p}}\frac{x^{-m}y^{-n}z^{-p}}{m!\,n!\,p!}\\
&=(-x)^{-a_1}\frac{\Gamma(b_1-a_1)\Gamma(c-b_2-b_3)}{\Gamma(b_1)\Gamma(c-a_1-b_2-b_3)}\\
&\qquad\times F_G\left(1-c+a_1+b_2+b_3,\,b_3,\,b_2,\,a_1;1-a_2+b_2+b_3,\,1+a_1-b_1\middle|\frac{1}{z},\,\frac{1}{y},\,\frac{1}{x}\right)
\end{aligned}
$$

$$+(-x)^{-b_1}\frac{\Gamma(a_1-b_1)\Gamma(c-b_2-b_3)}{\Gamma(a_1)\Gamma(c-b_1-b_2-b_3)}$$
$$\times F_G\left(1-c+b_1+b_2+b_3,\, b_3,\, b_2,\, b_1;1-a_2+b_2+b_3,\, 1+b_1-a_1\middle|\frac{1}{z},\,\frac{1}{y},\,\frac{1}{x}\right). \tag{56}$$

Thus, the analytic continuation of the $F_S^{(3)}$ around (∞,∞,∞) is the sum of the expressions in Eq. (52), Eq. (54) and Eq. (56) multiplied by appropriate prefactors. It is given by

$$F_S^{(3)} = (-y)^{-a_2}\frac{\Gamma(c)\Gamma(b_2-a_2)}{\Gamma(b_2)\Gamma(c-a_2)}\times S_1' + (-y)^{-b_2}(-z)^{b_2-a_2}\frac{\Gamma(c)\Gamma(a_2-b_2)\Gamma(-a_2+b_2+b_3)}{\Gamma(a_2)\Gamma(b_3)\Gamma(c-a_2)}\times S_2'$$
$$+(-y)^{-b_2}(-z)^{-b_3}\frac{\Gamma(c)\Gamma(a_2-b_2-b_3)}{\Gamma(a_2)\Gamma(c-b_2-b_3)}\times S_3'\,. \tag{57}$$

We do not write the expression explicitly due to its long length. The corresponding domain of convergence can be found using Horn's theorem as

$$\frac{1}{|x|}<1\wedge\frac{1}{|x|}+\frac{1}{|y|}<1\wedge\frac{1}{|y|}<1\wedge\frac{1}{|x|}+\frac{1}{|z|}<1\wedge\frac{1}{|z|}<1\wedge\left|\frac{z}{y}\right|<1\,.$$

Another analytic continuation of the $F_S^{(3)}$ around (∞,∞,∞) can be readily found by employing the symmetry relation Eq. (47).

5.3.1 `Olsson.wl` package and examples

We now briefly describe the `Olsson.wl` package[3] and its main functionality by taking Appell F_2 as our working example. The `Olsson` command can be called as follows

`Olsson[q, summation − indices − list, expression, options]`

The first argument `q` is an integer that dictates the summation index of the series with respect to which the transformation will be performed.

The summation indices in `summation-indices-list` can take only non negative integer values. As an example, if `{m,n}` is the list of summation indices and `q` is `1` (or `2`), then the analytic continuation is obtained for the series associated with the first (or second) summation index, i.e. `m`. (or `n`). Clearly `q` can take values from `1` to `Length[summation-indices-list]`.

The argument `expression` contains the series whose transformations are looked for. We emphasize that, in order to simplify the implementation of the package, we have built it in such a way that it takes as an input the general term of the series under study (written in terms of Pochhammer symbols). Therefore, the user should not include sums in `expression`. The latter, although not appearing explicitly, are understood to run from 0 to ∞ for each summation index.

The last argument of the `Olsson` command contains some of its possible options, which are

`sum,one,inf,PET1,PET2,PET3,sim,roc`

their default values being `False`. As we will see below, the options `one, PET1, PET2` and `PET3` can be used only if the ${}_2F_1$ series appears as a subseries of the starting point multivariable hypergeometric series. The further detailed description of these options and other useful commands of the package can be found in [52]. To find the analytic continuation of Appell F_2 around $y=\infty$ one first store the expression of the summand of the Appell F_2 in a variable

```
In[1]:= AppellF2 = (Pochhammer[a, m + p] Pochhammer[b1, m] Pochhammer[b2, p]
      x^m y^p)/(Pochhammer[c1, m] Pochhammer[c2, p] m! p!);
```

Now, we call Olsson to find the analytic continuation of F_2 around $(0,\infty)$ as shown below.

[3] The package is publicly available and can be downloaded from the supplementary material provided with the Ref. [52] on arXiv.

```
In[2]:= Olsson[2, {m, p}, AppellF2, inf → True,sim→True] // Expand

Out[2]= (x^m (-y)^(-a - m) y^-p Gamma[-a + b1] Gamma[c1] Pochhammer[a, m + p]
Pochhammer[b,m] Pochhammer[1+ a-c1,m+p])/(m!p!Gamma[b1]Gamma[-a+c1]
Pochhammer[1+a-b1,m+p]Pochhammer[c, m])
 + ((-1)^m x^m (-y)^-b1 y^-p Gamma[a-b1]Gamma[c1] Pochhammer[b,m]
 Pochhammer[b1,p] Pochhammer[1+b1-c1,p])/( m! p! Gamma[a]
 Gamma[-b1 + c1]  Pochhammer[1 - a + b1, -m + p]Pochhammer[c, m])
```

In this way, the package provides a quick and hassle-free implementation of analytic continuation using the method of Olsson. It is to be noted that the package can be used for series with more than two variables as well and has been recently used for the case of Lauricella and Lauricell-Saran series [54]. The only roadblock for a higher number of variables is the problem of finding the domains of convergence, which is a difficult problem even for the three-variable case [45].

5.4 `ROC2.wl` : Region of convergence of hypergeometric series

An important step in finding the analytic continuations of multivariable hypergeometric series is finding the region of convergence (ROC). Formally, Horn's theorem can be used to find the region of convergence of the multivariable hypergeometric series, which for the case of two variables is implemented in the package `ROC2.wl` .[4] Another important property of hypergeometric series is that the ROC is independent of the parameters in the series. Below, we briefly describe it and Horn's theorem.

1). **Cancellation of parameters**: It states that the ROC of a given hypergeometric series is independent of the Pochhammer parameters in the series [45].
As a simple application of the theorem, consider the following Kampé de Fériet function

$$S_1 = \sum_{m,\,n=0}^{\infty} \frac{(a)_{m+n}(b)_m(c)_n(d)_n}{(e)_m(f)_n(g)_n m!\, n!} x^m y^n \,. \tag{58}$$

Using the cancellation of parameters, we know that the ROC is independent of the Pochhammer parameters. We can choose $d = g$ and the two Pochhammer symbols in the numerator and denominator cancel, and the series effectively becomes similar to the Appell F_2 function and thus has the ROC: $|x|+|y|< 1$.
It is important to note that cancellation of parameters is automatically implemented inside the package `ROC2.wl` and used as a precursor before Horn's theorem is used.

2). **Horn's theorem**: Horn's theorem provides a more general way to find the ROC of a given hypergeometric series for any number of variables. The automatized implementation of Horn's theorem for two-variable hypergeometric series is performed in the package `ROC2.wl`. We will explain its working principle with an illustrative example below. Consider the following series

$$S_2 = \sum_{m,\,n=0}^{\infty} \frac{(a)_{m+n}(b)_{m+n}(c)_m}{(d)_{2m+n} m!\, n!} X^m Y^n \,. \tag{59}$$

Writing the above series in a compact form

$$S_2 = \sum_{m,\,n=}^{\infty} A_{m,\,n} X^m Y^n \,. \tag{60}$$

We then evaluate the following two ratios

$$f(m,\,n) = \frac{A_{m+1,\,n}}{A_{m,\,n}} = \frac{(a+m+n)(b+m+n)(c+m)}{(d+2m+n)(d+1+2m+n)(1+m)} \,, \tag{61}$$

[4] The package is publicly available and can be downloaded from the supplementary material provided with the Ref. [52] on arXiv.

$$g(m,\,n)=\frac{A_{m,\,n+1}}{A_{m,\,n}}=\frac{(a+m+n)(b+m+n)}{(d+2m+n)(1+n)}\,. \tag{62}$$

Now, we define two more functions as follows

$$\Phi(\mu,\,\nu)=|\lim_{t\to\infty} f(\mu t,\,\nu t)|^{-1}\,,$$
$$\Psi(\mu,\,\nu)=|\lim_{t\to\infty} g(\mu t,\,\nu t)|^{-1}\,.$$

From this, one can construct following two subsets of $\mathbb{R}^2_+$

$$C=\{(r,\,s)\mid 0<r<\Phi(1,\,0)\wedge 0<s<\Psi(0,\,1)\}\doteq K[\Phi(1,\,0),\,\Psi(0,\,1)]\,, \tag{63}$$

and

$$Z=\left\{(r,\,s)\mid \forall(m,\,n)\in\mathbb{R}^2_+ : 0<r<\Phi(m,\,n)\vee 0<s<\Psi(m,\,n)\right\}. \tag{64}$$

Horn's theorem for two-variable hypergeometric functions is then given as follows:

Theorem 5.1 The union of $Z\cap C$ and its projections upon the coordinate axes is the representation in the absolute quadrant $\mathbb{R}^2_+$ of the region of convergence in $\mathbb{C}^2$ for the series F.

For S_2 we then have

$$C=0<r<4\wedge 0<s<1\,,$$
$$Z=r+s<2s^{1/2}\,.$$

Using Horn's theorem the ROC of the series S_2 is then given by

$$|x|<4\wedge|y|<1\wedge|x|+|y|<2|y|^{1/2}\,. \tag{65}$$

5.4.1 Examples: two-variable case

The detailed algorithm along with the package `ROC2.wl` can be found in Ref. [52]. Here we will give some simple and well known double-variable examples where the package can be used. The main command is `ROC2` which takes the form

```
ROC2[m,n,num_ List,denom_ List,X,Y]
```

where `m` and `n` denote the two summation indices and `X` and `Y` the two variables of the studied double hypergeometric series. The two lists `num_List` and `denom_List` split the characteristic list of the series into two sets corresponding to the Gamma functions appearing in the numerator and in the denominator of the series. For Appell F_2 we can use `ROC2.wl` to find the region of convergence as follows

```
In[3]:= ROC2[m, n, {m, n, m + n}, {m, n}, x, y](*ROC of F2 *)

Out[3]= {"{R,S}, Cartesian Curve, ROC → ", {1,1}, {Abs[x] + Abs[y] == 1},

{Abs[x] < 1 && Abs[y] < 1 && Abs[y] < 1 - Abs[x]}}
```

The `{R,S}` determines the RHS of Eq. (63), the `Cartesian Curve` denotes the boundary of the ROC and the last element of the output above is the ROC as an inequality. The variables of the series may not be `x,y`. The command accepts other variables as well and the substitutions are automatically taken care of. As an example we consider F_2 with variables `x/y,y`:

```
In[4]:= ROC2[m, n, {m, n, m + n}, {m, n}, x/y, y](*ROC of F2 *)

Out[4]= {"{R,S}, Cartesian Curve, ROC → ", {1,1}, {Abs[x/y] + Abs[y] == 1},

{Abs[x/y] < 1 && Abs[y] < 1 && Abs[y] < 1 - Abs[x/y]}}
```

One might note that sometimes the package do not give textbook result for the ROC. For some cases it is possible to further simplify them, for other case it might not be possible, They can thought to be a different way to represent the same region.

6 Hypergeometric functions and Feynman integrals

In this section, we consider the intimate relationship between hypergeometric functions and Feynman Integrals in a variety of settings, with distinct subsections addressing the approaches we have studied.

6.1 Evaluating multiple MB integrals analytically

A general N-fold MB integral can be expressed as

$$I_N = \int_{-i\infty}^{+i\infty} \frac{dz_1}{2\pi i} \cdots \int_{-i\infty}^{+i\infty} \frac{dz_N}{2\pi i}\; x_1^{z_1} \cdots x_N^{z_N}\; \frac{\prod_{i=1}^{k} \Gamma^{a_i}(\mathbf{e}_i \cdot \mathbf{z} + g_i)}{\prod_{j=1}^{l} \Gamma^{b_j}(\mathbf{f}_j \cdot \mathbf{z} + h_j)}\,, \tag{66}$$

where a_i, b_j, k and l are positive integers, $\mathbf{e}_i$, $\mathbf{f}_j$ are N-dimensional coefficient real vectors, $\mathbf{z} = (z_1, ..., z_N)$ and g_i, h_j can be complex numbers. When not specified, the contours of integration are implicitly chosen such that they do not separate the set of poles of each of the numerator Gamma functions into different subsets. This implies that for some cases the contours may not be straight lines parallel to the imaginary axis of the integration variables.

The evaluation of one-fold MB integrals is straightforward and is described in detail in several books such as [55, 56]. However, the multifold case is much more complicated. Therefore, there have been many efforts to develop automated tools for computing MB representations in the context of the Feynman diagram calculations [57]. For instance, the *Mathematica* package `MBsums.m` [58] was created a few years ago for their analytic evaluation, but it is limited to MB integrals with straight contours and the analytic results derived from it are often bulky due to the appearance of spurious terms.

In parallel to the above developments, some mathematicians worked on a non-iterative and rigorous approach to evaluate MB integrals based on the theory of multidimensional residues [59], as detailed in a series of papers [60–62]. However, to the best of our knowledge, they did not explicitly provide the formulas necessary for evaluating N-fold MB integrals when $N > 2$, even in the non-logarithmic (or non-resonant) case.[5] Inspired by their work and with the aim of filling this gap, we developed a new and efficient method based on conic hulls and their intersections [63]. Although not established with the same level of rigor as in previous works [60–62], this method has been tested on many examples, either analytically when results were available in the literature or numerically using sector decomposition [64, 65]. In the following, we will describe this method in more detail, but first, we recall a few general features about MB integrals.

The MB integrals can be divided into two main categories (see Ref. [62] for more details)

- The *degenerate* type, where $\mathbf{\Delta} \doteq \sum a_i \mathbf{e_i} - \sum b_j \mathbf{f_j} = \mathbf{0}$ (see Eq. (66)). In this case, several hypergeometric series solutions of the corresponding MB integral coexist, which are, as a rule, analytic continuations of each other. It is observed that the MB representations of all scalar Feynman integrals fall into this class.
- The *non-degenerate* type, which satisfies $\mathbf{\Delta} \neq \mathbf{0}$. In this case, one or more convergent series representations converge for all values of $x_1 \cdots x_N$. In addition, there will be asymptotic series solutions.

Based on the singularity structure of the MB integrand, they can be further classified into two sub-types:

- The *non-resonant* case: Here, all the poles of the MB integrand are of order one. In the context of Feynman integrals, the MB representation usually falls into this category if the powers of the propagators are generic.

[5] For $N = 2$, the logarithmic case was considered for MB integrals with straight contours in Ref. [12].

– The *resonant* or the *logarithmic* case. Here, some or all poles of the MB integral are of order greater than one. Therefore, residue computation leads to logarithmic solutions. In the context of Feynman integrals, this typically happens when the powers of the propagators are set to integers.

In the following, we describe the conic hull and triangulation methods to compute N-fold MB integrals. Both of these methods can be used to compute MB integrals that fall into any of the above cases.

6.1.1 Brief overview of the conic hull method (non-resonant case)

We briefly outline the main steps of the conic hull in the non-resonant case. For more details on the technical aspects and the resonant case, we refer the reader to Ref. [63].

– *Step 1:* For a given N-fold MB integral, find all possible N-combinations of the numerator Gamma functions and retain only the non-singular ones.
– *Step 2:* Associate a series, which we call a *building block*, with each retained combination.
– *Step 3:* Construct a conic hull for each combination/building block.
– *Step 4:* Find the *largest* intersecting subsets of conic hulls. The sum of the building blocks associated with the conic hulls in each of these subsets yields a series representation of the MB integral.
– *Step 5:* The intersection region of the largest subset of conic hulls is usually a conic hull, which we call the *master conic hull*. Using it, we can derive a master series which considerably simplifies the convergence analysis of the series representation.

To make the method ready-to-use, we have automatized it in a *Mathematica* package called `MBConicHulls.wl` [63].[6] The package also works for the resonant case, which is more complicated because it involves multi-variable residues. Therefore, to handle the resonant case, we have internally used the package `MultivariateResidues.m` [66].

The first version of `MBConicHulls.wl` only worked for MB integrals with non-straight contours separating the poles of the integrand as described above. It has been successfully applied in the computation of various unsolved non-resonant and resonant MB representations of Feynman integrals [67–70]. Subsequently, we focused on the case of arbitrary straight contours of integration (parallel to the imaginary axis in the complex planes of the integration variables) since these integrals frequently appear if one performs an ϵ-expansion of the MB integral using `MB.m` [7] or `MBresolve.m` [8]. We solved the case of straight contours in Ref. [71] and implemented it in a new version of `MBConicHulls.wl`. The solution to this problem relies on the appropriate use of the generalized reflection formula

$$\Gamma(z-n) = \frac{\Gamma(z)\Gamma(1-z)(-1)^n}{\Gamma(n+1-z)}\,, \text{ for } n \in \mathbb{Z}\,, \tag{67}$$

in such a way that the real part of each numerator Gamma function of the MB integrand becomes positive along the integration contours. The conic hull method can then be applied in the same way as it is for non-straight contours.

6.1.2 The triangulation method

Although the conic hull method is very efficient, it is often too slow when dealing with (very) complicated higher-fold MB integrals. In trying to improve the method, we found that regular triangulations of a particular point configuration are dual to the relevant intersections of conic hulls and can thus be used to derive different series representations of a given MB integral [72]. Although the two approaches would yield the same set of series solutions, the great advantage of triangulations is that once automatized, they can provide the results for complicated integrals much faster than conic hulls. We have thus recently upgraded the `MBConicHulls.wl` package such that, in addition to the original analysis based on conic hulls, it offers the possibility of computing MB integrals using triangulations. This is possible by internally using the software `TOPCOM` [73] to perform triangulations. Therefore, one is now able to solve much more complicated MB integrals than before.

[6] The package is available at https://github.com/SumitBanikGit/MBConicHulls.

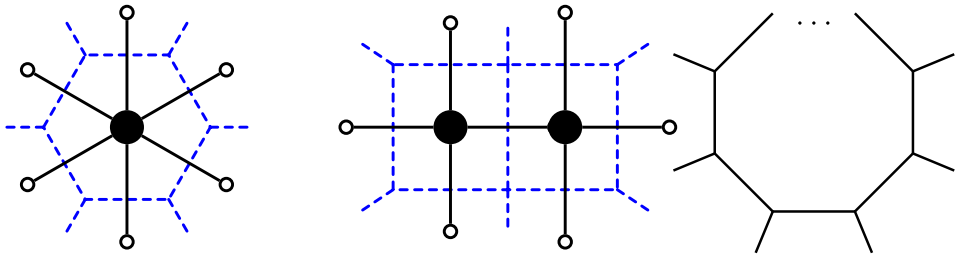

Fig. 3 Some of the one-loop and two-loop Feynman diagrams evaluated using the conic hull and triangulation methods in Table 1

(a) Conformal hexagon (b) Conformal double-box (c) One-Loop N-point Massless

In general, to apply the triangulation method, we need to perform a change of the integration variables to rewrite Eq. (66) in the *canonical form*

$$I_N = \int_{-i\infty}^{+i\infty} \frac{dz_1}{2\pi i} \cdots \int_{-i\infty}^{+i\infty} \frac{dz_N}{2\pi i} \frac{\Gamma(-z_1)\cdots\Gamma(-z_N)\prod_{i=N+1}^{k'} \Gamma^{a'_i}(s'_i(\mathbf{z}))}{\prod_{j=1}^{l} \Gamma^{b'_j}(t'_j(\mathbf{z}))} x_1'^{z_1} \cdots x_N'^{z_N} , \tag{68}$$

where we have pulled out the factors $\Gamma(-z_1)\cdots\Gamma(-z_N)$ in the numerator for convenience. The coefficient vectors s'_i and t'_j are expressed as follows:

$$s'_i(\mathbf{z}) = \sum_{k=1}^{N} e'_{ik} z_k + f'_i , \qquad t'_j(\mathbf{z}) = \sum_{k=1}^{N} g'_{jk} z_k + h'_j . \tag{69}$$

The next step is to construct the point configuration on which we perform triangulations. The configuration has a set of N points[7]

$$P_1 = e'_{l1} , \qquad P_2 = e'_{l2} , \qquad \cdots \qquad P_N = e'_{lN}$$

and $\sum_{i=N+1}^{k'} a'_i$ additional points corresponding to the unit vectors of dimension $\sum_{i=N+1}^{k'} a'_i$. The complete set of these $N + \sum_{i=N+1}^{k'} a'_i$ points is then used for triangulations, performed by calling `TOPCOM` internally from `MBConicHulls.wl`.

We applied the triangulation method to various Feynman integrals with higher-order MB representations. For example, we recomputed the massless conformal double-box and hexagon Feynman diagrams in Fig. 3, originally solved using the conic-hull approach [67]. Thanks to the efficiency of the triangulation approach, we could obtain all possible series representations that the method could offer. Due to this, we could derive new series solutions for both conformal integrals as a sum of 25 hypergeometric series, surpassing the results previously obtained in Ref. [67].

To further test the package, we computed the off-shell one-loop massless N-point Feynman integral in Fig. 3 with generic powers of the propagators and the hard diagram of the two-loop six-edged Wilson loop in [74] in order to gauge the computational power of the triangulation approach. We show in Table 1 the speed comparison of the triangulation and conic hull approaches.

6.2 Feynman integrals as GKZ hypergeometric functions

In Sect. 2.1 of this review, we discussed some widely used parametric representations for Feynman integrals. Another parametric representation, now more commonly known as the Lee-Pomeransky (LP) representation, was obtained in Ref. [75], where the question of determining the number of master integrals for multi-loop Feynman integrals was discussed. Later, in Refs. [76, 77], it was shown for the first time that a generalized version of Feynman integrals in the LP representation could be understood as the solutions to an associated holonomic system of partial differential equations, called a GKZ hypergeometric system [78]. Correspondingly, these solutions are called GKZ hypergeometric functions.

[7] Each of these N points has $\sum_{i=N+1}^{k'} a'_i$ coordinates as we include the possibility of non-unit positive powers of the numerator Gamma functions.

Table 1 Speed comparison of the conic hull and triangulation methods. More details can be found in the Ref. [72]

Feynman integral	MB folds	Total solution number	Conic hull method		Triangulation method	
			One solution	All solutions	One solution	All solutions
Conformal triangle	3	14	0.186 sec.	1.44 sec.	0.205 sec.	0.483 sec.
Massless pentagon	5	70	1.276 sec.	1.25 h.	0.318 sec.	2.78 sec.
Conformal hexagon	9	194160	1 min.	-	0.489 sec.	40 min.
Conformal double-box	9	243186	1.9 min.	-	0.635 sec.	1.8 h.
Hard diagram	8	1471926	6 min.	-	1.4 sec.	-

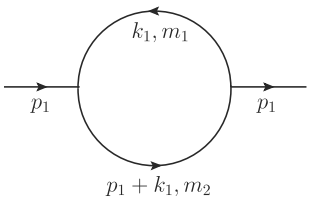

Fig. 4 One-loop bubble Feynman diagram with two unequal masses

To explore the scope of automated computation in the context of Feynman integrals using this newly understood correspondence, a *Mathematica* package called `FeynGKZ`[8] [79] was developed, which allows one to work with the mathematical machinery of GKZ systems to find series solutions to Feynman integrals.

`FeynGKZ` consists of a total of nine user-accessible commands. Six of them are necessary for the basic workflow of the program, namely, deriving the GKZ system for a given Feynman integral and solving the system in terms of hypergeometric series solutions. The remaining three commands provide some additional functionalities that are nice to have for certain cross-check purposes.

The general workflow using `FeynGKZ` consists of the following steps, where we also specify the relevant command for each step. Detailed documentation for each command (including the three secondary commands) can be found in Ref. [79].

1). `FindAMatrix`: Obtains the matrix $\mathcal{A}$ for some given scalar Feynman integral, using either the LP representation or the MB representation.
2). `FindTriangulations`: Computes the unimodular regular triangulations (URT) of the point configuration desctibed by the $\mathcal{A}$-matrix. To do this, `FeynGKZ` internally relies on the software `TOPCOM`.
3). `FindInitialIdeals`: Computes the square free initial ideals of $\mathcal{A}$. To do this, `FeynGKZ` internally calls the `gfanInterface` package from `Macaulay2`.
4). `SeriesRepresentation`: Finds the infinite series solution corresponding to a given URT, or a given square-free initial ideal.
5). `GetClosedForm`: Tries to obtain a closed-form expression for the infinite series solution obtained in the previous step. The *Mathematica* package `Olsson.wl` is used in case of series solutions involving two summation variables.
6). `NumericalSum`: A parallelized numerical-summation module to cross-check the results from `FeynGKZ` with those from other sources numerically. This is particularly useful for series solutions involving more than two summation variables, where a closed-form expression is usually difficult to obtain.

[8] `FeynGKZ` has been made available in the public domain at https://github.com/anant-group/FeynGKZ.

6.2.1 Example: bubble integral with two unequal masses

In the momentum representation, the integral corresponding to the one-loop bubble Feynman diagram with two unequal masses (Fig. 4) is given by

$$I_2(a_1, a_2, \mathrm{D}; p_1^2, m_1^2, m_2^2) = \int \frac{d^{\mathrm{D}}k_1}{i\pi^{\frac{\mathrm{D}}{2}}} \frac{1}{(k_1^2 - m_1^2)^{a_1}((p_1 + k_1)^2 - m_2^2)^{a_2}}\,. \tag{70}$$

`FeynGKZ` is very simple to load in *Mathematica*, once all the paths for the dependencies and for the package have been appropriately specified. It is important to use `FeynGKZ` in a fresh *Mathematica* kernel, after having saved the notebook in some given directory. Loading `FeynGKZ` creates a set of files in the current working *Mathematica* directory, which is by default set to `$UserBaseDirectory`. It is advised to set the current working directory to the one containing the notebook file, by using the command `SetDirectory[NotebookDirectory[]]`.

Once this is done, one can define the two-mass bubble integral of Eq. (70) as follows:

```
In[5]:= MomentumRep = {{k1, m1, a1}, {p1+k1, m2, a2}};
        LoopMomenta = {k1};
        InvariantList = {p1^2 → -s};
        Dim = 4 - 2ϵ;
        Prefactor = 1;
```

Using the external module `FindAMatrix`, the following $\mathcal{A}$-matrix is obtained, with co-dimension equal to 2.

```
In[6]:= FindAMatrixOut = FindAMatrix[{MomentumRep, LoopMomenta,
         InvariantList, Dim, Prefactor}, UseMB → False];

        The Symanzik polynomials → U = x1 + x2
          , F = m1^2 x1^2 + s x1 x2 + m1^2 x1 x2 + m2^2 x1 x2 + m2^2 x2^2
        The Lee-Pomeransky polynomial → G =
          x1 + m1^2 x1^2 + x2 + s x1 x2 + m1^2 x1 x2 + m2^2 x1 x2 + m2^2 x2^2

        The associated 𝒜-matrix → ⎛1 1 1 1 1⎞
                                  ⎜2 1 1 0 0⎟ , which has codim = 2.
                                  ⎝0 1 0 2 1⎠
        Normalized Volume of the associated Newton Polytope → 3
```

After this, the triangulations of the point configuration described by the $\mathcal{A}$-matrix could be obtained using `FindTriangulations`:

```
In[7]:= Triangulations = FindTriangulations[FindAMatrixOut];

        Finding all regular triangulations . . .
        Found 5 Regular Triangulations, out of which 3 are Unimodular
        The 3 Unimodular Regular Triangulations →
        1 :: {{1,2,3}, {2,3,4}, {3,4,5}}
        2 :: {{1,2,3}, {2,3,5}, {2,4,5}}
        3 :: {{1,2,5}, {1,3,5}, {2,4,5}}
```

In the next steps, one can select any of these triangulations to compute the infinite series solutions, by using `SeriesRepresentation`. Let's choose the second triangulation.

```
In[8]:= SeriesSolution = SeriesRepresentation[Triangulations,2];

Unimodular Triangulation → 2
Number of summation variables → 2
Non-generic limit → {z1→m1^2, z2→s+m1^2+m2^2, z3→1,
  z4→m2^2, z5→1}
  The series solution is the sum of following 3 terms.
Term 1 ::
  (((-1)^(-n1-n2) Γ[-2+ϵ+a1-n1-n2] Γ[4-2ϵ-a1-a2+n2]
      Γ[a2+2 n1+n2] (m1^2)^(2-ϵ-a1) (m1^2 m2^2/(s+m1^2+m2^2)^2)^n1 (m1^2/(s+m1^2+m2^2))^n2
      (s+m1^2+m2^2)^(-a2)) / (Γ[a1] Γ[4-2ϵ-a1-a2] Γ[a2]
      Γ[1+n1] Γ[1+n2]))
Term 2 ::
  (((-1)^(-n1-n2) Γ[-2+ϵ+a2-n1-n2] Γ[4-2ϵ-a1-a2+n2]
      Γ[a1+2 n1+n2] (m2^2)^(2-ϵ-a2) (m1^2 m2^2/(s+m1^2+m2^2)^2)^n1 (m2^2/(s+m1^2+m2^2))^n2
      (s+m1^2+m2^2)^(-a1)) / (Γ[a1] Γ[4-2ϵ-a1-a2] Gamma[a2]
      Γ[1+n1] Γ[1+n2]))
Term 3 ::
  (((-1)^(-n1-n2) Γ[2-ϵ-a2+n1-n2] Γ[2-ϵ-a1-n1+n2]
      Γ[-2+ϵ+a1+a2+n1+n2] (m1^2/(s+m1^2+m2^2))^n1 (m2^2/(s+m1^2+m2^2))^n2
      (s+m1^2+m2^2)^(2-ϵ-a1-a2)) / (Γ[a1] Γ[4-2ϵ-a1-a2]
      Γ[a2] Γ[1+n1] Γ[1+n2]))
```

Finally, we obtain the closed form expressions using `Olsson.wl` :

```
In[9]:= GetClosedForm[SeriesSolution];

Closed form found with Olsson!
Term 1 ::
1/Γ[a1] Γ[-2+ϵ+a1]
  H3[a2, 4-2ϵ-a1-a2, 3-ϵ-a1, m1^2 m2^2/(s+m1^2+m2^2)^2, m1^2/(s+m1^2+m2^2)]
  (m1^2)^(2-ϵ-a1) (s+m1^2+m2^2)^(-a2)
Term 2 ::
1/Γ[a2] Γ[-2+ϵ+a2]
  H3[a1, 4-2ϵ-a1-a2, 3-ϵ-a2, m1^2 m2^2/(s+m1^2+m2^2)^2, m2^2/(s+m1^2+m2^2)]
  (m2^2)^(2-ϵ-a2) (s+m1^2+m2^2)^(-a1)
Term 3 ::
((G1[-2+ϵ+a1+a2, 2-ϵ-a1, 2-ϵ-a2, -m2^2/(s+m1^2+m2^2),
  -m1^2/(s+m1^2+m2^2)] Γ[2-ϵ-a1] Γ[2-ϵ-a2]
  Γ[-2+ϵ+a1+a2] (s+m1^2+m2^2)^(2-ϵ-a1-a2)) / (Γ[a1]
  Γ[4-2ϵ-a1-a2] Γ[a2]))
```

6.3 The ϵ-expansion of multi-variable hypergeometric functions

As discussed in the previous section, Feynman integrals can be expressed in terms of multi-variable hypergeometric functions where the dimensional regulator parameter $\epsilon = (4 - \mathrm{D})/2$ appears in the Pochhammer parameters and the ratio of scales involved in the Feynman integral appear as the arguments. The result of the Feynman integrals is usually expressed as a series in the parameter ϵ. Thus, the resulting hypergeometric functions must be expanded around its Pochhammer parameters. In this section, we discuss one algorithm to do so.

Following Ref. [80], we summarize the steps of the algorithm below.

- *Step 1*: To determine if $F(\epsilon)$ is Taylor or Laurent series expandable, check the Pochhammer parameters of its series representation.
- *Step 2*: If the expansion of the function $F(\epsilon)$ is of Taylor type, find the series expansion of $F(\epsilon)$. The Taylor expansion can be found by taking successive derivatives of the function with respect to ϵ

$$F(\epsilon) = \sum_{i=0}^{\infty} \frac{1}{i!} \frac{d^i F}{d\epsilon^i}\bigg|_{\epsilon=0} .$$

  In this approach, we get a higher summation fold hypergeometric series appearing in the series coefficients which are not suitable for numerical evaluation. To express the series coefficients of well studied and much simpler function MPLs, we first find the PDE associated with the given hypergeometric function and bring it to the Pfaff system. Next, the Pfaff system is brought to the canonical form [81, 82] and solved order by order in ϵ with suitable boundary conditions.
- *Step 3*: If the series expansion is of Laurent type, find a secondary function, say $G(\epsilon)$ that can be related to $F(\epsilon)$ by a differential operator $H(\epsilon)$ as

$$F(\epsilon) = H(\epsilon) \bullet G(\epsilon) , \tag{71}$$

  and $G(\epsilon)$ can be expanded in Taylor series following *Step 2*. Here, the symbol $\bullet$ means the action of the differential operator $H(\epsilon)$ on the function $G(\epsilon)$.
- *Step 4*: Find the corresponding differential operator $H(\epsilon)$
- *Step 5*: Perform the series expansion of the operator $H(\epsilon)$ and apply it on the Taylor expansion of $G(\epsilon)$ and collect different powers of ϵ

This algorithm is implemented in the *Mathematica* based package `MultiHypExp.wl` [83] which is presently capable of expanding certain one, two and three-variable hypergeometric functions about integer-valued parameters. For the case of Appell F_4, the expansion is performed by using the transformation formulae of F_4 to F_1 or F_2, which impose restrictions on the parameters of F_4. To find the expansion of F_4 for general cases, a transformation of variables has to be performed which we discuss below.

It is well-known that the Appell $F_4(x, y)$ (defined in Eq. (42)) satisfies the following partial differential system

$$\begin{aligned}
&\big[(c_1 - x(a+b+1))\partial_x - (y(a+b+1))\partial_y - ab - (2xy)\partial_x\partial_y - ((x-1)x)\partial_x^2 - y^2\partial_y^2\big] \bullet F_4(x, y) = 0\,,\\
&\big[(c_2 - y(a+b+1))\partial_y - (x(a+b+1))\partial_x - ab - (2xy)\partial_x\partial_y - ((y-1)y)\partial_y^2 - x^2\partial_x^2\big] \bullet F_4(x, y) = 0\,.
\end{aligned}$$

Using the column vector

$$G = (1,\, x\partial_x,\, y\partial_y,\, xy\partial_x\partial_y) \bullet F_4\,.$$

The PDE can be brought to the Pfaffian system. However, the connection matrices are complicated. The Pfaffian system of F_4 is studied in mathematics literature [84, 85]. Following Ref. [84], we perform a transformation of variables

$$\phi : (x_1, y_1) \to (x, y) = (x_1 y_1,\, (x_1 - 1)(y_1 - 1))\,, \tag{72}$$

such that the connection matrix becomes the sum of constant matrices times logarithmic 1-forms. Now, it can be brought to the canonical form by using `CANONICA`.

Following the prescription described above, we find the expansion of $F_4(\epsilon, \epsilon, 1+2\epsilon, 1-\epsilon; x, y)$ in terms of GPL as

$$F_4(\epsilon, \epsilon, 1+2\epsilon, 1-\epsilon; x, y) = 1 + \left(\frac{\pi^2}{6} - G(0, x_1)G(1, y_1) - G(0, 1, y_1) - G(1, 0, x_1)\right)\epsilon^2 + \mathcal{O}(\epsilon^3)\,, \tag{73}$$

where G's are the MPLs and variables

$$\begin{aligned}
x_1 &= \frac{1}{2}\Big(\sqrt{(-x+y-1)^2 - 4x} + x - y + 1\Big),\\
y_1 &= \frac{1}{2}\Big(-\sqrt{(-x+y-1)^2 - 4x} + x - y + 1\Big)\,.
\end{aligned}$$

We also note that the expansion of hypergeometric functions around half-integer valued parameters, whose series coefficients can be expressed in terms of generalized polylogarithms, also requires a transformation of variables.

6.4 Algebraic relations for products of propagators

Feynman integrals play an important role in precision calculations in quantum field theory. There are various methods to evaluate them [86, 87] as has been discussed in previous sections. Even with all these methods and their advancements, it is at times still challenging to compute Feynman integrals. More often, other techniques are used in conjunction to facilitate their computation. In this section, we consider the formalism first proposed by Tarasov to derive algebraic relations for the product of propagators for functional reduction [88]. However, for the ease of automation of the method, a slightly modified algorithm was developed in Ref. [89], inspired by the original work and a realization for the same was provided as a *Mathematica* package called `AlgRel.wl` .[9] The package was used to simplify and analyze many important and interesting Feynman integrals that are amenable to treatment using the formalism. These relations reduce the original integral into a sum of integrals that are easier to evaluate. The focus of the section is to find a new way to obtain functional relations by deriving the algebraic relations for the product of propagators. This method, in turn then leaves some undetermined free parameters which can be chosen at will. Appropriate choices of these parameters result in various functional equations for Feynman integrals [90–94]. We now discuss in detail the method, the formalism used for the automation process, its relation with the existing method and finally its usage in uncovering various previously unknown relations amongst hypergeometric functions.

[9] The package and an example notebook are publicly available at https://github.com/TanayPathak-17/Algebraic-relation-for-the-product-of-propagators.

6.4.1 The method

To provide a brief explanation of the working of the method, we consider the integral corresponding to the one-loop bubble diagram with two unequal masses, as shown in Fig. 4. We will explain how the method can be used to find the algebraic relations of the product of propagators for this one-loop integral, explain how it leads to the reduction of complexity of this integral and finally discuss the implications of these relations in deriving new relations and reduction formulae for hypergeometric functions. Finally, we will develop a recursive strategy to use the method for cases when there are more than 2 propagators and also for certain cases of multi-loop integrals.

In this subsection, we discuss a very special case in which our propagator indices are unity for the one-loop bubble diagram with two different masses given in Eq. (70). For notational convenience, we make the following redefinition of variables compared to Sect. 6.2.1:

$$k_1 \to k, \tag{74}$$

$$p_1 \to p \tag{75}$$

$$I_2(p^2, m_1^2, m_2^2) \equiv I_2(a_1 = 1, a_2 = 1, \mathrm{D}; p_1^2, m_1^2, m_2^2) = \int \frac{d^{\mathrm{D}}k}{i\pi^{\frac{\mathrm{D}}{2}}} \frac{1}{(k^2 - m_1^2)((k+p)^2 - m_2^2)}\,. \tag{76}$$

To find the algebraic relation for the product of propagators, we instead consider a more general propagator, depending on only one loop momentum, of the following form

$$d_i = (k + q_i)^2 - m_i^2\,, \tag{77}$$

where k is the loop-momentum, q_i's are dependent on external momenta and can be zero as well and m_i is the mass of the propagator.

With the general propagators, we now have

$$I_2((q_1 - q_2)^2, m_1, m_2) = \int \frac{d^{\mathrm{D}}k}{d_1 d_2}\,, \tag{78}$$

where substituting: $q_1 = 0$ and $q_2 = p$, we recover Eq. (76).

We seek the algebraic relation for the integrand, by introducing a new denominator D_1 along with coefficients x_1 and x_2, of the following form

$$\frac{1}{d_1 d_2} = \frac{x_1}{D_1 d_1} + \frac{x_2}{D_1 d_2}\,, \tag{79}$$

where $D_i = (k + P_i)^2 - M_i^2$ is defined similar to Eq. (77).

The unknowns introduced can be fixed using the above equation, while the remaining parameters are arbitrary and can be fixed at will in such a way that the resulting relationship gives rise to integrals that are easier to compute.

Using Eq. (79), we get

$$D_1 = x_1 d_2 + x_2 d_1\,. \tag{80}$$

Comparing the coefficients of k^2, k and the remaining k independent term we get

$$\begin{aligned} &x_1 + x_2 = 1\,,\\ &x_1\mathbf{q_2} + x_2\mathbf{q_1} = \mathbf{P_1}\,,\\ &\quad - M_1^2 + P_1^2 - (-m_2^2 + q_2^2)x_1 - (-m_1^2 + q_1^2)x_2 = 0\,. \end{aligned} \tag{81}$$

Solving for x_1, x_2 and $\mathbf{P_1}$, we get following two sets of solutions

$$x_1 = \frac{D_1 + m_1^2 - m_2^2 + q_1^2 + q_2^2 - 2q_1q_2}{2(q_1 - q_2)^2}\,, \tag{82}$$

$$x_2 = \frac{-D_1 - m_1^2 + m_2^2 + q_1^2 + q_2^2 - 2q_1q_2}{2(q_1 - q_2)^2}\,, \tag{83}$$

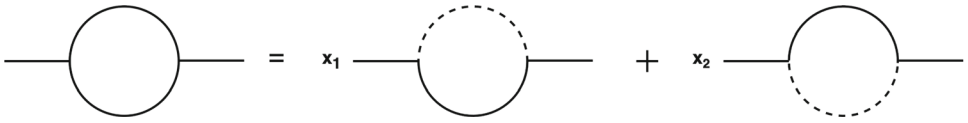

Fig. 5 Diagrammatic representation of Eq. (88)

$$\mathbf{P_1} = \mathbf{q_2} + \frac{(\mathbf{q_1} - \mathbf{q_2})\left(-D_1 - m_1^2 + m_2^2 + q_1^2 + q_2^2 - 2q_1q_2\right)}{2(q_1 - q_2)^2}\,, \tag{84}$$

with $D_1 = \sqrt{\left(m_1^2 - m_2^2 + (q_1 - q_2)^2\right)^2 - 4(q_1 - q_2)^2(m_1^2 - M_1^2)}$ and

$$x_1 = \frac{-D_1 + m_1^2 - m_2^2 + q_1^2 + q_2^2 - 2q_1q_2}{2(q_1 - q_2)^2}\,, \tag{85}$$

$$x_2 = \frac{D_1 - m_1^2 + m_2^2 + q_1^2 + q_2^2 - 2q_1q_2}{2(q_1 - q_2)^2}\,, \tag{86}$$

$$\mathbf{P_1} = \mathbf{q_2} + \frac{(\mathbf{q_1} - \mathbf{q_2})(D_1 - m_1^2 + m_2^2 + q_1^2 + q_2^2 - 2q_1q_2)}{2(q_1 - q_2)^2}\,. \tag{87}$$

We remark that both of the above sets can be used for the purpose of finding the algebraic relation. However, for convenience, we would use the set given by Eq. (82). For the algebraic relations, both of the choices are equivalent. One can use either of the solutions and check that it satisfies the algebraic relation that we seek to find. In the above equation, M_1 is still an arbitrary variable that can be chosen at will. Choosing various values of M_1 results in different functional equations [95] for the bubble integral. For the present work, we focus on one of the simple choices, i.e., $M_1 = 0$. Integrating Eq. (79) and substituting $q_1 = 0$ and $q_2 = p$ we have

$$I_2(p^2, m_1, m_2) = x_1 I_2((P_1 - p)^2, 0, m_2) + x_2 I_2(P_1^2, m_1, 0)\,. \tag{88}$$

Hence, we see that the general two-point bubble integral with non-zero masses can be written in terms of two integrals with just one mass. Diagrammatically, Eq. (88) can be represented as in Fig. 5.

To see how the complexity in the computation has been reduced in the Eq. (88), we refer to a few analytic results. The general result for the massive bubble diagram can be written in terms of the Appell F_4 function [96].

$$\begin{aligned} I_2(p, m_1, m_2) = {} & \frac{(m_2^2)^{\frac{\mathrm{D}}{2}-2}\Gamma(\frac{\mathrm{D}}{2}-1)\Gamma(2-\frac{\mathrm{D}}{2})}{\Gamma(\frac{\mathrm{D}}{2})} F_4\Big(2-\frac{\mathrm{D}}{2}, 1; \frac{\mathrm{D}}{2}, 2-\frac{\mathrm{D}}{2}; \frac{p^2}{m_2^2}, \frac{m_1^2}{m_2^2}\Big) \\ & + \frac{(m_1^2)^{\frac{\mathrm{D}}{2}-1}\Gamma(1-\frac{\mathrm{D}}{2})}{m_2^2} F_4\Big(\frac{\mathrm{D}}{2}, 1; \frac{\mathrm{D}}{2}, \frac{\mathrm{D}}{2}; \frac{p^2}{m_2^2}, \frac{m_1^2}{m_2^2}\Big)\,, \end{aligned} \tag{89}$$

where,

$$F_4(a, b, c, d, x, y) = \sum_{m,n=0}^{\infty} \frac{(a)_{m+n}(b)_{m+n}}{(c)_m(d)_n m!\, n!} x^m y^n\,, \tag{90}$$

is the Appell F_4 hypergeometric series with the region of convergence (ROC) given by $\sqrt{|x|} + \sqrt{|y|} < 1$.

The analytic expression result for $I_2(p, m, 0)$, in D-dimension, is given by

$$I_2^{(\mathrm{D})}(p^2; m^2, 0) = -\Gamma\left(1 - \frac{\mathrm{D}}{2}\right) m_2^{d-4}\, {}_2F_1\left[\begin{matrix} 1, 2 - \frac{\mathrm{D}}{2}; \\ \frac{\mathrm{D}}{2}; \end{matrix} \frac{p^2}{m^2}\right], \tag{91}$$

is readily available in Refs. [97, 98]. Using the above relation in Eq. (88), we get the following for the right-hand side

$$- \frac{m_1^{\mathrm{D}-4}\Gamma\left(1 - \frac{\mathrm{D}}{2}\right)\left(\sqrt{(-m_1^2 + m_2^2 + p^2)^2 - 4m_1^2p^2} + m_1^2 - m_2^2 + p^2\right)}{2p^2}$$

$$\times\ {}_2F_1\left[\begin{matrix}1,\ 2-\frac{\mathrm{D}}{2};\\ \frac{\mathrm{D}}{2};\end{matrix}\frac{\left(p^2+m_1^2-m_2^2+\sqrt{(p^2+m_1^2-m_2^2)^2-4p^2m_1^2}\right)^2}{4p^2m_1^2}\right]$$
$$-\frac{m_2^{\mathrm{D}-4}\Gamma\left(1-\frac{\mathrm{D}}{2}\right)}{2p^2}(m_1^2-m_2^2+p^2+\sqrt{(-m_1^2+m_2^2+p^2)^2-4m_1^2p^2})$$
$$\times\ {}_2F_1\left[\begin{matrix}1,\ 2-\frac{\mathrm{D}}{2};\\ \frac{\mathrm{D}}{2};\end{matrix}\frac{\left(-p^2+m_1^2-m_2^2+\sqrt{(p^2-m_1^2+m_2^2)^2-4p^2m_1^2}\right)^2}{4p^2m_2^2}\right]. \tag{92}$$

The above relation can be viewed as a reduction formula without making reference to the underlying Feynman integral. In a similar manner, the evaluation of other Feynman integrals can be used to obtain the relationship between hypergeometric functions [99]. Such a reduction of hypergeometric functions with a higher number of variables to those with a lesser number of variables also helps when the analytic continuation has to be done to reach a certain kinematical region. For the case of Appell F_4, the elaborate analytic continuation has been performed explicitly in Ref. [100] or using automated algorithms [52] for more general multi-variable hypergeometric functions. This whole process still does not guarantee convergence for all the values of the parameter space [101]. While for the case of ${}_2F_1$ complete table of analytic continuations is available [102]. The procedure to find the analytic continuations also gets more complicated with the increase in the number of variables, even with the use of automated packages, thus such a reduction is desirable.

The above algorithm can be generalized for the case when we have N denominators, to find an algebraic relation recursively. For this general situation, it is important to notice that all the denominators are assumed to be functions of the same loop momenta. Consider the general situation with product of N denominators as $\frac{1}{d_1\cdots d_N}$. This step is the same as used for the bubble integral.

1). We first find the algebraic relation by taking d_1 and d_2

$$\frac{1}{d_1d_2}=\frac{x_1}{D_1d_1}+\frac{x_2}{D_1d_2}. \tag{93}$$

2). We then multiply the above equation by $\frac{1}{d_3}$

$$\frac{1}{d_1d_2d_3}=\frac{x_1}{D_1d_1d_3}+\frac{x_2}{D_1d_2d_3}. \tag{94}$$

3). We then find the algebraic relation of each pair of d_is again using Eq. (93).
4). Then, in the resulting relation, we repeat this process until all the denominators are exhausted.

For the special case when there are N products of propagators with the same loop momenta, then the final result is a sum of 2^{N-1} terms.

It is to be noted that the above procedure is a slight modification of the original method [88]. In Ref. [88], we start by seeking the following algebraic relation for the product of N propagators

$$\frac{1}{d_1\cdots d_N}=\frac{x_1}{D_1d_1\cdots d_{N-1}}+\cdots+\frac{x_N}{d_2\cdots d_ND_1}. \tag{95}$$

Comparing the coefficients of k^2, k, and using the constant term, we get an over-determined set of equations. Such a system leave x_3, $x_4\cdots x_N$ undetermined. Such a procedure, when used recursively with each term on the RHS of the above equation, finally results in $N!$ total number of terms, unlike 2^{N-1} terms using the procedure presented here. It is also important to note that the arbitrariness in the choice of coefficients x_is in the original Tarasov's algorithm is now present in the choice of parameters M_is.

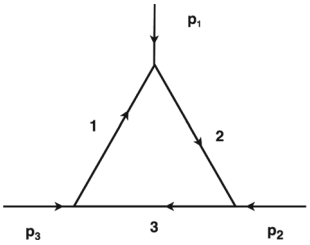

Fig. 6 Triangle diagram

6.4.2 Example: one-loop vertex integral

As an application of the package `AlgRel.wl` , we consider the reduction of the one-loop vertex integral corresponding to Fig. 6, which is given by

$$I_3 = \int \frac{d^{\mathrm{D}}k}{(k^2-m_1^2)((k+p_1)^2-m_2^2)((k+p_1+p_2)^2-m_3^2)}\,, \tag{96}$$

We proceed as described in the previous section and use the generalized propagators as well as do the substitutions accordingly, such that the result reduces to Eq. (96). This can be done using the following command

```
In[10]:= AlgRel[{1,2,3},{k,q,m},{P,M},x,{q[1]→0,q[2]→p1,q[3]→p1+p2}]
```

The result of the above code is a sum of 4 terms given as follows

$$\begin{aligned}&\frac{x_2x_5}{(k+P_1)^2(k+P_3)^2((k+p_1)^2-m_2^2)}+\frac{x_2x_6}{(k+P_1)^2(k+P_3)^2((k+p_1+p_2)^2-m_3^2)}\\&+\frac{x_1x_3}{(k^2-m_1^2)(k+P_1)^2(k+P_2)^2}+\frac{x_1x_4}{(k+P_1)^2(k+P_2)^2((k+p_1+p_2)^2-m_3^2)},\end{aligned} \tag{97}$$

where

$$\begin{aligned}
x_1 &= \frac{\sqrt{(m_1^2-m_2^2+p_1^2)^2-4m_1^2p_1^2}+m_1^2-m_2^2+p_1^2}{2p_1^2},\\
x_2 &= \frac{-\sqrt{(m_1^2-m_2^2+p_1^2)^2-4m_1^2p_1^2}-m_1^2+m_2^2+p_1^2}{2p_1^2},\\
\mathbf{P_1} &= \mathbf{P_1}-\frac{\mathbf{P_1}\left(-\sqrt{\left(m_1^2-m_2^2+p_1^2\right)^2-4m_1^2p_1^2}-m_1^2+m_2^2+p_1^2\right)}{2p_1^2},\\
x_3 &= \frac{\sqrt{(m_1^2-m_3^2+(-p_1-p_2)^2)^2-4m_1^2(-p_1-p_2)^2}+m_1^2-m_3^2+(p_1+p_2)^2}{2(-p_1-p_2)^2},\\
x_4 &= \frac{-\sqrt{(m_1^2-m_3^2+(-p_1-p_2)^2)^2-4m_1^2(-p_1-p_2)^2}-m_1^2+m_3^2+(p_1+p_2)^2}{2(-p_1-p_2)^2},\\
\mathbf{P_2} &= \frac{(-\mathbf{p_1}-\mathbf{p_2})\left(-\sqrt{\left(m_1^2-m_3^2+(p_1+p_2)^2\right)^2-4m_1^2(p_1+p_2)^2}-m_1^2+m_3^2+(p_1+p_2)^2\right)}{2(p_1+p_2)^2}\\
&\quad+(\mathbf{p_1}+\mathbf{p_2}),\\
x_5 &= \frac{\sqrt{(m_2^2-m_3^2+p_2^2)^2-4m_2^2p_2^2}+m_2^2-m_3^2+p_1^2+(p_1+p_2)^2-2p_1(p_1+p_2)}{2p_2^2},\\
x_6 &= \frac{-\sqrt{(m_2^2-m_3^2+p_2^2)^2-4m_2^2p_2^2}-m_2^2+m_3^2+p_1^2+(p_1+p_2)^2-2p_1(p_1+p_2)}{2p_2^2},
\end{aligned}$$

$$\mathbf{P_3} = (\mathbf{p_1} + \mathbf{p_2}) - \frac{\mathbf{P_2}\left(-\sqrt{-2(m_2^2+m_3^2)p_2^2 + (m_2^2-m_3^2)^2 + p_2^4} - m_2^2 + m_3^2 + p_2^2\right)}{2p_2^2}\,.$$

Integrating Eq. (97) over loop momenta k results in a vertex integral that can be written as a sum of vertex integrals but with just one massive propagator. For the detailed numerical check of the above obtained relation, we refer to Ref. [89] for further details.

7 Recent aplications

In this section, we present recent applications of the Mellin–Barnes technique to the analytical evaluation of Feynman diagrams. These examples can now be studied with the `MBConicHulls` and `MultiHypExp` packages.

7.1 The conformal double-box and triangle integrals

We follow in our computations the notational conventions of Ref. [103], where the six-point off-shell massless double-box with generic propagator powers is written, in dual momentum space, as

$$I_{3,3} = \int \frac{\mathrm{d}^{\mathrm{D}}x_0 \mathrm{d}^{\mathrm{D}}x_{0'}}{x_{10}^{2a}x_{20}^{2b}x_{30}^{2c}x_{00'}^{2\ell}x_{40'}^{2d}x_{50'}^{2e}x_{60'}^{2f}} = V_{3,3}\phi_{3,3}\,, \tag{98}$$

with $\phi_{3,3}$ a conformal invariant function of nine cross ratios (u_i, $i = 1, ..., 9$) and $V_{3,3}$ is the prefactor

$$V_{3,3} = x_{13}^{2\ell-\mathrm{D}}x_{14}^{\mathrm{D}-2\ell}x_{15}^{-2d-2e}x_{16}^{2d+2e-2a}x_{26}^{-2b}x_{36}^{\mathrm{D}-2c-2\ell}x_{46}^{2\ell-2d-\mathrm{D}}x_{56}^{2d}\,. \tag{99}$$

The dual conformal Feynman parameter representation of the double-box is given in [103], where

$$\phi_{3,3}(u_1, ..., u_9, \mathrm{D}) = Q_{3,3}\int_0^\infty \mathrm{d}\beta_2\mathrm{d}\beta_3\mathrm{d}\beta_4\mathrm{d}\beta_5 \frac{\beta_2^{b-1}\beta_3^{c-1}\beta_4^{d-1}\beta_5^{e-1}}{X_2^{\mathrm{D}/2-\ell}Y^{\mathrm{D}/2-f}Z_4^f}\,, \tag{100}$$

with

$$Q_{3,3} = \frac{\pi^{\mathrm{D}}\Gamma(\mathrm{D}/2-\ell)\Gamma(\mathrm{D}/2-f)}{\Gamma(a)\Gamma(b)\Gamma(c)\Gamma(l)\Gamma(d)\Gamma(e)}, \tag{101}$$

$$X_2 = \beta_2u_6u_9 + \beta_3u_9 + \beta_2\beta_3u_1u_2u_3u_9, \tag{102}$$

$$Y = u_8X_2 + \beta_4u_9 + \beta_2\beta_4u_2u_3u_9 + \beta_3\beta_4u_2u_3u_4u_5u_9 + \beta_5 + \beta_2\beta_5u_3 + \beta_3\beta_5u_3u_5 + \beta_4\beta_5u_3u_5u_7, \tag{103}$$

and

$$Z_4 = 1 + \beta_2 + \beta_3 + \beta_4 + \beta_5\,. \tag{104}$$

In the above expressions, $x_{ij}^\mu = x_i^\mu - x_j^\mu$ and the momenta are related to their duals by $p_j^\mu = x_j^\mu - x_{j+1}^\mu$. Note that the conformal constraints are $a + b + c + \ell = \mathrm{D}$ and $d + e + f + \ell = \mathrm{D}$.

A similar analysis yields the hexagon integral given by [103]

$$I_6 = \int \frac{\mathrm{d}^{\mathrm{D}}x_0}{x_{10}^{2a}x_{20}^{2b}x_{30}^{2c}x_{40}^{2d}x_{50}^{2e}x_{60}^{2f}} = V_6\phi_6\,, \tag{105}$$

where

$$\phi_6(u_1, ..., u_9, \mathrm{D}) = Q_6\int_0^\infty \mathrm{d}\beta_2\mathrm{d}\beta_3\mathrm{d}\beta_4\mathrm{d}\beta_5 \frac{\beta_2^{b-1}\beta_3^{c-1}\beta_4^{d-1}\beta_5^{e-1}}{Y^{\mathrm{D}/2-f}Z_4^f}\,, \tag{106}$$

with

$$Q_6 = \frac{\pi^{\mathrm{D}/2}\Gamma(\mathrm{D}/2-f)}{\Gamma(a)\Gamma(b)\Gamma(c)\Gamma(d)\Gamma(e)}\,. \tag{107}$$

and $V_6 = x_{15}^{2f-\mathrm{D}} x_{16}^{\mathrm{D}-2a-2f} x_{26}^{-2b} x_{36}^{-2c} x_{46}^{-2d} x_{56}^{\mathrm{D}-2e-2f}$.

In this case, the conformal constraint is $a+b+c+d+e+f = \mathrm{D}$. It is straightforward to derive the MB representations of the double-box and hexagon from the Feynman parameterizations given in Eqs (100) and (106), which can be written as

$$\begin{aligned}\phi_{3,3} = &\frac{Q_{3,3}\, u_8^{\mathrm{D}/2-\ell}}{\Gamma(\mathrm{D}/2-f)\Gamma(f)}\frac{1}{(2i\pi)^9}\int_{-i\infty}^{+i\infty}\mathrm{d}z_1 ... \int_{-i\infty}^{+i\infty}\mathrm{d}z_9 \Pi_{i=1}^{9}(w_i^{z_i}\Gamma(-z_i))\\
&\times\Gamma(d+z_3+...+z_6)\Gamma(-b-c-d-e+\mathrm{D}-\ell-z_1-z_2-z_3-z_5-z_6-z_8)\\
&\times\Gamma(\mathrm{D}-f-\ell+z_1+...+z_9)\Gamma(b+z_1+z_5+z_8+z_9)\Gamma(c+z_2+z_6+z_7+z_8)\\
&\times\Gamma(e+f+\ell-\mathrm{D}-z_4-...-z_9)\times\frac{\Gamma(\ell-\mathrm{D}/2-z_7-z_8-z_9)}{\Gamma(-z_7-z_8-z_9)}\,,\end{aligned} \tag{108}$$

and

$$\begin{aligned}\phi_6 = &\frac{Q_6}{\Gamma(\mathrm{D}/2-f)\Gamma(f)}\frac{1}{(2i\pi)^9}\int_{-i\infty}^{+i\infty}\mathrm{d}z_1 ... \int_{-i\infty}^{+i\infty}\mathrm{d}z_9 \Pi_{i=1}^{9}(w_i^{z_i}\Gamma(-z_i))\\
&\times\Gamma(\mathrm{D}/2-f+z_1+...+z_9)\Gamma(c+z_2+z_6+z_7+z_8)\Gamma(d+z_3+...+z_6)\\
&\times\Gamma(b+z_1+z_5+z_8+z_9)\Gamma(e+f-\mathrm{D}/2-z_4-...-z_9)\\
&\times\Gamma(-b-c-d-e+\mathrm{D}/2-z_1-z_2-z_3-z_5-z_6-z_8)\end{aligned} \tag{109}$$

where w_i are combinations of the u_i (see Eq. (A20) in Ref. [103]).

The two integrals in Eqs. (108) and (109) belong to a class of MB integrals for which several series representations of the latter coexist, converging in various regions. We solve these MB integrals using `MBConicHulls` to get the following series solution for the double-box integral

$$\begin{aligned}\phi_{3,3} = &\frac{Q_{3,3}\, u_8^{\mathrm{D}/2-\ell}}{\Gamma(\mathrm{D}/2-f)\Gamma(f)}(\mathcal{D}_1+\mathcal{D}_4+\mathcal{D}_{10}+\mathcal{D}_{18}+\mathcal{D}_{27}+\mathcal{D}_{45}+\mathcal{D}_{76}+\mathcal{D}_{140}+\mathcal{D}_{158}\\
&+\mathcal{D}_{190}+\mathcal{D}_{208}+\mathcal{D}_{318}+\mathcal{D}_{340}+\mathcal{D}_{440}+\mathcal{D}_{542}+\mathcal{D}_{674}+\mathcal{D}_{1063}+\mathcal{D}_{1091}+\mathcal{D}_{1435}\\
&+\mathcal{D}_{1581}+\mathcal{D}_{1646}+\mathcal{D}_{2382}+\mathcal{D}_{3047}+\mathcal{D}_{3068}+\mathcal{D}_{3786}+\mathcal{D}_{4580}+\mathcal{D}_5+\mathcal{D}_{19}+\mathcal{D}_{28}\\
&+\mathcal{D}_{142}+\mathcal{D}_{210}+\mathcal{D}_{826}+\mathcal{D}_{926}+\mathcal{D}_{942}+\mathcal{D}_{988}+\mathcal{D}_{1094}+\mathcal{D}_{1112}+\mathcal{D}_{1330}+\mathcal{D}_{1449}\\
&+\mathcal{D}_{1647}+\mathcal{D}_{2436}+\mathcal{D}_{3069}+\mathcal{D}_{3806}+\mathcal{D}_{46})\,,\end{aligned} \tag{110}$$

where the $\mathcal{D}_i$ are hypergeometric series, where the subscript corresponds to their ranking in the obtained list of 4834 series in Ref. [67][10] that are used to constitute the different series representations of the double box. Their analytic expressions are long and interested readers can find them in Ref. [67]. While for the hexagon integral, we obtain

$$\begin{aligned}\phi_6 = &\frac{Q_6}{\Gamma(\mathrm{D}/2-f)\Gamma(f)}(\mathcal{H}_1+\mathcal{H}_4+\mathcal{H}_9+\mathcal{H}_{15}+\mathcal{H}_{22}+\mathcal{H}_{35}+\mathcal{H}_{58}+\mathcal{H}_{94}+\mathcal{H}_{103}\\
&+\mathcal{H}_{123}+\mathcal{H}_{133}+\mathcal{H}_{199}+\mathcal{H}_{210}+\mathcal{H}_{270}+\mathcal{H}_{331}+\mathcal{H}_{409}+\mathcal{H}_{637}+\mathcal{H}_{653}\\
&+\mathcal{H}_{838}+\mathcal{H}_{925}+\mathcal{H}_{960}+\mathcal{H}_{1375}+\mathcal{H}_{1664}+\mathcal{H}_{1675}+\mathcal{H}_{2062}+\mathcal{H}_{2442})\,,\end{aligned} \tag{111}$$

where $\mathcal{H}_i$ corresponds to i^{th}[11] series among 2530 series obtained in Ref. [67] that are used to constitute the different series representations of the hexagon integrals. More details about these series can be found in Ref. [67].

To validate our results, we first compared the series solution with direct numerical integration and found excellent agreement. Additionally, we verified that the series solutions for the double-box and hexagon satisfy the known

[10] We have slightly changed the notation to $\mathcal{D}_i$ to avoid confusion with the propagator used in previous sections.

[11] We have slightly changed the notation to $\mathcal{H}_i$ to avoid confusion with the Horn functions.

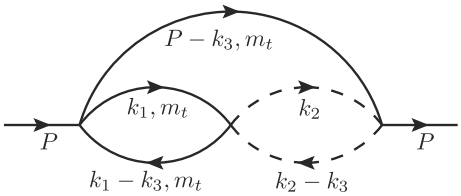

Fig. 7 The master integral $I_{110011001000}$ from Ref. [70]; $P^2 = m_t^2$

differential equation

$$\partial_{u_8}\phi_{3,3}(u_1, \ldots, u_9, \mathrm{D}) = -\frac{\pi^{\mathrm{D}/2-1}}{\Gamma(l)}\,\phi_6(u_1, \ldots, u_9, \mathrm{D}+2)\,, \tag{112}$$

when $\mathrm{D}/2 - l = 1$, which holds both at the level of Feynman parameterizations and MB representations.

7.2 The ϵ-expansion of hypergeometric functions with non-integer parameters using `MultiHypExp`

In this section, we demonstrate a non-trivial use of an in-house version of the `MultiHypExp` package, suitable for expansion of hypergeometric functions around half-integer valued parameters, by considering the master integral $I_{110011001000}$ (sector 307) from Table 1 in Ref. [70], shown in Fig. 7. After obtaining 1-fold series solutions to this master integral through the MB representation, using `AMBRE` and `MBConicHulls.wl`, we find the following result

$$\begin{aligned} I_{110011001000} = &-\left(m_t^2\right)^{1-3\epsilon}\frac{\Gamma(1-2\epsilon)\Gamma(1-\epsilon)^2\Gamma(\epsilon)\Gamma(2\epsilon)^2\Gamma(3\epsilon-1)}{\Gamma(2-2\epsilon)\Gamma(2-\epsilon)\Gamma(4\epsilon)} \\ &\times {}_3F_2\left(\frac{1}{2}, 1, 3\epsilon-1; 2-\epsilon, 2\epsilon+\frac{1}{2}; 1\right) \\ &-\left(m_t^2\right)^{1-3\epsilon}\frac{\Gamma(3-4\epsilon)\Gamma(1-\epsilon)^2\Gamma(\epsilon)^2\Gamma(2\epsilon-1)}{\Gamma(3-3\epsilon)\Gamma(2-2\epsilon)} \\ &\times {}_3F_2\left(1, \frac{3}{2}-2\epsilon, \epsilon; \frac{3}{2}, 3-3\epsilon; 1\right), \end{aligned} \tag{113}$$

which needs to be expanded in the dimensional regularization parameter ϵ till transcendental weight 11.

We start with the hypergeometric function in the first term in the RHS of Eq. (113):

$${}_3F_2\left(\frac{1}{2}, 1, 3\epsilon-1; 2-\epsilon, 2\epsilon+\frac{1}{2}; 1\right). \tag{114}$$

Unlike the Gauss ${}_2F_1$, there does not exist any formula of ${}_3F_2(...;z)$ at $z=1$ in terms of Gamma functions. We expand the above ${}_3F_2(...;z)$ with argument z instead of 1 and take the limit $z \to 1$ at the end. So, the relevant function to be expanded is given by

$${}_3F_2\left(\frac{1}{2}, 1, 3\epsilon-1; 2-\epsilon, 2\epsilon+\frac{1}{2}; z\right). \tag{115}$$

The limit $z \to 1$ can be performed in the coefficients of the series expansion of the ${}_3F_2(...;z)$.

By observing the Pochhammer parameters, we can infer that the expansion of the above function is of Taylor series. Furthermore, we use the relation

$${}_3F_2\left(\frac{1}{2}, 1, 3\epsilon-1; 2-\epsilon, 2\epsilon+\frac{1}{2}; z\right) = H(\epsilon) \bullet {}_3F_2\left(\frac{1}{2}, 1, 3\epsilon; 1-\epsilon, 2\epsilon+\frac{1}{2}; z\right).$$

The reason is that the ${}_3F_2$ appearing on the right-hand side of the relation is much simpler to expand.

The differential operator $H(\epsilon)$ can be obtained using Takayama's algorithm [104], and found to be

$$H(\epsilon) = A\partial_z^2 + B\partial_z + C\,,$$

with

$$A = -\frac{(\epsilon-1)(z-1)\big(2\epsilon^2((z-30)z+9)+\epsilon(z(3z+14)-9)+(z+1)^2\big)}{4(1-2\epsilon)^2(\epsilon+1)(2\epsilon+1)(4\epsilon-1)},$$
$$B = -\frac{(\epsilon-1)}{8(1-2\epsilon)^2(\epsilon+1)(2\epsilon+1)(4\epsilon-1)z}\quad[5\epsilon+z\big(5z^2+z+11\big)-8\epsilon^3(z(53z-42)+9)$$
$$+2\epsilon^2(z(z(5z-61)-17)+9)+\epsilon z(3z(5z+29)-59)-1],$$
$$C = -\frac{(\epsilon-1)\big(27\epsilon(1-2\epsilon)+(\epsilon+1)(2\epsilon+1)z^2-2(8\epsilon-1)(\epsilon(2\epsilon(8\epsilon+11)-7)-1)z-3\big)}{8(1-2\epsilon)^2(\epsilon+1)(2\epsilon+1)(4\epsilon-1)z},$$

Let us now focus on the expansion of the following ${}_3F_2$

$$f := {}_3F_2\left(\frac{1}{2},\,1,\,3\epsilon;1-\epsilon,\,2\epsilon+\frac{1}{2};z\right).$$

It is well-known that ${}_3F_2$ satisfies a third-order ordinary differential equation, which can be brought to the Pfaffian system

$$dF = \Omega F,$$

where $F=(f,\,z\partial_z f,\,z^2\partial_z^2 f)^T$ and Ω is a differential 1-form

$$\Omega = \Omega_1\frac{\mathrm{d}z}{z}+\Omega_2\frac{d(z-1)}{z-1},$$

with

$$\Omega_1=\begin{pmatrix}0 & 1 & 0\\ 0 & 1 & 1\\ 0 & \frac{1}{2}\big(4\epsilon^2-3\epsilon-1\big) & \frac{1}{2}(-2\epsilon-1)\end{pmatrix},\qquad \Omega_2=\begin{pmatrix}0 & 0 & 0\\ 0 & 0 & 0\\ -\frac{1}{2}(3\epsilon) & \frac{1}{2}\big(-4\epsilon^2-12\epsilon-5\big) & -2(\epsilon+1)\end{pmatrix}.$$

Next, to bring the Pfaffian system to the canonical form using `CANONICA` [105], we perform a change of variable $z=x^2$ and obtain

$$\Omega\to\Omega'=\Omega_1'\frac{\mathrm{d}x}{x}+\Omega_2'\frac{d(x-1)}{x-1}+\Omega_3'\frac{d(x+1)}{x+1},$$

with

$$\Omega_1'=\begin{pmatrix}0 & 2 & 0\\ 0 & 2 & 2\\ 0 & (\epsilon-1)(4\epsilon+1) & -2\epsilon-1\end{pmatrix},\qquad \Omega_2'=\begin{pmatrix}0 & 0 & 0\\ 0 & 0 & 0\\ -\frac{1}{2}(3\epsilon) & -\frac{1}{2}(2\epsilon+1)(2\epsilon+5) & -2(\epsilon+1)\end{pmatrix},$$
$$\Omega_3'=\begin{pmatrix}0 & 0 & 0\\ 0 & 0 & 0\\ -\frac{1}{2}(3\epsilon) & -\frac{1}{2}(2\epsilon+1)(2\epsilon+5) & -2(\epsilon+1)\end{pmatrix}.$$

Now, it can be brought to the canonical form by a fibre change (obtained using the `CANONICA`),

$$T=\begin{pmatrix}1 & 0 & 0\\ -3\epsilon & \frac{\epsilon}{x-1} & \frac{\epsilon}{x+1}\\ \frac{3\epsilon\left(\epsilon+(3\epsilon+1)x^2-1\right)}{x^2-1} & -\frac{\epsilon\left(2(\epsilon-1)+(6\epsilon+3)x^2-4\epsilon x+x\right)}{2(x-1)^2(x+1)} & \frac{\epsilon\left(-3x^2-2\epsilon(x(3x+2)+1)+x+2\right)}{2(x-1)(x+1)^2}\end{pmatrix},$$

and the canonical form looks as follows, $F=T\tilde{F}$

$$d\tilde{F}=\epsilon\tilde{\Omega}\tilde{F},$$

with

$$\tilde{\Omega} = \begin{pmatrix} -\frac{6}{x} & \frac{2}{x-1} - \frac{2}{x} & \frac{2}{x} - \frac{2}{x+1} \\ \frac{12}{x} & \frac{2}{x} - \frac{2}{x-1} & \frac{6}{x+1} - \frac{6}{x} \\ -\frac{12}{x} & \frac{6}{x-1} - \frac{6}{x} & \frac{2}{x} - \frac{2}{x+1} \end{pmatrix} \mathrm{d}x\,.$$

The boundary condition can be easily found as

$$F(z=0) = (1,\,0,\,0)^T\,.$$

Note that the point $z = 0$ mapped to $x = 0$, thus, the boundary condition in terms of the basis $\tilde{F}$ is given by

$$\tilde{F}(x=0) = (T^{-1}F)\big|_{x=0} = \left(1, -\frac{3}{2}, \frac{3}{2}\right)^T,$$

which is true for all orders in ϵ. So, we find the solutions of $\tilde{F}$ as

$$\begin{aligned}\tilde{F} = \left(1, -\frac{3}{2}, \frac{3}{2}\right)^T &+ \epsilon\Big(-3G(-1,\,x) - 3G(1,\,x),\, 9G(-1,\,x) + 3G(1,\,x) \\ &- 3G(-1,\,x) - 9G(1,\,x)\Big)^T + \epsilon^2\Big(6G(-1,\,-1,\,x) + 18G(-1,\,1,\,x) \\ &- 6G(0,\,-1,\,x) - 6G(0,\,1,\,x) + 18G(1,\,-1,\,x) + 6G(1,\,1,\,x), \\ &- 18G(-1,\,-1,\,x) - 54G(-1,\,1,\,x) + 24G(0,\,1,\,x) - 18G(1,\,-1,\,x) \\ &- 6G(1,\,1,\,x) + 6G(-1,\,-1,\,x) + 18G(-1,\,1,\,x) - 24G(0,\,-1,\,x) \\ &+ 54G(1,\,-1,\,x) + 18G(1,\,1,\,x)\Big)^T + \mathcal{O}(\epsilon^3)\,. \end{aligned} \tag{116}$$

Performing the inverse change of variable $x \to \sqrt{z}$, applying the operator $H(\epsilon)$ and setting the limit $z \to 1$, we find the expansion of Eq. (114) as

$$\begin{aligned}{}_3F_2\Big(\frac{1}{2},\,1,\,3\epsilon-1;2-\epsilon,\,2\epsilon+\frac{1}{2};1\Big) = \frac{1}{2} + \frac{5}{2}\epsilon + (9 - 24\log(2))\epsilon^2 \\ + \big(2\big(\pi^2 + 16 + 48\log^2(2) - 48\log(2)\big)\big)\epsilon^3 + \mathcal{O}(\epsilon^4)\,, \end{aligned} \tag{117}$$

which matches with the result from `HypExp` [106].

In a similar manner, the other ${}_3F_2$ that appears in the RHS of Eq. (113) can be expanded:

$$\begin{aligned}{}_3F_2\left(1,\,\frac{3}{2}-2\epsilon,\,\epsilon;\frac{3}{2},\,3-3\epsilon;1\right) = 1 + \frac{\epsilon}{2} + [16\log(2) - 11]\epsilon^2 \\ + 4\big[\pi^2 - 23 - 16\log^2(2) + 30\log(2)\big]\epsilon^3 + \mathcal{O}(\epsilon^4)\,. \end{aligned} \tag{118}$$

Thus, we obtain the expansion of the integral in the parameter ϵ as,

$$I_{110011001000} = \left(m_t^2\right)^{1-3\epsilon} e^{-3\gamma_E\epsilon}\left[\frac{2}{3}\frac{1}{\epsilon^3} + \frac{10}{3}\frac{1}{\epsilon^2} + \left(\frac{26}{3} + \frac{\pi^2}{2}\right)\frac{1}{\epsilon} + \left(\frac{14\zeta(3)}{3} + \frac{9\pi^2}{2} + 2\right) + \mathcal{O}(\epsilon)\right], \tag{119}$$

which matches with the numerical result from `AMFlow` [107].

7.3 Sunsets in ChPT and three-loop QED corrections to charged lepton $(g-2)_l$

The low-energy interactions of pions, kaons, and η-mesons can be described by ChPT [108, 109]. One can also use the $SU(3)$ version of it, which allows the parameters of these mesons, such as masses and decay constants, to be written in terms of the bare parameters of the ChPT Lagrangian when calculated at higher loops. Such higher loop calculations get complicated due to multiple scales present in the Feynman diagrams. These limitations can

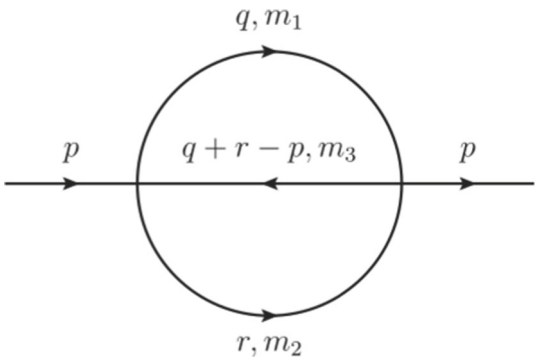

Fig. 8 The two-loop self-energy sunset diagram

sometimes restrict the results to be expressed either in numerical or semi-analytical way [110], and the full analytic structure remains hidden.

The MB technique has been found very useful to evaluate many such multiscale Feynman diagrams at two loops analytically. One of such classes of Feynman diagrams is the sunset topology presented in Fig. 8. The results of these diagrams are evaluated in terms of the masses of pseudoscalar mesons, and one can also study the analytic continuation for different values of input parameters. The generality of this method also allows one to explore the examples beyond ChPT, and some of the three-loop contributions to charged lepton $(g-2)_l$ with two internal loops have been explored in Ref. [111]. Interestingly, the new results obtained are expressed in the closed form, and we outline some details in the rest of the subsection.

The QED contributions to the anomalous magnetic moment of the charged leptons can be expressed perturbatively as

$$a_l^{\rm QED} = A_{1,l} + A_{2,l}\left(\frac{m_l}{m_{l'}}\right) + A_{2,l}\left(\frac{m_l}{m_{l''}}\right) + A_{3,l}\left(\frac{m_l}{m_{l'}}, \frac{m_l}{m_{l''}}\right), \tag{120}$$

with

$$A_{i,l} = A_{i,l}^{(2)}\left(\frac{\alpha}{\pi}\right) + A_{i,l}^{(4)}\left(\frac{\alpha}{\pi}\right)^2 + A_{i,l}^{(6)}\left(\frac{\alpha}{\pi}\right)^3 + \cdots, \tag{121}$$

where α is fine structure constant, $A_{i,l}^{(2n)}$ is the sum of the $n^{\rm th}$ loop contributions with $A_{2,l}^{(2)} = A_{3,l}^{(2)} = A_{3,l}^{(4)} = 0$ and dots represent higher-order corrections in α. The status of various terms in Eq. (121) can be found in Ref. [111]. Here, we focus our attention only to three-loop coefficient $A_3^{(6)}\left(\frac{m_1}{m_2}, \frac{m_1}{m_3}\right)$ which corresponds to Feynman diagram presented in Fig. 9.

In contrast to all other three loop QED contributions to the $a_l^{\rm QED}$, $A_{3,\mu}^{(6)}(m_\mu/m_\tau, m_\mu/m_e)$ is the only one whose exact analytic form has not been derived so far, as pointed out in Ref. [112]. In [113], the first few terms of a series expansion in powers and logarithms of the mass ratios, using large-momentum, heavy mass, and eikonal expansions techniques, were obtained which are later confirmed and extended in Ref. [114]. However, the missing analytical expression in terms of generalized hypergeometric and Kampé de Fériet double hypergeometric series has recently

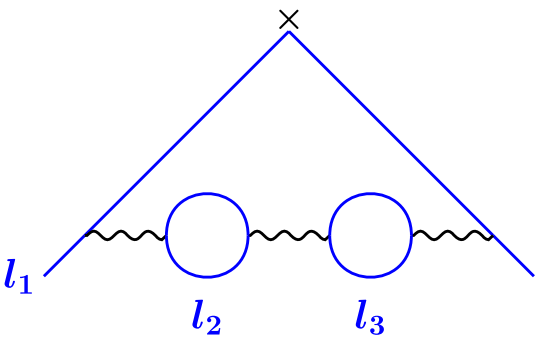

Fig. 9 The 3-loop QED Feynman diagram corresponding to $A_3^{(6)}(m_1/m_2, m_1/m_3)$

been obtained in Ref. [111] using the MB technique. Defining $r_1 \equiv m_{l_1}^2/m_{l_2}^2$, $r_2 \equiv m_{l_1}^2/m_{l_3}^2$, $A_{3,e}^{(6)}(m_e/m_\tau, m_e/m_\mu)$ can be written as:

$$A_{3,l}^{(6)}(\sqrt{r_1}, \sqrt{r_2}) = \frac{\sqrt{\pi}}{8} \int\limits_{\gamma+i\mathbf{R}^2} \frac{ds}{2i\pi} \wedge \frac{dt}{2i\pi}\, r_1^{-s}\, r_2^{-t}\;\; \Gamma(s)\Gamma(-s)\Gamma(t)\Gamma(-t)\Gamma(2-s)\Gamma(2-t) \times \frac{\Gamma\left(\frac{1}{2}-s-t\right)\Gamma(1-s-t)\Gamma(2+s+t)}{\Gamma\left(\frac{5}{2}-s\right)\Gamma\left(\frac{5}{2}-t\right)\Gamma(3-s-t)}, \tag{122}$$

where $\gamma \equiv (\mathrm{Re}(s), \mathrm{Re}(t)) \in]-1, 0[\times]-1, 0[$ (see the yellow region in Fig. 10a).

The symmetry properties of the MB integral in Eq. (122) under the exchange of r_1 and r_2 (or s and t) that arises from the symmetry of the Feynman diagram under the exchange of l_2 and l_3, is also reflected in the singular structure of the integrand (see Fig. 10a) as well as the convergence regions of the series representations in the first quadrant of the (r_1, r_2)-plane (see Fig. 10b).

It is easy to find the different sets of residues (cones) associated with each convergent series, and a detailed procedure can be found in Ref. [12], which, in passing, can now be replaced by the automated one presented in Sect. 6.1. There are six such cones, plotted in Fig. 11 and, due to symmetry properties, the series representations associated to only three of them have to be computed (the blue cones), the others (coming from the red cones) being derived from the latter by exchanging r_1 and r_2 in the final results. Final exact expressions are rather long, so we refer to Ref. [111] where one can also find the analytic continuation into different regions.

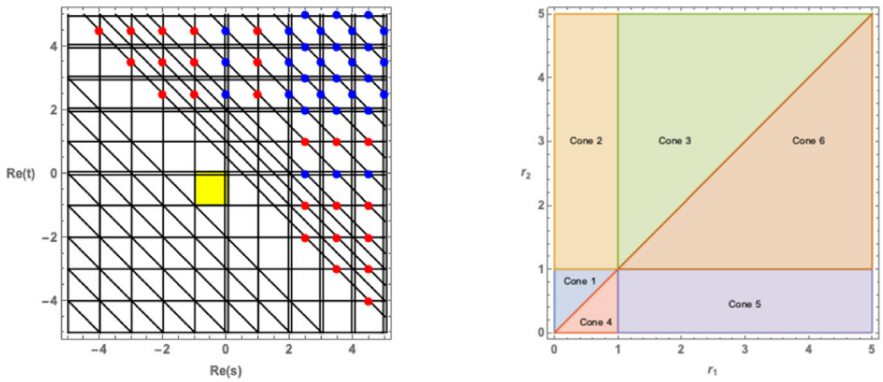

Fig. 10 Visualization of analytic features in the Mellin-Barnes representation of Eq. (122)

(a) Singular structure of the integrand of Eq. (122). Red dots mark cancelled singularities; blue dots show reduced-order singularities due to factors in the denominator.

(b) Convergence regions of the series representations of Eq. (122), labeled by their associated cones.

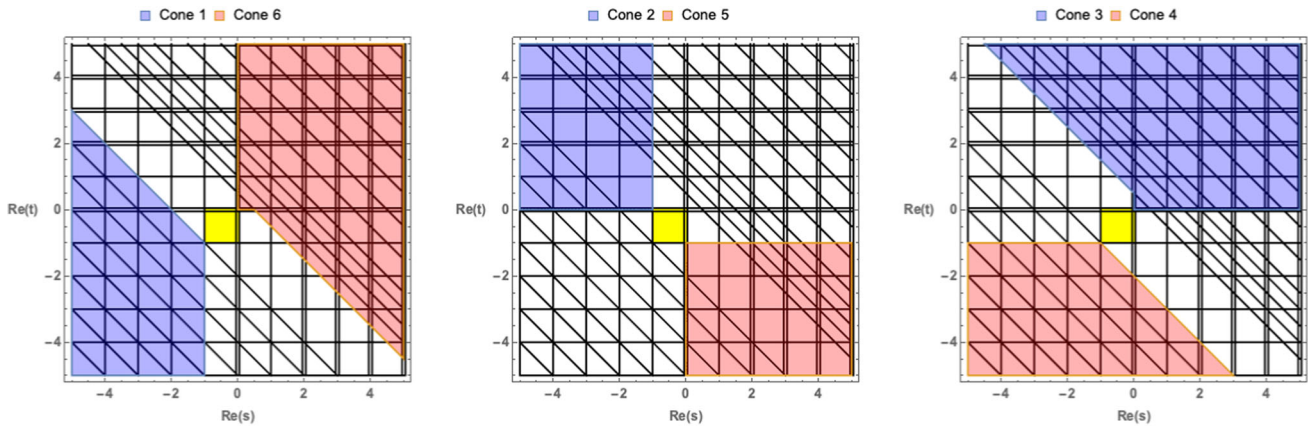

Fig. 11 The cones associated to the MB integral of Eq. (122)

We now present our final prediction $A_{3,l}^{(6)}$ for the charged leptons using the CODATA 2018 lepton mass ratios values [115]:

$$\frac{m_\mu}{m_e} = 206.7682830(46)\,,\ \frac{m_\mu}{m_\tau} = 5.94635(40)\times 10^{-2}\,,$$
$$\frac{m_e}{m_\mu} = 4.83633169(11)\times 10^{-3}\,,\ \frac{m_e}{m_\tau} = 2.87585(19)\times 10^{-4}\,,$$

and results in the following values:

$$A_{3,\mu}^{(6)} = 5.27737(71)\times 10^{-4}\,,$$
$$A_{3,\tau}^{(6)} = 3.34778(17)\,,$$
$$A_{3,e}^{(6)} = 1.90972(25)\times 10^{-13}\,.$$

8 Leading logarithms of the two-point function in simple massless models

In Sects. 8 and 9, we turn to other important investigations carried out in the framework of quantum field theory, which are a parallel stream of investigations carried out by us. These are, of course, indirectly related to higher loop results, but express themselves in terms of renormalization group analysis, another cornerstone of particle physics and field theory research.

In this section, we briefly review some results in a class of massless models that were obtained in Ref. [116]. This presentation follows closely that paper. An in-depth introduction to the subject may be found in, see e.g. Ref. [117]. We recall that (large) logarithms arise in radiative loop calculations and often modify substantially tree-level results. In renormalizable theories, these so-called leading logs (those with the lowest power of the coupling constants in the theory) can be conveniently summed up by renormalization group techniques combined with a simple one-loop calculation. Indeed, this often leads to large corrections and a substantial reduction of the (artificial) scale dependence. Similarly, next-to-leading logarithms can be treated in a similar way based on two-loop calculations, and similarly for higher loop orders. In this way, theoretical predictions have reached impressive accuracy, and some of the discussion for QCD can be found in the next section.

However, the situation in non-renormalizable theories is not so well explored. But such theories are increasingly important, because of the need and use of effective theories which are seen as low-energy approximations to a full renormalizable 'true' theory. Weinberg, in a prophetic work [118], showed that the leading logarithms at two-loop level could be obtained by a one-loop calculation, see also Ref. [119, 120]. Since then, several papers (see Ref. [116]) indicate that in various models the leading logarithms could be summed up, by using the general principles of analyticity and unitarity which impose surprisingly strong constraints. Extending these works, we have, for massless $O(N)$ models, obtained the leading logarithms of the scalar two-point function to arbitrary orders; and the partial waves and form factors and two-point functions for $SU(N)$ models. More details can be found in the publication [116] supplemented with the *Mathematica* codes.

The scalar and vector form factors are important quantities in many applications of field theory. They are defined as the matrix elements of the scalar (vector) current between two (physical) one-particle states $\phi(p)$, namely the lowest mass states, such as the pions in QCD after the symmetry breaking from which we adopt as the name for all the theories considered here

$$\langle \phi^a(p_f)|-j_0^s|\phi^a(p_i)\rangle = F_S(s)\,, \tag{123}$$

and

$$\langle \phi^a(p_f)|j_{V,\mu}^c|\phi^b(p_i)\rangle = \langle T^c(T^bT^a - T^aT^b)\rangle (p_f+p_i)_\mu F_V(s)\,, \tag{124}$$

respectively. Here, $s=(p_f-p_i)^2$ and T^a are the algebra generators of the particle representation with a, b, c as the group indices. The leading log expansion for these quantities is given by [121]

$$F_{S,V}(s) = \sum_{n=0}^{\infty} f_n^{S,V}\hat{S}(s)^n \log^n\left(-\frac{\mu^2}{s}\right), \tag{125}$$

where the $f_n^{S,V}$ are coefficients of the leading logs and $\hat{S}(s) = \frac{s}{(4\pi F)^2}$ is a dimensionless quantity with F being the tree-level pion decay constant. Unitarity and analyticity dictate that the discontinuity of the scalar and vector form factors satisfy

$$\text{disc } F_S(s) = 2\, i\, t_0^0(s) F_S^*(s)\,, \tag{126}$$

and

$$\text{disc } F_V(s) = 2\, i\, t_1^1(s) F_V^*(s)\,, \tag{127}$$

respectively, where $t_l^I(s)$ is the partial wave amplitude of $\pi\pi$ scattering, and

$$t_l^I(s) = \frac{\pi}{2} \sum_{n=1}^{\infty} \omega_{nl}^I \frac{\hat{S}(s)^n}{2l+1} \log^{n-1}\left(\frac{\mu^2}{s}\right) + \mathcal{O}(\text{NLL})\,, \tag{128}$$

where ω_{nl}^I are the leading log coefficients of the pion-pion scattering amplitudes. The index I of t_l^I enumerates the irreducible representations in the expansion of $(R \times R)$, where R is the representation of the scattered particle. In the case of $O(N)$ models, the pions belong to the defining (or vector) representation and thus the product $(R \times R)$ has three entries. In terms of isospin components of $O(4)/O(3)$, they correspond to the isospin of the produced system equal to 0, 1, and 2, respectively. For $SU(N)$ models, the pions belong to the adjoint representation, and the product $(R \times R)$ contains 7 irreducible representations, $I = 1, \ldots, 7$ [122].

The scalar two-point function between two scalar currents in both $O(N)$ and $SU(N)$ is of special interest in ChPT. In the chiral limit of the $O(4)/O(3)$ model, two-point function is defined by

$$H(s = p^2) = i \int \mathrm{d}x\; e^{ipx} \langle 0 | T j_0^s(x) j_0^s(0) | 0 \rangle,\,. \tag{129}$$

A leading log expansion for the current correlator in Eq. (129) is given by

$$H(s) = \frac{B^2}{16\pi^2} \sum_{n=0}^{\infty} p_n \hat{S}(s)^n \log^n\left(-\frac{\mu^2}{s}\right), \tag{130}$$

where p_n is the leading log coefficient at order n, and B is related to the quark condensate. In analogy to the expression given in for $O(3)$ and $SU(2)$ the discontinuity across its cut is given by

$$\text{disc}(H(s)) = \frac{i\,M}{16\pi} |F_S(s)|^2\,, \tag{131}$$

where the M is an overall multiplicative factor denoting the number of Goldstone bosons arising from the sum over intermediate states. Therefore, for $O(N+1)/O(N)$ models, it is given by given by N. For the $SU(N) \times SU(N)/SU(N)$ models, $M = N^2 - 1$.

The coefficients of the leading log expansion of the scalar and vector form factors are given as recursion relations that depend on the partial wave decomposition of the crossing matrix Ω_p^{li} which are solved to provide expressions for $f_n^{S,V}$ in terms of the leading log coefficients of the $\pi - \pi$ scattering amplitudes ω_{nl}^I.

For the scalar form factor, this solution reads

$$f_n^S(N) = \frac{1}{2(n-1)} \sum_{i=1}^{n-1} \omega_{i0}^{I=0} f_{n-i}^S(N)\,, \tag{132}$$

and for the vector form factor, we get

$$f_n^V(N) = \frac{1}{6(n-1)} \sum_{i=1}^{n-1} \omega_{i0}^{I=1} f_{n-i}^V(N), \tag{133}$$

where $f_1^S(N) = f_1^V(N) = 1$, and n denotes the loop order.

Using a similar approach, we obtain for the leading log coefficients of the scalar correlator:

$$p_n(N) = \frac{M}{2(n-1)} \sum_{i=1}^{n-1} f_i^S f_{n-i}^S \,, \tag{134}$$

which is one of the principal results of the Ref. [116].

Using a recursion relation, the coefficients of the form factor expansion are obtained as:

$$f_n^{S,V} = \frac{1}{n} \sum_{m=0}^{n-1} \sum_{\substack{j=0 \\ j \text{ even}}}^{n-m} \Gamma_{S,V}^{(n-m,j)} f_m^{S,V} \omega_{(n-m-1)j} \,, \tag{135}$$

where

$$\Gamma_S^{(p,l)} = \frac{N}{2} \delta_{l0} + \Omega_p^{l0} \,, \tag{136}$$

and

$$\Gamma_V^{(p,l)} = \frac{1}{3} \Omega_p^{l1} \,, \tag{137}$$

with

$$\omega_{nl} = (\omega_{nl}^0 - \omega_{nl}^2)/N \,. \tag{138}$$

The functions $\Omega_p^{ll'}$ are the components of the crossing matrix ($s \leftrightarrow t$) for the amplitude in the partial wave basis. The values for coefficients $f_n^{S,V}$ are given in Table 1 of Ref. [116] for the scalar form factor. Those values are reproduced by solving Eq. (132) with its initial condition $f_1^S = 1$. Solving the recursion relation of Eq. (133) produces the same set of values of the expansion coefficients as using the correct $\Gamma_V^{(p,l)}$ in Eq. (135) does.

Using the values of f_n^S generated from Eq. (132), and Eq. (134), the coefficients of the leading log expansion of the scalar current $H(s)$ are obtained and given in Table 1 of Ref. [116]. Also, the values of p_n for both general $O(N+1)/O(N)$ and for $O(4)/O(3)$, upto 7-loop order are given. They are a generalization to arbitrary loop order n, and arbitrary group dimension N.

For $SU(N)$ models, the two-particle scattering amplitude is given by two functions of the Mandelstam variables, which parameterize independent group structures. The leading log coefficients for these functions are denoted in the following as ω_{nl} and v_{nl}. They could be decomposed into seven irreducible representations, ω_{nl}^I. Those corresponding to $I = 1$ and 5 are special in that their $S-$ and $P-$ waves enter the discontinuity equations for the scalar and vector form factors, respectively. For the case of $N = 2$, the seven amplitudes collapse to three and have a direct correspondence with those of the $O(N)$ model. In the massless theory, the amplitudes that correspond to B and C are the charges denoted by ω and v. Recall that in the $O(N)$ model there is a single charge, and it has a closed evolution equation. In contrast, the charges in the $SU(N)$ theory have a coupled system of closed evolution equations. Furthermore, in the large N limit, there is an essential simplification. From the evolution equations for arbitrary N for the ω and v, one can obtain corresponding solutions for the ω^I which wires in the full crossing matrices for the seven amplitudes, as well as for all the waves that enter a particular order. It is this system that is solved and used by us in our computations, both for the ω, which are then inserted into the relations for the expansion coefficients for the scalar and vector form factors and eventually for the two-point function. The equations for the charges can be used directly in the direct formula Eq. (140) to obtain the vector form factor in general as well as in the large N limit.

An expression for the vector form factor in $SU(N)$, analogous to Eq. (135) in Ref. [116] and which is based on a recursion relation is

$$\Gamma_V^{(p,l)} = \frac{1}{3} \Omega_p^{l1} \,, \tag{139}$$

$$f_n^V = \frac{1}{n}\sum_{m=0}^{n-1}\sum_{\substack{j=0\\ j\in \text{ even}}}^{n-m} \Gamma_V^{(n-m,\,j)} f_{m+1}^V\left(\frac{N}{2}\omega_{n-m-1,\,j} + 2v_{n-m-1,\,j}\right), \tag{140}$$

where $f_0^V = 1$ and $n = 0, 1, 2, 3, \cdots$. We see that this recursion formula generates the entries given in Table 4 of Ref. [116] for f_n^V.

In the large-N limit, the full set of coupled RG equations is replaced by a simpler one, $\omega_{nl}^{\text{large-}N}$. This leads to a simpler set of equations for f_n^V which produce the correct coefficient for the highest power of N as found from Eq. (140). For completeness, Eq. (140) is replaced by the following:

$$f_n^{V\,\text{large-}N} = \frac{1}{n}\sum_{m=0}^{n-1}\sum_{\substack{j=0\\ j\ \text{even}}}^{n-m} \Gamma_V^{(n-m,\,j)} f_{m+1}^V \frac{N}{2}\omega_{n-m-1,\,j}^{\text{large-}N}. \tag{141}$$

The expansion coefficients in Eq. (140) for the $S-$wave of the scalar and the $P-$wave of the vector form factors are given in Tables 2 and 3 of [116] for both general $SU(N)$ and $SU(2)$ models up to 7-loop order. These quantities are inserted into the unitarity, which then yields the scalar and vector form factors to the same order and are listed in Table 4 of Ref. [116]. In the *Mathematica* notebooks provided with Ref. [116], we perform consistency checks by putting $N = 2$ and compare them with the corresponding results for the orthogonal models with $N = 3$. In Ref. [121], f_n^S and f_n^V are listed for massive $SU(N)$ models to 5-loop order. By taking their massless limit and results against the entries of Table 4, one finds perfect agreement. Finally, in Table 5 of Ref. [116], we list the expansion coefficients of the two-point scalar currents for $SU(N)$ and $SU(2)$ models. These results offer checks to the published results of Bijnens, Kampf and Lanz and also provide a basis for comparison with a future computation to higher loops or for the scalar two-point function.

The results presented in this section illustrate the somewhat surprising fact that even in non-renormalizable theories, the leading logs can be reliably summed up when analyticity and unitarity are imposed. The coefficients of the leading log expansion for the quantities of interest such as the scalar and vector form factors can then be calculated. This simplification has been traced to the vanishing of tadpoles in massless theories.

The topic of large logarithms in non-renormalizable theories remains of interest. Existing results, like the ones discussed here, are obtained within the context of specific theories with spontaneous symmetry breaking, where there is an underlying proper (renormalizable) gauge theory. There remain various open questions, such as what are the necessary (symmetry) conditions for an effective theory that allows the summation of leading (next-to-leading) logs? Non-renormalizable theories arise when going beyond the standard model or even when considering gravity [123]. It is worthwhile returning to these questions so that more insights may be obtained.

9 Higher-order corrections and renormalization group improvement

In previous sections, we discussed various methods used in the literature to calculate the higher-order corrections and numerical evaluations of various special functions using automated *Mathematica* codes. These developments have paved a path to the precise determination of some of the theoretical quantities in the standard model of particle physics.[12] Even with these higher-order calculations, renormalization scale and scheme ambiguities are still present on the theoretical side and it is necessary to minimize them using various prescriptions. After renormalization to a fixed order, a perturbative series for a physical quantity of interest is expressed as a polynomial expansion in the coupling constant, masses of the particles, and large logarithms containing the renormalization scale. This form of perturbation series is known as the fixed-order perturbation theory (FOPT). Since the observables are independent of the prescriptions used in the theoretical calculations, it is expected that such ambiguities must cancel among various parameters present in the theory.

FOPT is the most commonly used prescription as it simplifies many calculations and the renormalization scale is varied in a certain range to quantify theoretical uncertainty arising from this variation. These uncertainties sometimes can be very large and the effects of large logarithms should be minimized for which various methods available in the literature are used to control them by using renormalization group (RG) summation. Various theoretical prescriptions developed in the literature rely on the fact that an infinite series can be reordered in such a way that maximum information can be accessed with a few first terms. Here, RG can be used as a guiding principle

[12] Non-perturbative aspects are ignored here as they are beyond the scope of this review.

to gain more insight into the rearrangement. However, it should be kept in mind that this reorganization must not underestimate the truncation uncertainties by neglecting important terms. Among various other prescriptions present in the literature, we will discuss formalism and applications of renormalization group summed perturbation theory (RGSPT) [124, 125] in quantum chromodynamics (QCD) in great detail.

9.1 RGSPT

RGSPT is a summation method in which RG is used to sum the running logarithms accessible from a given order of the perturbation theory in closed form. These closed-form solutions are obtained by finding the recurrence relation among the coefficients present in the perturbation series at different orders of perturbation theory using the RG equation (RGE). It was first introduced in Ref. [124] and soon after robustness of this prescription was detailed for various QCD processes in Ref. [125]. Theoretical uncertainties arising due to variation of the renormalization scale are found to be significantly reduced by summing the running RG logarithm in closed form. These logarithms are of special interest when a perturbation series is used in the QCD sum rules [126, 127] in the determination of the SM parameters.

In FOPT prescription, a perturbative series $S(Q^2)$ in perturbative QCD (pQCD) can be written as:

$$\mathcal{S}(Q^2) \equiv \sum_{i,\,j} T_{i,\,j} x^i L^j \,, \tag{142}$$

where the couplant $x = \alpha_{\rm s}(\mu)/\pi$ is defined from the strong coupling constant $\alpha_{\rm s}(\mu)$, RG logarithm is $L = \log(\mu^2/Q^2)$ and μ is the renormalization scale. One can sum these logarithms by choosing $\mu^2 = Q^2$ and also regenerate them using the RG evolution of the perturbative series in Eq. (142). If a quantity has an anomalous dimension, $\gamma_S(x)$, associated with it then it is required to solve the following set of RGEs:

$$\mu^2 \frac{d}{d\mu^2} \mathcal{S}(Q^2) = \gamma_S(x)\, \mathcal{S}(Q^2) \,, \tag{143}$$

$$\mu^2 \frac{d}{d\mu^2} x(\mu) = \beta(x) \,, \tag{144}$$

where $\gamma_S(x)$ and QCD beta function $\beta(x)$ also has a series expansion in x:

$$\begin{aligned} \gamma_S(x) &= \sum_{i=0} \gamma_i x^{i+1} \,, \\ \beta(x) &= -\sum_{i=0} \beta_i x^{i+2} \,. \end{aligned} \tag{145}$$

One must be careful with the convergence of the perturbation series while solving the RG evolution of the perturbation series in Eq. (142). One is only allowed to go to various scales as long as x is small enough that the series is strictly convergent. For FOPT, which has analytical logarithms present, one must check the convergence by setting $\mu^2 \simeq Q^2$ and the large logarithms L do not spoil it when μ^2 is varied in a certain range. It is common practice to evaluate the theoretical uncertainties by including

1). Uncertainties in the value of the theoretical parameters such as strong coupling constant x, quark masses, non-perturbative condensates, etc.
2). Truncation uncertainty due to finite numbers of terms known which is usually estimated by the difference in the predictions when the known last term is ignored.
3). Scale uncertainties usually calculated by setting $\mu^2 = \xi Q^2$ and varying parameter $\xi \in [1/2,\, 2]$.

In RGSPT, perturbative series in Eq. (142) is organized as follows:

$$\mathcal{S}^{\Sigma}(Q^2) = \sum_i x^i S_i(x\,L) \,, \tag{146}$$

where the goal is to obtain a closed-form expression for coefficients:

$$S_i(u) = \sum_{j=0}^{\infty} T_{i+j,\,j} u^j \,, \tag{147}$$

where we have defined $u \equiv x\,L$. The closed-form coefficients of the series $S_i(u)$ are functions of one variable where $u \sim \mathcal{O}(1)$ and their solution is obtained solving RGE. It should be noted that RG-inaccessible coefficients $T_{i,\,0}$ can only be obtained by direct Feynman diagram calculation and can not be obtained using RGE. Coefficients $T_{i,\,j}$ for $j > 0$ are known as RG-accessible coefficients and are obtained using RGE for the FOPT series.

To get a closed-form summation, RGE in Eq. (143) is applied to the perturbative series in Eq. (142). A set of coupled differential equations are obtained for $S_i(u)$, which in compact form can be written as:

$$\left(\sum_{i=0}^{n} \frac{\beta_i}{u^{n-i-1}} \frac{d}{d\,u}\big(u^{n-i} S_{n-i}(u)\big) + \gamma_i S_{n-i}(u)\right) - S_n'(u) = 0\,, \tag{148}$$

The first three coefficients are obtained as:

$$\begin{aligned}
S_0(u) &= T_{0,\,0} w^{-\tilde{\gamma}_0}\,,\\
S_1(u) &= T_{1,\,0} w^{-\tilde{\gamma}_0-1} + T_{0,\,0} w^{-\tilde{\gamma}_0-1}\Big[(1-w)\tilde{\gamma}_1 + \tilde{\beta}_1\tilde{\gamma}_0(w-\log(w)-1)\Big]\,,\\
S_2(u) &= T_{2,\,0} w^{-\tilde{\gamma}_0-2} - T_{1,\,0} w^{-\tilde{\gamma}_0-2}\Big[(w-1)\tilde{\gamma}_1 + \tilde{\beta}_1(\tilde{\gamma}_0(-w+\log(w)+1)+\log(w))\Big]\\
&\quad + \frac{1}{2} T_{0,\,0} w^{-\tilde{\gamma}_0-2}\Big\{ - \tilde{\beta}_1\tilde{\gamma}_1\Big[1-w^2+2\log(w)+2(w-1)\tilde{\gamma}_0(w-\log(w)-1)\Big]\\
&\quad + (w-1)\Big[(w-1)\tilde{\beta}_2\tilde{\gamma}_0 + (w-1)\tilde{\gamma}_1^2 - (w+1)\tilde{\gamma}_2\Big]\\
&\quad + \tilde{\beta}_1^2\tilde{\gamma}_0(\tilde{\gamma}_0-1)(w-\log(w)-1)^2\Big\}\,,
\end{aligned} \tag{149}$$

where $w \equiv 1-\beta_0\,u$, for anomalous dimension and higher order beta function coefficients, we have used $\tilde{X} \equiv X/\beta_0$. Now, one can obtain the RG summed expression for various observables and parameters of the theory such as the strong coupling constant and running of the quark masses by substituting appropriate values of the anomalous dimensions to Eq. (149).

For demonstration purposes, the strong coupling constant can be obtained by setting $T_{i,\,0} = \delta_{i,\,1}$ and $\tilde{\gamma}_i = 0$ in Eq. (149). The leading order (LO) and next-to-leading order (NLO) RG summed coefficients are given by:

$$S_0[xL] = \frac{1}{1-\beta_0 x\,L}\,, \tag{150}$$

$$S_1[xL] = \frac{-\beta_1\log(1-\beta_0 x\,L)}{\beta_0(1-\beta_0 x\,L)^2}\,. \tag{151}$$

The form of Eq. (150) looks familiar and can be found in the textbooks involving one-loop renormalization of QCD after the summation of large logarithms. However, the appearance of $\log(1-\beta_0 x\,L)$ term in Eq. (151) is new that is obtained using RGSPT. It should be noted that the above solutions have an explicit Landau pole at $q^2 = \Lambda^2_{\rm QCD} > 0$ in the LO coefficient and a cut for NLO coefficient extending from $q^2 \in (-\infty,\,\Lambda^2_{\rm QCD}]$. An important feature of the above procedure is that the most general term present in the summed coefficient using RGSPT is given by:

$$\Omega_{n,\,a} \equiv \frac{\log^n(w)}{w^a} = \frac{\log^n(1-\beta_0\,x(\mu)\log(\mu^2/Q^2))}{(1-\beta_0\,x(\mu)\log(\mu^2/Q^2))^a}\,, \tag{152}$$

where n is a positive integer and $a \propto \gamma_0/\beta_0 +$ integer appearing in Eq. (145).

It should be noted that for $\mu^2 = Q^2$, both RG summed series in Eq. (146) reduce to FOPT series in Eq. (142). However, two approaches give different results when computed at different scales by setting $\mu^2 = \xi Q^2$. The presence of logarithms in the numerator and denominator in term (152) results in extra stability when ξ is varied. These improvements are found to be very significant in QCD static energy [128], moments of hadronic tau decay width [129], low-energy moments of heavy quark vector current correlator [130], Higgs to two gluons [131], and strong coupling constant from hadronic tau decays [132], etc.

One can also use the RG-improved series to sum kinematical π^2-terms arising from the analytic continuation of the perturbative series from spacelike regions to timelike regions. The observable $R(s)$, which is analog of spectral density, can be measured in experiments for energies $s > 0$ related to the discontinuity of theoretical quantity

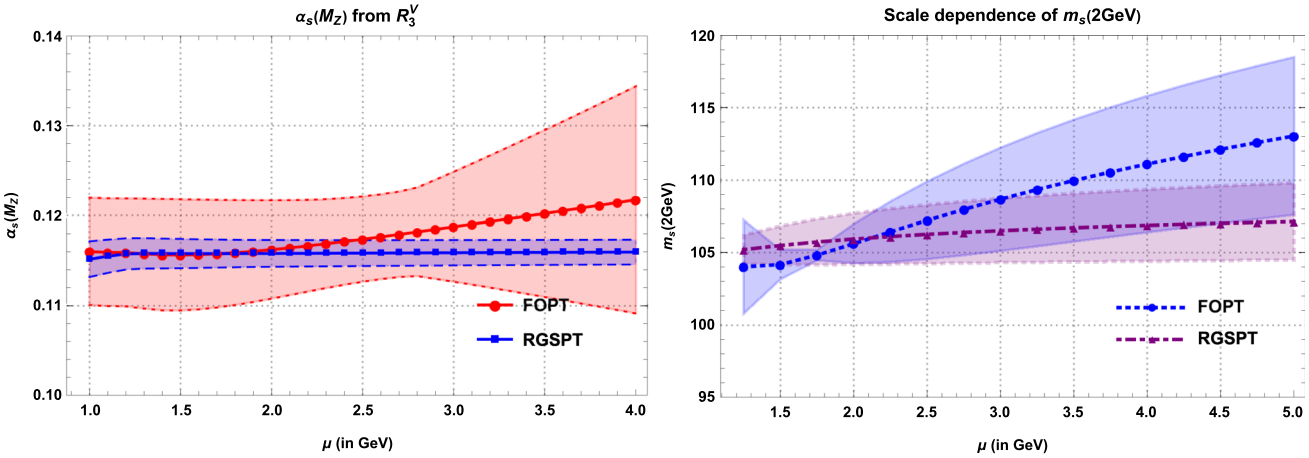

Fig. 12 The strong-coupling constant obtained from the third moment of the low-energy (R_3^V) of the vector current correlator at different renormalization scales is presented in the left figure. The strange quark mass obtained at different renormalization scales from the Borel-Laplace sum rule for the pseudoscalar current correlator is presented on the right. Bands represent the 1σ uncertainty in the determination using the FOPT and RGSPT prescriptions

such as polarization functions $\Pi(q^2)$ or Adler functions $\widetilde{D}(q^2) \equiv -q^2 \frac{d}{dq^2}\Pi(q^2)$ calculated at $q^2 < 0$. The analytic continuation is achieved by

$$R(s) \equiv \frac{1}{2\pi i} \lim_{\epsilon \to 0} [\Pi(-s - i\epsilon) - \Pi(-s + i\epsilon)] = \frac{-1}{2\pi i} \oint_{|x_c|=1} \frac{dx_c}{x_c} \widetilde{D}(-x_c s)\,. \tag{153}$$

For FOPT, these extra terms arise at N^{2}LO in α_s and can significantly alter the convergence of the series. In RGSPT, these contributions can be summed to all orders using the general formula:

$$\frac{1}{2\pi i} \oint_{|q^2|=s} \frac{dq^2}{q^2} \frac{\log^m\left(1 - u_1 \log\left(\frac{\mu^2}{-q^2}\right)\right)}{\left(1 - u_1 \log\left(\frac{\mu^2}{-q^2}\right)\right)^n} \tag{154}$$

$$= \lim_{\delta \to 0} \partial_\delta^m \begin{cases} \dfrac{\tan^{-1}\left(\frac{\pi u_1}{1 - u_1 L_s}\right)}{\pi u_1}\,, & n = 1 \\ \dfrac{w_s^{-\frac{1}{2}(n-\delta-1)} \sin\left((n-\delta-1)\tan^{-1}\left(\frac{\pi u_1}{1-u_1 L_s}\right)\right)}{\pi u_1 (n-\delta-1)}\,, & n \neq 1 \end{cases} \tag{155}$$

where, $w_s = (1 - u_1 L_s)^2 + \pi^2 u_1^2$, $u_1 = \beta_0 x$ and $L_s = \log(\mu^2/s)$. This result has profound effects in reducing the theoretical uncertainties in Borel-Laplace type sum rules [133, 134]. One can also test the application of the procedure for various perturbation series known at even lower orders by first getting the estimate of higher order terms using Padé approximants. Interested readers can also find *Mathematica* implementation of the two-variable generalization of the diagonal Padé approximants called the Chisholm approximants in the package `ChisholmD.wl`[13] [135]. More details and application of analytic continuation can be found in Ref. [136]. Some improvements in the determination of the strong-coupling constant from the low-energy moments of the heavy quark vector current correlator [130] and strange quark mass determination from the Borel-Laplace sum rule for the pseudoscalar current correlator [133] are presented in Fig. 12. A more recent review of the application of RGSPT in QCD sum rule determination can be found in Ref. [137].

[13]The package along with a notebook containing various examples is available at https://github.com/TanayPathak-17/Chisholm_Approximant.

10 Conclusion and outlook

The tremendous improvements in our ability to perform precision measurements at particle colliders and other experiments necessarily demand comparable progress in theoretical precision predictions, so that promising deviations could be filtered out from seemingly important ones. Such deviations could pave the path to novel search strategies for discovering new particles and interactions, which could possibly help make sense of the observations that cannot be accounted for by the Standard Model as it stands today. Standard Model-based predictions for observables such as cross-sections and decay-widths are primarily obtained from a perturbative evaluation of particle scattering amplitudes using Feynman diagrams, particularly at NNLO and beyond. We reviewed some theoretical concepts and automated implementations that help in the analytic evaluation of integrals corresponding to multi-loop Feynman diagrams appearing at higher orders in perturbation.

Calculation of Feynman integrals having multiple scales and loops is quite non-trivial. The MoR provides a systematic way to simplify such integrals using hierarchies between various scales of the problem. The identification of regions becomes more subtle with the increase in loops and scales in given Feynman integrals. We described a novel algorithm ASPIRE, which helps in isolating the regions based on Landau singularities and Newton polytopes. We also presented a simple one-loop three-point function as an example to demonstrate the systematic way to calculate the contribution of each region with the consideration of generic analytic regulators. This method provides a useful way to calculate the boundary conditions for the evaluation of master integrals for given high-energy scattering processes.

It is often possible to express planar Feynman integrals in terms of transcendental functions called MPLs, which in the Feynman integral context could be understood as appearing after a Laurent expansion in the parameter ϵ of the relevant hypergeometric function/series results. The MPLs satisfy a mathematical structure known as the Hopf algebra, which enables us to employ their symbol calculus to analyse the analytic structure of a given Feynman integral. The symbol alphabet of the integral is related to its cut. Hence, by evaluating the simpler cut-integral, we can evaluate the original Feynman integral analytically. We examined this method by considering the case of a non-planar Feynman integral, and using the *Mathematica* codes `PolyLogTools` and `HypExp`.

We then provided a brief introduction to multi-variable generalizations of the Gauss hypergeometric function, namely, the double-variable Appell functions and the triple-variable Lauricella and Lauricella-Saran functions. These functions frequently appear in the literature dealing with Feynman integral calculus. The defining series representations of these functions are valid in certain domains of convergence. Thus, analytic continuations are necessary to find representations for these functions beyond the defining domains of convergence, and for evaluating them. In this article, we have discussed the method of Olsson to find analytic continuations of these functions, with the triple-variable Lauricella-Saran $F_S^{(3)}$ function as a demonstrative example. Olsson's method has also been implemented in the *Mathematica* package `Olsson.wl`, which enables one to automatically obtain the analytic continuations of multi-variable hypergeometric functions. We have briefly demonstrated the application of the main command `Olsson`, choosing the Appell F_2 function as an example. Determination of the domain of convergence plays an essential role in obtaining the analytic continuations, and thus, for numerically evaluating a given multi-valued complex function. In this regard, we briefly discussed Horn's theorem to find the domain of convergence of hypergeometric functions with multiple variables. We demonstrated the *Mathematica* package `ROC2.wl` to find the region of convergence of double-variable hypergeometric functions.

Concerning Mellin-Barnes integrals, in this article, we have briefly described the steps to convert a Feynman integral into a Mellin-Barnes integral. We then showed that multi-fold MB integrals can be analytically computed in a non-iterative way using conic hulls or triangulations of point configurations. These methods, which can handle both the resonant and non-resonant cases, are automated in the `MBConicHulls.wl` package. We then discussed one application of this package by computing the massless off-shell conformal hexagon and double-box for both generic and unit powers of the propagators. In addition, we discussed that `MBConicHulls.wl` can be used to systematically study the transformation theory of multi-variable hypergeometric functions, an area of research that remains largely unexplored. We also briefly summarized how the program `FeynGKZ` can be used to obtain series solutions to Feynman integrals using GKZ hypergeometric theory. When analytic results for Feynman integrals are expressed in terms of multi-variable hypergeometric functions, the dimensional regulator ϵ appears in the parameters. These hypergeometric functions need to be expanded in a Laurent series in ϵ. We sketched an algorithm to find this expansion, which is the backbone of the `MultiHypExp.wl` package. An example of ϵ-expansion of the Appell F_4 function with integer-valued parameters is presented, which requires a non-linear change of variables. The expansion coefficients are expressed in terms of the MPLs. We have also presented an example of ϵ-expansion of the ${}_3F_2$ function with half-odd-integer valued parameters, which appears in the evaluation of a certain three-loop two-point Feynman integral.

The evaluation of Feynman integrals continues to be computationally challenging at higher loops, even with all the above methods. Thus, it becomes important to use other techniques in conjunction to facilitate the computation of these integrals. We described briefly one such method that can be used to derive algebraic relations for the product of propagators. These relations, once derived, allow us to rewrite our original Feynman integral as a sum

of integrals with reduced complexity. We discussed the method in detail using the one-loop bubble integral as an example. The method has also been implemented in the *Mathematica* package `AlgRel.wl`, a basic usage of which has been demonstrated using the one-loop vertex integral as an example. Apart from helping in Feynman integral evaluation, the method also allows for the determination of reduction formulae of multi-variable hypergeometric functions, which is demonstrated using the one-loop bubble integral as well.

The large logarithms obtained after evaluating the Feynman diagrams in a theory can interfere with the convergence of the perturbation series. It is therefore very important to find a way to sum them to extend the validity of the perturbation theory in a wide energy region. This is a non-trivial task for non-renormalizable theories where the method of analyticity and unitarity are guiding principles. We discussed the leading logarithm summation for the case of $O(N)$ and $SU(N)$ non-renormalizable massless models. In renormalizable theories, the renormalization group provides a very powerful method to sum these logarithms. In QCD, the strong coupling constant is large at lower energies, where the convergence of the perturbation series can be spoiled by the large logarithms. The RGSPT prescription is found to significantly improve the milder dependence on the renormalization scale, which is a free parameter introduced during the regularization procedure. An improved convergence is also obtained if the analytic continuation of the current correlators from spacelike to timelike regions is performed for some observables. Impact of these issues in the determination of some Standard Model parameters using QCD sum rules is found to significantly improve the reduction in the theoretical uncertainties, especially those coming from the renormalization scale. These parameters are now calculated with alternative computationally expensive lattice QCD simulations with improved precision.

In this review, we have presented a survey of many techniques and a summary of a large body of work that has addressed the complex issues addressed herein. We feel that this is a rich area where a lot of further work is needed to take forward the themes discussed here and to automate as much as possible the methods that are available. It brings together diverse fields of mathematics, physics and computer algebra to name a few and is a fertile ground for progress in all these subjects.

Acknowledgements S.B. has been supported by an appointment to the JRG Program at the APCTP through the Science and Technology Promotion Fund and Lottery Fund of the Korean Government and by the Korean Local Governments—Gyeongsangbuk-do Province and Pohang City. TP acknowledges the support of the grant JST CREST (Grant No. JPMJCR19T2). A.K. acknowledges support from the SERB Grant SPG/2022/001238.

Funding Open access funding provided by University of Zurich.

Data Availability Data sharing is not applicable to this article as no datasets were generated or analyzed during the current study.

Declarations

Conflict of interest We have no conflict of interest to disclose.

References

1. B. Ananthanarayan, M.S.A.A. Khan, D. Wyler, Chiral perturbation theory: reflections on effective theories of the standard model. Indian J. Phys. **97**(11), 3245–3267 (2023)
2. G. Heinrich, Collider physics at the precision frontier. Phys. Rept. **922**, 1–69 (2021)
3. T. Gehrmann, B. Malaescu, Precision QCD Physics at the LHC. Ann. Rev. Nucl. Part. Sci. **72**, 233–258 (2022)
4. R. Boughezal et al. Theory Techniques for Precision Physics – Snowmass 2021 TF06 Topical Group Report. 9 (2022)
5. Wolfram Research, Inc. Mathematica, Version 12.3.1. Champaign, IL (2021)
6. V.A. Smirnov, *Feynman integral calculus* (Springer, Berlin, Heidelberg, 2006)
7. M. Czakon, Automatized analytic continuation of Mellin-Barnes integrals. Comput. Phys. Commun. **175**, 559–571 (2006)
8. A.V. Smirnov, V.A. Smirnov, On the Resolution of Singularities of Multiple Mellin-Barnes Integrals. Eur. Phys. J. C **62**, 445–449 (2009)

9. J. Usovitsch, I. Dubovyk, T. Riemann, MBnumerics: Numerical integration of Mellin-Barnes integrals in physical regions. PoS **LL2018**, 046 (2018)
10. V.A. Smirnov, Analytical result for dimensionally regularized massless on shell double box. Phys. Lett. B **460**, 397–404 (1999)
11. J.B. Tausk, Nonplanar massless two loop Feynman diagrams with four on-shell legs. Phys. Lett. B **469**, 225–234 (1999)
12. S. Friot, D. Greynat, On convergent series representations of Mellin-Barnes integrals. J. Math. Phys. **53**, 023508 (2012)
13. A.I. Davydychev, General results for massive N-point Feynman diagrams with different masses. J. Math. Phys. **33**, 358–369 (1992)
14. M.Y. Kalmykov, B.A. Kniehl, Mellin-Barnes representations of Feynman diagrams, linear systems of differential equations, and polynomial solutions. Phys. Lett. B **714**, 103–109 (2012)
15. T.-F. Feng, C.-H. Chang, J.-B. Chen, H.-B. Zhang, GKZ-Hypergeometric Systems for Feynman integrals. Nucl. Phys. B **953**, 114952 (2020)
16. M.Y. Kalmykov, B.A. Kniehl, Counting the number of master integrals for sunrise diagrams via the Mellin-Barnes representation. JHEP **07**, 031 (2017)
17. B. Ananthanarayan, T. Pathak, K. Sharma, Closed Form Expressions for Certain Improper Integrals of Mathematical Physics. Eur. Phys. J. Spec. Top. **233**, 2057–2074 (2024)
18. M. Beneke, V.A. Smirnov, Asymptotic expansion of Feynman integrals near threshold. Nucl. Phys. B **522**, 321–344 (1998)
19. V.A. Smirnov, Applied asymptotic expansions in momenta and masses. Springer Tracts Mod. Phys. **177**, 1–262 (2002)
20. B. Jantzen, Foundation and generalization of the expansion by regions. JHEP **12**, 076 (2011)
21. T. Becher, A. Broggio, A. Ferroglia, *Introduction to Soft-Collinear Effective Theory*, vol. 896 (Springer, 2015)
22. V.A. Smirnov, Expansion by Regions: An Overview. (2021)
23. T.Y. Semenova, A.V. Smirnov, V.A. Smirnov, On the status of expansion by regions. Eur. Phys. J. C **79**(2), 136 (2019)
24. G. Heinrich, S. Jahn, S.P. Jones, M. Kerner, F. Langer, V. Magerya, A. Pöldaru, J. Schlenk, E. Villa, Expansion by regions with pySecDec. Comput. Phys. Commun. **273**, 108267 (2022)
25. E. Gardi, F. Herzog, S. Jones, Y. Ma, J. Schlenk, The on-shell expansion: from Landau equations to the Newton polytope. JHEP **07**, 197 (2023)
26. Y. Ma, Identifying regions in wide-angle scattering via graph-theoretical approaches. JHEP **09**, 197 (2024)
27. E. Gardi, F. Herzog, S. Jones, Y. Ma, Dissecting polytopes: Landau singularities and asymptotic expansions in $2 \to 2$ scattering. JHEP **08**, 127 (2024)
28. V.A. Smirnov, F. Wunder, Expansion by regions meets angular integrals. JHEP **08**, 138 (2024)
29. Y. Ma, Identifying regions for asymptotic expansions of amplitudes: fundamentals and recent advances. 5 (2025)
30. T. Becher, P. Hager, S. Jaskiewicz, M. Neubert, D. Schwienbacher, Factorization Restoration through Glauber Gluons. Phys. Rev. Lett. **134**(6), 061901 (2025)
31. T. Pathak, R. Sreekantan, Singularities of Feynman Integrals. Eur. Phys. J. Spec. Top. **232**, 3191–3206 (2023)
32. S. Srednyak, V. Khachatryan, Vanishing Cycles and Analysis of Singularities of Feynman Diagrams. Mathematics **13**(6), 969 (2025)
33. V.A. Smirnov, *Feynman integral calculus* (Springer, Berlin, Heidelberg, 2006)
34. S. Weinzierl, *Feynman Integrals* (Springer, A Comprehensive Treatment for Students and Researchers. UNITEXT for Physics, 2022)
35. A. Pak, A. Smirnov, Geometric approach to asymptotic expansion of feynman integrals. Eur. Phys. J. C **71**, 1626 (2011)
36. B. Jantzen, A.V. Smirnov, V.A. Smirnov, Expansion by regions: revealing potential and Glauber regions automatically. Eur. Phys. J. C **72**, 2139 (2012)
37. A.D. Bruno, A.B. Batkhin, Resolution of an algebraic singularity by power geometry algorithms. Program. Comput. Softw. **38**(2), 57–72 (2012)
38. B. Ananthanarayan, A. Pal, S. Ramanan, R. Sarkar, Unveiling Regions in multi-scale Feynman Integrals using Singularities and Power Geometry. Eur. Phys. J. C **79**(1), 57 (2019)
39. G. Mishima, High-Energy Expansion of Two-Loop Massive Four-Point Diagrams. JHEP **02**, 080 (2019)
40. T. Becher, G. Bell, Analytic Regularization in Soft-Collinear Effective Theory. Phys. Lett. B **713**, 41–46 (2012)
41. B. Ananthanarayan, A.B. Das, R. Sarkar, Asymptotic analysis of Feynman diagrams and their maximal cuts. Eur. Phys. J. C **80**(12), 1131 (2020)
42. S. Abreu, R. Britto, C. Duhr, E. Gardi, From multiple unitarity cuts to the coproduct of Feynman integrals. JHEP **10**, 125 (2014)
43. B. Ananthanarayan, A.B. Das, D. Wyler, Hopf algebra structure of the two loop three mass nonplanar Feynman diagram. Phys. Rev. D **104**(7), 076002 (2021)
44. N.I. Usyukina, A.I. Davydychev, Some exact results for two loop diagrams with three and four external lines. Phys. Atom. Nucl. **56**, 1553–1557 (1993)
45. M. Hari, *Srivastava and Per Wennerberg Karlsson* (Multiple Gaussian hypergeometric series. E, Horwood, 1985)
46. H. Bateman, *Higher Transcendental Functions* (McGraw-Hill Book Company, 1953)
47. P.O.M. Olsson, Integration of the partial differential equations for the hypergeometric functions F_1 and F_D of two and more variables. J. Math. Phys. **5**(3), 420–430 (1964)

48. P.J. Appell, K. de Fériet, *Fonctions Hypergéométriques et Hypersphériques* (Polynômes d'Hermite. Gauthier-Villars, Paris, 1926)
49. P. Appell, Sur les séries hypergéométriques de deux variables et sur dés équations différentielles linéaires aux dérivés partielles. C. R. Acad. Sci. Paris **90**(296–299), 731–735 (1880)
50. B. Ananthanarayan, S. Bera, S. Friot, O. Marichev, T. Pathak, On the evaluation of the Appell F_2 double hypergeometric function. Comput. Phys. Commun. **284**, 108589 (2023)
51. H. Exton, On the system of partial differential equations associated with Appell's function F_4. J. Phys. A: Math. Gen. **28**(3), 631–645 (1995)
52. B. Ananthanarayan, S. Bera, S. Friot, T. Pathak, Olsson.wl & ROC2.wl: Mathematica packages for transformations of multivariable hypergeometric functions & regions of convergence for their series representations in the two variables case. Comput. Phys. Commun. **300**, 109162 (2024)
53. M.A. Bezuglov, B.A. Kniehl, A.I. Onishchenko, O.L. Veretin, PrecisionLauricella: Package for numerical computation of Lauricella functions depending on a parameter. Comput. Phys. Commun. **316**, 109812 (2025)
54. S. Bera, T. Pathak, Analytic continuations and numerical evaluation of the Appell F_1, F_3, Lauricella $F_D(3)$ and Lauricella-Saran $F_S(3)$ and their application to Feynman integrals. Comput. Phys. Commun. **306**, 109386 (2025)
55. O.I. Marichev, *Handbook of integral transforms of higher transcendental functions: Theory and Algorithmic tables* (Ellis Horwood Ltd, 1983)
56. R.B. Paris, D. Kaminski, *Asymptotics and Mellin-Barnes Integrals* (Cambridge University Press, Encyclopedia of Mathematics and its Applications, 2001)
57. MBtools Collaboration. Mbtools: A toolbox for Mellin–Barnes integrals. https://mbtools.hepforge.org/
58. M. Ochman, T. Riemann, MBsums - a Mathematica package for the representation of Mellin-Barnes integrals by multiple sums. Acta Phys. Polon. B **46**(11), 2117 (2015)
59. A.K. Tsikh, *Multidimensional residues and their applications*, vol. 103 (Citeseer, 1992)
60. M. Passare, A. Tsikh, O. Zhdanov, A multidimensional Jordan residue lemma with an application to Mellin-Barnes integrals. Aspects Math. pp. 233–241 (1994)
61. M. Passare, A.K. Tsikh, A.A. Cheshel, Multiple Mellin-Barnes integrals as periods of Calabi-Yau manifolds with several moduli. Teor. Mat. Fiz. **109N3**, 381–394 (1996)
62. A. Tsikh, O. Zhdanov, Investigation of multiple Mellin-Barnes integrals by means of multidimensional residues. Siberian Math. J. **39**(2), 245–260 (1998)
63. B. Ananthanarayan, S. Banik, S. Friot, S. Ghosh, Multiple Series Representations of N-fold Mellin-Barnes Integrals. Phys. Rev. Lett. **127**(15), 151601 (2021)
64. A.V. Smirnov, N.D. Shapurov, L.I. Vysotsky, FIESTA5: Numerical high-performance Feynman integral evaluation. Comput. Phys. Commun. **277**, 108386 (2022)
65. S. Borowka, G. Heinrich, S. Jahn, S.P. Jones, M. Kerner, J. Schlenk, T. Zirke, pySecDec: a toolbox for the numerical evaluation of multi-scale integrals. Comput. Phys. Commun. **222**, 313–326 (2018)
66. K.J. Larsen, R. Rietkerk, MultivariateResidues: a Mathematica package for computing multivariate residues. Comput. Phys. Commun. **222**, 250–262 (2018)
67. B. Ananthanarayan, S. Banik, S. Friot, S. Ghosh, Double box and hexagon conformal Feynman integrals. Phys. Rev. D **102**(9), 091901 (2020)
68. B. Ananthanarayan, S. Banik, S. Friot, S. Ghosh, Massive One-loop Conformal Feynman Integrals and Quadratic Transformations of Multiple Hypergeometric Series. Phys. Rev. D **103**(9), 096008 (2021)
69. S. Datta, N. Rana, V. Ravindran, R. Sarkar, Three loop QCD corrections to the heavy-light form factors in the color-planar limit. JHEP **12**, 001 (2023)
70. S. Datta, N. Rana, Three loop QCD corrections to the heavy-light form factors: fermionic contributions. JHEP **10**, 254 (2024)
71. S. Banik, S. Friot, Multiple Mellin-Barnes integrals with straight contours. Phys. Rev. D **107**(1), 016007 (2023)
72. S. Banik, S. Friot, Multiple Mellin-Barnes integrals and triangulations of point configurations. Phys. Rev. D **110**(3), 036002 (2024)
73. J. Rambau, Topcom: Triangulations of point configurations and oriented matroids. In Proceedings of the International Congress of Mathematical Software, (2002)
74. V. Del Duca, C. Duhr, V.A. Smirnov, The Two-Loop Hexagon Wilson Loop in N = 4 SYM. JHEP **05**, 084 (2010)
75. R.N. Lee, A.A. Pomeransky, Critical points and number of master integrals. JHEP **11**, 165 (2013)
76. L. de la Cruz, Feynman integrals as A-hypergeometric functions. JHEP **12**, 123 (2019)
77. René Pascal Klausen, Hypergeometric Series Representations of Feynman Integrals by GKZ Hypergeometric Systems. JHEP **04**, 121 (2020)
78. I.M. Gelfand, M.M. Kapranov, A.V. Zelevinsky, Discriminants, resultants, and multidimensional determinants. (1994)
79. B. Ananthanarayan, S. Banik, S. Bera, S. Datta, FeynGKZ: A Mathematica package for solving Feynman integrals using GKZ hypergeometric systems. Comput. Phys. Commun. **287**, 108699 (2023)
80. S. Bera, ϵ-expansion of multivariable hypergeometric functions appearing in Feynman integral calculus. Nucl. Phys. B **989**, 116145 (2023)
81. J.M. Henn, Multiloop integrals in dimensional regularization made simple. Phys. Rev. Lett. **110**, 251601 (2013)
82. J.M. Henn, Lectures on differential equations for Feynman integrals. J. Phys. A **48**, 153001 (2015)

83. S. Bera, MultiHypExp: A Mathematica package for expanding multivariate hypergeometric functions in terms of multiple polylogarithms. Comput. Phys. Commun. **297**, 109060 (2024)
84. M. Kato, A Pfaffian system of Appell's F_4. Bull. College Educ. Univ. Ryukyus **33**, 331–334 (1988)
85. Y. Goto, J. Kaneko, K. Matsumoto, Pfaffian of Appell's Hypergeometric System $\mathcal{F}_\triangle$ in Terms of the Intersection Form of Twisted Cohomology Groups. Publ. Res. Inst. Math. Sci. **52**(2), 223–247 (2016)
86. S. Weinzierl, *Feynman Integrals* (Springer, A Comprehensive Treatment for Students and Researchers. UNITEXT for Physics, 2022)
87. V.A. Smirnov, V.A. Smirnov, *Feynman Integral Calculus*, vol. 10 (Springer, 2006)
88. O.V. Tarasov, Derivation of Functional Equations for Feynman Integrals from Algebraic Relations. JHEP **11**, 038 (2017)
89. B. Ananthanarayan, S. Bera, T. Pathak, AlgRel.wl: Algebraic relations for the product of propagators in Feynman integrals. Nucl. Phys. B **995**, 116345 (2023)
90. O.V. Tarasov, Calculation of One-Loop Integrals for Four-Photon Amplitudes by Functional Reduction Method. Phys. Part. Nucl. Lett. **20**(3), 287–291 (2023)
91. O.V. Tarasov, Using Functional Equations to Calculate Feynman Integrals. Theor. Math. Phys. **200**(2), 1205–1221 (2019)
92. O.V. Tarasov, Functional reduction of Feynman integrals. JHEP **02**, 173 (2019)
93. O.V. Tarasov, Methods for deriving functional equations for Feynman integrals. J. Phys: Conf. Ser. **920**(1), 012004 (2017)
94. B.A. Kniehl, O.V. Tarasov, Counting master integrals: Integration by parts vs. functional equations. 1 (2016)
95. O.V. Tarasov, Functional reduction of one-loop Feynman integrals with arbitrary masses. JHEP **06**, 155 (2022)
96. I. Gonzalez, V.H. Moll, Definite integrals by the method of brackets. Adv. Appl. Math. **45**(1), 50–73 (2010)
97. C.G. Bollini, J.J. Giambiagi, Lowest order "divergent" graphs in ν-dimensional space. Phys. Lett. B **40**(5), 566–568 (1972)
98. E.E. Boos, A.I. Davydychev, A Method of evaluating massive Feynman integrals. Theor. Math. Phys. **89**, 1052–1063 (1991)
99. B.A. Kniehl, O.V. Tarasov, Finding new relationships between hypergeometric functions by evaluating Feynman integrals. Nucl. Phys. B **854**, 841–852 (2012)
100. H. Exton, On the system of partial differential equations associated with Appell's function F_4. J. Phys. A: Math. Gen. **28**(3), 631 (1995)
101. S. Bera, T. Pathak, Analytic continuations of the Horn H_1 and H_5 functions. Eur. Phys. J. Spec. Top., (2023)
102. W. Becken, P. Schmelcher, The analytic continuation of the Gaussian hypergeometric function ${}_2F_1(a, b; c; z)$ for arbitrary parameters. J. Comput. Appl. Math. **126**(1–2), 449–478 (2000)
103. F. Loebbert, D. Müller, H. Münkler, Yangian Bootstrap for Conformal Feynman Integrals. Phys. Rev. D **101**(6), 066006 (2020)
104. N. Takayama, Groebner basis and the problem of contiguous relation. Japan Journal of Applied Mathematics **6**, 147–160 (1989)
105. C. Meyer, Algorithmic transformation of multi-loop master integrals to a canonical basis with CANONICA. Comput. Phys. Commun. **222**, 295–312 (2018)
106. T. Huber, D. Maitre, HypExp 2, Expanding Hypergeometric Functions about Half-Integer Parameters. Comput. Phys. Commun. **178**, 755–776 (2008)
107. X. Liu, Y.-Q. Ma, AMFlow: A Mathematica package for Feynman integrals computation via auxiliary mass flow. Comput. Phys. Commun. **283**, 108565 (2023)
108. J. Gasser, H. Leutwyler, Chiral Perturbation Theory to One Loop. Annals Phys. **158**, 142 (1984)
109. J. Gasser, H. Leutwyler, Chiral Perturbation Theory: Expansions in the Mass of the Strange Quark. Nucl. Phys. B **250**, 465–516 (1985)
110. G. Amoros, J. Bijnens, P. Talavera, Two-point functions at two loops in three flavour chiral perturbation theory. Nucl. Phys. B **568**, 319–363 (2000)
111. B. Ananthanarayan, S. Friot, S. Ghosh, Three-loop QED contributions to the $g-2$ of charged leptons with two internal fermion loops and a class of Kampé de Fériet series. Phys. Rev. D **101**(11), 116008 (2020)
112. F. Jegerlehner, *The Anomalous Magnetic Moment of the Muon*, vol. 274 (Springer, Cham, 2017)
113. A. Czarnecki, M. Skrzypek, The Muon anomalous magnetic moment in QED: Three loop electron and tau contributions. Phys. Lett. B **449**, 354–360 (1999)
114. S. Friot, D. Greynat, E. De Rafael, Asymptotics of Feynman diagrams and the Mellin-Barnes representation. Phys. Lett. B **628**, 73–84 (2005)
115. CODATA. Codata recommended values of the fundamental physical constants: 2018, (2018)
116. B. Ananthanarayan, S. Ghosh, A. Vladimirov, D. Wyler, Leading Logarithms of the Two Point Function in Massless O(N) and SU(N) Models to any Order from Analyticity and Unitarity. Eur. Phys. J. A **54**(7), 123 (2018)
117. A. Vladimirov, Infrared logarithms in effective field theories. PhD thesis, Ruhr U., Bochum (main), (2010)
118. S. Weinberg, Pion scattering lengths. Phys. Rev. Lett. **17**, 616–621 (1966)
119. D.I. Kazakov, On a Generalization of Renormalization Group Equations to Quantum Field Theories of an Arbitrary Type. Theor. Math. Phys. **75**, 440–442 (1988)

120. M. Buchler, G. Colangelo, Renormalization group equations for effective field theories. Eur. Phys. J. C **32**, 427–442 (2003)
121. J. Bijnens, K. Kampf, S. Lanz, Leading logarithms in N-flavour mesonic Chiral Perturbation Theory. Nucl. Phys. B **873**, 137–164 (2013)
122. J. Bijnens, L. Jie, Meson-meson Scattering in QCD-like Theories. JHEP **03**, 028 (2011)
123. J. Donoghue, Quantum gravity as a low energy effective field theory. Scholarpedia **12**(4), 32997 (2017)
124. D.G.C. McKeon, Summing logarithms in quantum field theory: The renormalization group. Int. J. Theor. Phys. **37**, 817–826 (1998)
125. M.R. Ahmady, F.A. Chishtie, V. Elias, A.H. Fariborz, N. Fattahi, D.G.C. McKeon, T.N. Sherry, T.G. Steele, Closed form summation of RG accessible logarithmic contributions to semileptonic B decays and other perturbative processes. Phys. Rev. D **66**, 014010 (2002)
126. M.A. Shifman, A.I. Vainshtein, V.I. Zakharov, QCD and Resonance Physics. Theoretical Foundations. Nucl. Phys. B **147**, 385–447 (1979)
127. M.A. Shifman, A.I. Vainshtein, V.I. Zakharov, QCD and Resonance Physics: Applications. Nucl. Phys. B **147**, 448–518 (1979)
128. B. Ananthanarayan, D. Das, M.S.A.A. Khan, QCD static energy using optimal renormalization and asymptotic Padé-approximant methods. Phys. Rev. D **102**(7), 076008 (2020)
129. B. Ananthanarayan, D. Das, M.S.A. Khan, Renormalization group improved m_s and —V_{us}— determination from hadronic τ decays. Phys. Rev. D **106**(11), 114036 (2022)
130. M.S.A.A. Khan, Renormalization group improved determination of αs, mc, and mb from the low energy moments of heavy quark current correlators. Phys. Rev. D **108**(7), 074029 (2023)
131. G. Abbas, A. Jain, V. Singh, N. Singh, Renormalization-group improved Higgs to two gluons decay rate. Eur. Phys. J. Plus **139**(2), 114 (2024)
132. G. Abbas, B. Ananthanarayan, I. Caprini, J. Fischer, Perturbative expansion of the QCD Adler function improved by renormalization-group summation and analytic continuation in the Borel plane. Phys. Rev. D **87**(1), 014008 (2013)
133. M.S.A.A. Khan, Renormalization group improved determination of light quark masses from Borel-Laplace sum rules. Phys. Rev. D **108**(9), 094016 (2023)
134. S. Narison, Laplace Sum Rules in Quantum ChromoDynamics. 9 (2023)
135. S. Bera, T. Pathak, ChisholmD. wl: Automated rational approximant for bi-variate series. The European Physical Journal Special Topics, pages 1–22, (2025)
136. M.S.A.A. Khan, Renormalization group summation and analytic continuation from spacelike to timeline regions. Phys. Rev. D **108**(1), 014028 (2023)
137. M.S.A.A. Khan, Renormalization group improvement and QCD sum rules. Nucl. Part. Phys. Proc. **344**, 1–7 (2024)